# Morphology-dependent Hashin–Shtrikman bounds on the effective properties of stress-gradient materials

Vinh Phuc Tran, Karam Sab, Sébastien Brisard

# Morphology-dependent Hashin–Shtrikman bounds on the effective properties of stress-gradient materials

**Sébastien Brisard, Vinh-Phuc Tran, Karam Sab**

This is the accepted version of the following article: “Morphology-dependent Hashin–Shtrikman bounds on the effective properties of stress-gradient materials”, which has been published in final form at https://doi.org/10.1016/j.euromechsol.2020.104072.

# Morphology-dependent Hashin–Shtrikman bounds on the effective properties of stress-gradient materials

S. Brisard[a], V.P. Tran[a,b], K. Sab[a]

[a]*Navier, Ecole des Ponts, Univ Gustave Eiffel, IFSTTAR, CNRS, Marne-la-Vallée, France*
[b]*Laboratoire Modélisation et Simulation Multi Échelle (MSME), Univ Gustave Eiffel, CNRS, Marne-la-Vallée, France*

**Abstract**

Stress-gradient materials are generalized continua with two generalized stress variables: the Cauchy stress field and its gradient. For homogenization purposes, we introduce an extension to stress-gradient materials of the principle of Hashin and Shtrikman. The variational principle is first stated within the framework of periodic homogenization, then extended to random homogenization. Contrary to the usual derivation of the classical principle, we adopt here a stress-based approach, much better suited to stress-gradient materials. We show that, in many cases of interest, the third-order trial eigenstrain may be discarded, leaving only one (second-order) trial eigenstrain in the functional to optimize. For $N$-phase material, the bounds are very similar in structure to their classical counterpart. One notable difference is the fact that, even in the case of isotropy, the bounds depend on some additionnal microstructural parameters (besides the usual volume fractions).

*Keywords:* Stress-gradient, Homogenization, Variational methods, Bounds

## 1. Introduction

The complementary elastic energy of stress-gradient materials depends on the stress *and* its gradient. This class of generalized materials was first introduced by Forest and Sab (2012) as an alternative to strain-gradient materials. Since then, other similar models have been proposed, which mostly differ by the boundary conditions; see e.g. Polizzotto (2018) and references therein. Such models are relevant for nanocomposites exhibiting "negative" size-effect (Tran et al., 2018) and foams (Hütter et al., 2020).

The model of Forest and Sab (2012) (including the boundary conditions) was fully justified mathematically by Sab et al. (2016). It was subsequently extended to finite strains by Forest and Sab (2017). Homogenization of heterogeneous, stress-gradient materials as homogeneous, Cauchy materials was then considered in the work by Tran et al. (2018), where a simplified stress-gradient model, akin to the simplified strain-gradient model of Altan and Aifantis (1992, 1997), was also proposed. The converse homogenization problem (Cauchy material at the microscale, stress-gradient material at the macroscale) has recently been addressed by Hütter et al. (2020), who offer a microscopic interpretation of the generalized strain that is work-conjugate to the gradient of the stresses.

The present paper builds upon the results obtained by Tran et al. (2018). More specifically, we propose a variational framework that allows the derivation of rigorous bounds on the macroscopic, classical stiffness of microscopically heterogeneous, stress-gradient materials, within the framework of both periodic and random homogenization. The variational principle that we introduce is an extension to stress-gradient materials of the celebrated principle of Hashin and Shtrikman (1962a). The classical version of this principle is usually presented within a strain-based approach, where *eigenstresses* are used as trial functions. A stress-based approach, where *eigenstrains* are used as trial functions, was found to be much better suited to stress-gradient materials and was therefore adopted. Both strain- and stress-based approaches are known to be equivalent in the classical case. For stress-gradient materials, we also verified this equivalence, since in early versions of the work presented here, we used a strain-based approach (Tran, 2016). Note that the variational principle of Hashin and Shtrikman was extended to strain-gradient materials by Smyshlyaev and Fleck (1994).

This paper is organized as follows. Sec. 2 provides an overview of the stress-gradient model of Forest and Sab (2012) and recalls how periodic, heterogenous stress-gradient materials can be homogenized as Cauchy materials through the so-called *corrector problem* (Tran et al., 2018). In the stress-based formulation of the principle of Hashin and Shtrikman (1962a), the trial function is an eigenstrain; we therefore discuss eigenstrained, stress-gradient materials in Sec. 3. For homogeneous materials, we then introduce in Sec. 4 the Delta operator that maps the eigenstrains to the stresses. This operator is the key ingredient of the Lippmann–Schwinger equation, which is introduced in Sec. 5 as an equivalent, alternative formulation of the corrector problem. Then, the principle of Hashin and Shtrikman (1962a) is stated in Sec. 6, first as the weak form of the Lippmann–Schwinger equation, then (under some conditions) as a variational principle.

These results, which are first introduced within the framework of periodic homogenization, are then extended to random

*Email addresses:* sebastien.brisard@univ-eiffel.fr (S. Brisard), karam.sab@enpc.fr (K. Sab)

homogenization.

In Sec. 7, we define the apparent and effective compliances of random composites. Then, in Sec. 8, we extend the principle of Hashin and Shtrikman (1962a) to the random case, and derive an operational formula for the resulting bounds on the effective compliance. This formula is simplified in Sec. 9, where it is shown that in some circumstances, it is possible to discard the third-order eigenstrain, the minimization problem being reduced to one trial field only. In Sec. 10, we specialize the general framework to $N$-phase materials with piece-wise constant trial eigenstrains; the resulting bounds are very close in spirit to the classical bounds of Hashin and Shtrikman (1962b). Finally, these bounds are evaluated numerically in Sec. 11 for a simple (boolean) microstructure.

## 2. Background

### 2.1. Nomenclature

The space of second-order, *symmetric* tensors is denoted $\mathcal{T}_2$; $\mathbf{I}_2 \in \mathcal{T}_2$ is the second-order identity tensor and $\mathbf{I}_4$ is the fourth-order identity tensor over $\mathcal{T}_2$

$$\mathbf{I}_2 = \delta_{ij}\mathbf{e}_i\otimes\mathbf{e}_j \quad \text{and} \quad \mathbf{I}_4 = \tfrac{1}{2}(\delta_{ip}\delta_{jq}+\delta_{iq}\delta_{jp})\mathbf{e}_i\otimes\mathbf{e}_j\otimes\mathbf{e}_p\otimes\mathbf{e}_q, \quad (1)$$

in cartesian coordinates. The double contraction ":" defines a scalar product over $\mathcal{T}_2$

$$\mathbf{a} : \mathbf{b} = a_{ij}x_{ij} \quad \text{for all } \mathbf{a}, \mathbf{b} \in \mathcal{T}_2. \quad (2)$$

It will be convenient to introduce the classical fourth-order spherical and deviatoric projection tensors $\mathbf{J}_4 = \frac{1}{3}\mathbf{I}_2 \otimes \mathbf{I}_2$ and $\mathbf{K}_4 = \mathbf{I}_4 - \mathbf{J}_4$, such that

$$\mathbf{J}_4 : \mathbf{K}_4 = \mathbf{K}_4 : \mathbf{J}_4 = \mathbf{0}, \quad \mathbf{J}_4 : \mathbf{J}_4 = \mathbf{J}_4 \quad \text{and} \quad \mathbf{K}_4 : \mathbf{K}_4 = \mathbf{K}_4. \quad (3)$$

The space of third-order tensors that are symmetric with respect to their first two indices is denoted $\mathcal{T}_3$: $\mathbf{T} \in \mathcal{T}_3$ iff $T_{ijk} = T_{jik}$. The triple contraction "$\therefore$" defines a scalar product over $\mathcal{T}_3$

$$\mathbf{a} \therefore \mathbf{b} = a_{ijk}b_{ijk} \quad \text{for all } \mathbf{a}, \mathbf{b} \in \mathcal{T}_3. \quad (4)$$

Note that for both double and triple contractions, we do not reverse the order of indices in the right-hand side.

The trace of a second-order tensor is classically defined as its double contraction with the second-order identity tensor $\mathbf{I}_2$. Likewise, we define in this paper the *trace of a third-order tensor* $\mathbf{T} \in \mathcal{T}_3$ as the *vector* $\mathbf{T} : \mathbf{I}_2$; in cartesian coordinates, this quantity coincides with $T_{ijj}\mathbf{e}_i$. A third-order tensor $\mathbf{T} \in \mathcal{T}_3$ is *trace-free* if its trace is null, $\mathbf{T} : \mathbf{I}_2 = \mathbf{0}$, and we introduce the space $\mathcal{T}_3'$ of third-order, trace-free tensors: $\mathbf{T} \in \mathcal{T}_3'$ iff $\mathbf{T} \in \mathcal{T}_3$ and $\mathbf{T} : \mathbf{I}_2 = \mathbf{0}$; in index form

$$\mathbf{T} \in \mathcal{T}_3' \quad \text{iff} \quad T_{ijk} = T_{jik} \quad \text{and} \quad T_{ijj} = 0. \quad (5)$$

Since $\mathcal{T}_3'$ is a subspace of $\mathcal{T}_3$, it is possible to define the orthogonal projection $\mathbf{I}_6'$ onto $\mathcal{T}_3'$: for all $\mathbf{T} \in \mathcal{T}_3$, $\mathbf{R} = \mathbf{I}_6' \therefore \mathbf{T} \in \mathcal{T}_3'$ with

$$\mathbf{R} : \mathbf{I}_2 = \mathbf{0} \quad \text{and} \quad \mathbf{R} \therefore (\mathbf{T} - \mathbf{R}) = (\mathbf{T} - \mathbf{R}) \therefore \mathbf{R} = 0, \quad (6)$$

orthogonality being here understood in the sense of the "$\therefore$" scalar product. The projection tensor $\mathbf{I}_6'$ is a sixth-order tensor which is fully defined by how it operates on third-order tensors $\mathbf{T} \in \mathcal{T}_3$ (Tran et al., 2018)

$$\mathbf{I}_6' \therefore \mathbf{T} = \mathbf{T} - \tfrac{1}{2}\mathbf{I}_4 \cdot \mathbf{T} : \mathbf{I}_2. \quad (7)$$

For isotropic, stress-gradient elasticity, it will be convenient to introduce the following sixth-order, isotropic tensors $\mathbf{J}_6'$ and $\mathbf{K}_6'$

$$\mathbf{J}_6' = \tfrac{2}{5}\mathbf{I}_6' \therefore (\mathbf{I}_2 \otimes \mathbf{e}_k \otimes \mathbf{I}_2 \otimes \mathbf{e}_k) \therefore \mathbf{I}_6' \quad \text{and} \quad \mathbf{K}_6' = \mathbf{I}_6' - \mathbf{J}_6', \quad (8)$$

with the simple multiplication rules (see also Tran et al., 2018)

$$\mathbf{J}_6' \therefore \mathbf{J}_6' = \mathbf{J}_6', \quad \mathbf{K}_6' \therefore \mathbf{K}_6' = \mathbf{K}_6' \quad (9a)$$

and

$$\mathbf{J}_6' \therefore \mathbf{K}_6' = \mathbf{K}_6' \therefore \mathbf{J}_6' = \mathbf{0}. \quad (9b)$$

The domain $\Omega \subset \mathbb{R}^3$ being fixed, $\mathcal{T}_2(\Omega)$ denotes the space of second-order, symmetric tensor fields defined over $\Omega$, with square-integrable components. The spaces of third-order tensor fields $\mathcal{T}_3(\Omega)$ and $\mathcal{T}_3'(\Omega)$ are defined similarly.

The gradient of a tensor field $\mathbf{T}$ is denoted $\mathbf{T} \otimes \nabla$; its divergence is denoted $\mathbf{T} \cdot \nabla$. In cartesian coordinates

$$\mathbf{T} \otimes \nabla = \partial_i\mathbf{T} \otimes \mathbf{e}_i \quad \text{and} \quad \mathbf{T} \cdot \nabla = \partial_i\mathbf{T} \cdot \mathbf{e}_i. \quad (10)$$

Note that in this paper, the nabla operator is applied *to the right* to recall that spatial derivation is operated with respect to the last index. This is important, since the theory of stress-gradient materials involves third-order tensors, which have by construction no symmetries with respect to the first and last indices. To conclude this section, it is observed that the divergence of a second-order tensor field $\boldsymbol{\sigma} \in \mathcal{T}_2(\Omega)$ appears as the trace of its gradient: $\boldsymbol{\sigma} \cdot \nabla = (\boldsymbol{\sigma} \otimes \nabla) : \mathbf{I}_2$.

### 2.2. An overview of stress-gradient materials

*Strain-gradient* materials were introduced by Mindlin (1964) as a class of generalized materials for which the elastic energy depends on the strain *and its gradient(s)*. Since their inception, they have grown in popularity (Askes and Aifantis, 2011). In principle, it is quite natural to introduce *stress-gradient* materials as materials whose complementary elastic energy depends on the stress and its first gradient. Quite surprisingly, this small theoretical leap was performed only recently by Forest and Sab (2012). This significant time-lapse is probably due to the misconception that strain- and stress-gradient materials where somehow equivalent, while it was shown by Tran et al. (2018) that these two classes of materials were in fact *complementary*.

We consider a stress-gradient body occupying the domain $\Omega \subset \mathbb{R}^3$ and subjected to body forces $\mathbf{b}$. The stresses $\boldsymbol{\sigma}$ are in equilibrium with $\mathbf{b}$ in the classical sense: $\boldsymbol{\sigma} \cdot \nabla + \mathbf{b} = \mathbf{0}$. It would be natural to postulate the complementary energy of the stress-gradient body as the following expression

$$W^c(\boldsymbol{\sigma}) = \int_{\mathbf{x}\in\Omega} w^c[\boldsymbol{\sigma}(\mathbf{x}), \boldsymbol{\sigma} \otimes \nabla(\mathbf{x})]\mathrm{d}V. \quad (11)$$

However, as was previously argued (Forest and Sab, 2012; Tran et al., 2018), the trace of the gradient of the stresses, $\boldsymbol{\sigma}\otimes\nabla$: $\mathbf{I}_2 = \boldsymbol{\sigma}\cdot\nabla = -\mathbf{b}$, is prescribed and plays the role of a prestress in Eq. (11). The physical meaning of this prestress is unclear and it was proposed, as a first step towards stress-gradient materials, to ommit this contribution. This suggests to adopt the following expression of the complementary elastic energy

$$W^{\mathrm{c}}(\boldsymbol{\sigma}) = \int_{\mathbf{x}\in\Omega} w^{\mathrm{c}}[\boldsymbol{\sigma}(\mathbf{x}), \mathbf{I}'_6 \therefore \boldsymbol{\sigma}\otimes\nabla(\mathbf{x})]\mathrm{d}V, \tag{12}$$

where $\mathbf{I}'_6$ is the orthogonal projection onto the space of trace-free tensors introduced in Sec. 2.1. In expression (12) which will be adopted below, only the trace-free part of the gradient of the stresses, which is not prescribed by equilibrium, is involved. The mechanical model resulting from assumption (12) was fully derived by Forest and Sab (2012) and mathematically justified by Sab et al. (2016). The most unusual consequence of the above modelling assumption is probably the fact that the *full* stress *tensor* (rather than the traction *vector*) is continuous at any point of a stress-gradient body; it is therefore in principle possible to prescribe the full stress tensor at the boundary of a stress-gradient body.

This paper is devoted to *linearly* elastic, stress-gradient materials, for which the volume density of complementary elastic energy $w^{\mathrm{c}}$ is given by the following expression

$$w^{\mathrm{c}}(\boldsymbol{\sigma}, \mathbf{R}) = \tfrac{1}{2}\boldsymbol{\sigma} : \mathbf{S} : \boldsymbol{\sigma} + \tfrac{1}{2}\mathbf{R} \therefore \mathbf{M} \therefore \mathbf{R}, \tag{13}$$

for all $\boldsymbol{\sigma} \in \mathcal{T}_2$ and $\mathbf{R} \in \mathcal{T}'_3$. The fourth-order tensor $\mathbf{S}$ is the classical compliance; it has both major and minor symmetries. The sixth-order tensor $\mathbf{M}$ is the generalized compliance; it has the following symmetries

$$M_{ijkpqr} = M_{pqrijk} = M_{jikpqr} = M_{ijkqpr}, \tag{14}$$

furthermore

$$\mathbf{I}'_6 \therefore \mathbf{M} = \mathbf{M} \therefore \mathbf{I}'_6 = \mathbf{M} \tag{15a}$$

and

$$\mathbf{M} \therefore (\mathbf{I}'_6 \therefore \boldsymbol{\sigma}\otimes\nabla) = \mathbf{M} \therefore \boldsymbol{\sigma}\otimes\nabla, \tag{15b}$$

since the complementary energy density $w^{\mathrm{c}}$ operates only on the trace-free part of the gradient of the stresses (Tran et al., 2018).

With these considerations in mind, it is possible to derive the equations that govern the equilibrium of a linearly elastic, stress-gradient material (Forest and Sab, 2012; Tran et al., 2018)

$$\boldsymbol{\sigma}\cdot\nabla + \mathbf{b} = \mathbf{0}, \tag{16a}$$
$$\mathbf{e} = \mathbf{S} : \boldsymbol{\sigma}, \tag{16b}$$
$$\boldsymbol{\phi} = \mathbf{M} \therefore (\boldsymbol{\sigma}\otimes\nabla), \tag{16c}$$
$$\mathbf{e} = \boldsymbol{\phi}\cdot\nabla + \mathbf{sym}(\mathbf{u}\otimes\nabla), \tag{16d}$$

where $\mathbf{e} \in \mathcal{T}_2(\Omega)$ and $\boldsymbol{\phi} \in \mathcal{T}'_3(\Omega)$ are the generalized strains that are energy-conjugate to the stress field $\boldsymbol{\sigma}$ and its gradient $\boldsymbol{\sigma}\otimes\nabla$, respectively. The vector field $\mathbf{u}$ has dimension of a classical displacement. For heterogeneous Cauchy materials that are homogenized as stress-gradient materials, Hütter et al. (2020) have recently shown that $\boldsymbol{\phi}$ can be interpreted as the trace-free part of the first moment of the microscopic strain-field.

The above field equations must be complemented with appropriate boundary conditions

$$\boldsymbol{\sigma}|_{\partial\Omega_\sigma} = \mathbf{0}, \tag{16e}$$
$$[\boldsymbol{\phi}\cdot\mathbf{n} + \mathbf{sym}(\mathbf{u}\otimes\mathbf{n})]|_{\partial\Omega_u} = \mathbf{0}, \tag{16f}$$

where $\partial\Omega_\sigma \cup \partial\Omega_u = \partial\Omega$ and $\partial\Omega_\sigma \cap \partial\Omega_u = \emptyset$. More general (mixed and non-homogeneous) boundary conditions are possible (Sab et al., 2016).

To close this section, we provide a brief discussion of linearly elastic, isotropic stress-gradient materials. Tran et al. (2018) proved that the compliance $\mathbf{S}$ and generalized compliance $\mathbf{M}$ are defined in general by five material parameters, namely: two elastic constants (e.g. shear modulus and Poisson ratio) and three material internal lengths. A simplified model with only one material internal length was then introduced by analogy with the simplified model of Altan and Aifantis (1992, 1997) for strain-gradient materials. For this simplified model, the volume density of complementary elastic energy reads

$$w^{\mathrm{c}}(\boldsymbol{\sigma}, \mathbf{R}) = \frac{1}{4\mu}\Big(\sigma_{ij}\sigma_{ij} - \frac{\nu}{1+\nu}\sigma_{ii}\sigma_{jj}\Big) + \frac{\ell^2}{4\mu}\Big(R_{ijk}R_{ijk} - \frac{\nu}{1+\nu}R_{iik}R_{jjk}\Big), \tag{17}$$

for all $\boldsymbol{\sigma} \in \mathcal{T}_2$ and $\mathbf{R} \in \mathcal{T}'_3$. In the above expression, $\mu$ and $\nu$ are the shear modulus and Poisson ratio, while $\ell$ is the sole material internal length. Identification with Eq. (13) delivers the following expressions of the compliance $\mathbf{S}$ and generalized compliance $\mathbf{M}$

$$\mathbf{S} = \frac{1}{2\mu}\Big(\mathbf{I}_4 - \frac{3\nu}{1+\nu}\mathbf{J}_4\Big), \tag{18a}$$
$$\mathbf{M} = \frac{\ell^2}{2\mu}\Big(\mathbf{I}'_6 - \frac{5}{2}\frac{\nu}{1+\nu}\mathbf{J}'_6\Big), \tag{18b}$$

where $\mathbf{J}_4$ and $\mathbf{J}'_6$ were defined in Sec. 2.1.

**Remark 1.** *Expressions (20) and (21) of the generalized compliance* $\mathbf{M}$ *and generalized stiffness* $\mathbf{L} = \mathbf{M}^{-1}$ *in the paper by Tran et al. (2018) are not correct and should be replaced with the following*

$$\mathbf{M} = \frac{\ell^2}{2\mu}\Big[\frac{2-3\nu}{2(1+\nu)}\mathbf{J}'_6 + \mathbf{K}'_6\Big], \tag{19a}$$
$$\mathbf{L} = \frac{2\mu}{\ell^2}\Big[\frac{2(1+\nu)}{2-3\nu}\mathbf{J}'_6 + \mathbf{K}'_6\Big], \tag{19b}$$

*where* $\mathbf{J}'_6$ *and* $\mathbf{K}'_6$ *were defined in Sec. 2.1.*

### 2.3. Periodic homogenization of heterogeneous, stress-gradient materials

Homogenization of stress-gradient materials was discussed by Tran et al. (2018). We only give a brief summary here, with a focus on periodic homogenization.

We consider a structure made of the periodic repetition of the brick-like unit-cell $\Omega = (0, L_1) \times (0, L_2) \times (0, L_3)$ with unequal sides $L_1 \neq L_2 \neq L_3$. The material at point $\mathbf{x} \in \Omega$ is a linearly elastic, stress-gradient material, with compliance $\mathbf{S}(\mathbf{x})$ and generalized compliance $\mathbf{M}(\mathbf{x})$. From the $\Omega$-periodicity of the structure, we have

$$\begin{cases} \mathbf{S}(\mathbf{x}+\mathbf{r}) = \mathbf{S}(\mathbf{x}) \\ \mathbf{M}(\mathbf{x}+\mathbf{r}) = \mathbf{M}(\mathbf{x}) \end{cases} \quad \text{with} \quad \mathbf{r} = \sum_{i=1}^{3} n_i L_i \mathbf{e}_i, \tag{20}$$

$n_1$, $n_2$ and $n_3$ being integers such that $\mathbf{x} \in \Omega$ and $\mathbf{x} + \mathbf{r} \in \Omega$.

It is assumed that *separation of scales* prevails. As discussed by Tran et al. (2018), this entails two conditions

1. $L_1, L_2, L_3 \ll L_\mathrm{M}$, where $L_\mathrm{M}$ denotes the macroscopic length-scale (typical span of the structure),
2. $\|\mathbf{M}\|/\|\mathbf{S}\| \ll L_1^2, L_2^2, L_3^2$ or $\|\mathbf{M}\|/\|\mathbf{S}\| \sim L_1^2, L_2^2, L_3^2$ for some tensor norms.

The first assumption is classical: it states that the heterogeneities are small compared to the characteristic length scale of the structure. The second assumption was discussed in (Tran et al., 2018) and is specific to stress-gradient materials: it states that all material internal lengths are at most of the same order as the heterogeneities.

Under these assumptions of separation of scales, the complex, heterogeneous, periodic microstructure can be replaced with an effective, homogeneous material through a homogenization process. More precisely, the effective material is expected to be linear elastic *in the classical sense* owing to the second assumption (Tran et al., 2018).

The elastic properties of the effective material can be retrieved from the solution to the following boundary-value problem over the unit-cell $\Omega$

$$\boldsymbol{\sigma} \cdot \nabla = \mathbf{0}, \tag{21a}$$
$$\mathbf{e} = \mathbf{S} : \boldsymbol{\sigma}, \tag{21b}$$
$$\boldsymbol{\phi} = \mathbf{M} \therefore (\boldsymbol{\sigma} \otimes \nabla), \tag{21c}$$
$$\mathbf{e} = \boldsymbol{\phi} \cdot \nabla + \mathbf{sym}(\mathbf{u} \otimes \nabla), \tag{21d}$$

which must be complemented with appropriate boundary conditions that ensure that the generalized Hill–Mandel lemma holds, namely $\langle \boldsymbol{\sigma} : \mathbf{e} + \mathbf{R} \therefore \boldsymbol{\phi} \rangle = \langle \boldsymbol{\sigma} \rangle : \langle \mathbf{e} \rangle$, where $\langle \bullet \rangle$ denotes the volume average over the statistical volume element (SVE) $\Omega$. Tran et al. (2018) have extended the classical static uniform, kinematic uniform and periodic boundary conditions. In the present paper, we make exclusive use of periodic boundary conditions

$$\boldsymbol{\sigma} \text{ and } \mathbf{u} - \bar{\mathbf{e}} \cdot \mathbf{x} \text{ are } \Omega\text{-periodic}, \tag{22a}$$
$$\boldsymbol{\phi} \cdot \mathbf{n} \text{ is } \Omega\text{-skew-periodic}, \tag{22b}$$

where $\bar{\mathbf{e}}$ denotes the (prescribed) macroscopic strain, $\bar{\mathbf{e}} = \langle \mathbf{e} \rangle$.

In the remainder of this paper, we will consistently use a stress-based approach, for which it is more natural to prescribe the macroscopic stress $\overline{\boldsymbol{\sigma}}$, rather than the macroscopic strain $\bar{\mathbf{e}}$. The above boundary conditions are therefore replaced with

$$\boldsymbol{\sigma} \text{ and } \mathbf{u} - \langle \mathbf{e} \rangle \cdot \mathbf{x} \text{ are } \Omega\text{-periodic}, \tag{23a}$$
$$\boldsymbol{\phi} \cdot \mathbf{n} \text{ is } \Omega\text{-skew-periodic}, \tag{23b}$$
$$\langle \boldsymbol{\sigma} \rangle = \overline{\boldsymbol{\sigma}}, \tag{23c}$$

where angle brackets $\langle \bullet \rangle$ denote volume averages over the unit-cell $\Omega$.

Owing to the linearity of problem (21)$\wedge$(23), the strain field $\mathbf{e}$ and its volume average $\langle \mathbf{e} \rangle$ depend linearly on the loading parameter $\overline{\boldsymbol{\sigma}}$. The effective compliance $\mathbf{S}^\mathrm{eff}$ is defined as the linear operator that maps the prescribed macroscopic stress $\overline{\boldsymbol{\sigma}}$ onto the macroscopic strain $\langle \mathbf{e} \rangle$

$$\langle \mathbf{e} \rangle = \mathbf{S}^\mathrm{eff} : \overline{\boldsymbol{\sigma}} = \mathbf{S}^\mathrm{eff} : \langle \boldsymbol{\sigma} \rangle. \tag{24}$$

Our goal in this paper is to derive a Hashin–Shtrikman-like variational principle for stress-gradient materials. In order to do so, we must transform problem (21) $\wedge$ (23), which is formulated on a heterogeneous material, into an equivalent problem, now formulated on a *homogeneous* material, where material heterogeneities are accounted for by means of appropriate "polarizations", which are eigenstresses/eigenstrains. While stress-polarizations (eigenstresses) are usually considered for classical materials, our experience shows that the derivations are substantially simpler with eigenstrains for stress-gradient materials. In the next section, we therefore discuss eigenstrained, stress-gradient materials and derive the associated complementary energy principle.

## 3. On eigenstrained stress-gradient materials

Deformation of stress-gradient materials is defined through two strain measures, namely: $\mathbf{e}$ and $\boldsymbol{\phi}$. It is therefore a priori possible to introduce *two* eigenstrains: the second-order eigenstrain $\mathbf{e}^* \in \mathcal{T}_2(\Omega)$ and the third-order eigenstrain $\boldsymbol{\phi}^* \in \mathcal{T}_3'(\Omega)$. In the present section, we first state the equilibrium of linearly elastic, eigenstrained, stress-gradient as a minimization problem. We then extend Clapeyron's theorem, that delivers the value of the complementary energy.

### 3.1. Minimum complementary energy principle

The following problem states the equilibrium of a linearly elastic, eigenstrained, stress-gradient body occupying the unit-cell $\Omega = (0, L_1) \times (0, L_2) \times (0, L_3)$

$$\boldsymbol{\sigma} \cdot \nabla = \mathbf{0}, \tag{25a}$$
$$\mathbf{e} = \mathbf{S} : \boldsymbol{\sigma} + \mathbf{e}^*, \tag{25b}$$
$$\boldsymbol{\phi} = \mathbf{M} \therefore (\boldsymbol{\sigma} \otimes \nabla) + \boldsymbol{\phi}^*, \tag{25c}$$
$$\mathbf{e} = \boldsymbol{\phi} \cdot \nabla + \mathbf{sym}(\mathbf{u} \otimes \nabla), \tag{25d}$$
$$\boldsymbol{\sigma} \text{ and } \mathbf{u} - \langle \mathbf{e} \rangle \cdot \mathbf{x} \text{ are } \Omega\text{-periodic}, \tag{25e}$$
$$\boldsymbol{\phi} \cdot \mathbf{n} \text{ is } \Omega\text{-skew-periodic}, \tag{25f}$$
$$\langle \boldsymbol{\sigma} \rangle = \overline{\boldsymbol{\sigma}}, \tag{25g}$$

where $\mathbf{e}^* \in \mathcal{T}_2(\Omega)$ and $\boldsymbol{\phi}^* \in \mathcal{T}_3'(\Omega)$ are second- and third-order tensor fields ("eigenstrains"), respectively; note that we require $\boldsymbol{\phi}^*$ to be trace-free (see Remark 2 below).

The minimum complementary energy principle can be stated as follows: the unique solution to Problem (25) minimizes the total complementary energy

$$\Pi^\mathrm{c}(\boldsymbol{\sigma}, \mathbf{e}^*, \boldsymbol{\phi}^*) = W^\mathrm{c}(\boldsymbol{\sigma}) - V^\mathrm{c}(\boldsymbol{\sigma}, \mathbf{e}^*, \boldsymbol{\phi}^*), \tag{26}$$

subject to $\boldsymbol{\sigma} \in \overline{\boldsymbol{\sigma}} + \mathcal{S}_0(\Omega)$, where

$$W^{\mathrm{c}}(\boldsymbol{\sigma}) = \tfrac{1}{2}\langle \boldsymbol{\sigma} : \mathbf{S} : \boldsymbol{\sigma} + (\boldsymbol{\sigma} \otimes \nabla) \therefore \mathbf{M} \therefore (\boldsymbol{\sigma} \otimes \nabla)\rangle, \tag{27a}$$

$$V^{\mathrm{c}}(\boldsymbol{\sigma}, \mathbf{e}^*, \boldsymbol{\phi}^*) = -\langle \boldsymbol{\sigma} : \mathbf{e}^* + (\boldsymbol{\sigma} \otimes \nabla) \therefore \boldsymbol{\phi}^* \rangle \tag{27b}$$

and $\mathcal{S}_0(\Omega)$ denotes the space of $\Omega$-periodic, divergence-free stress tensors with null average. It should be noted that, in line with our ultimate homogenization goal, $W^{\mathrm{c}}$, $V^{\mathrm{c}}$ and $\Pi^{\mathrm{c}}$ thus defined are rather volume densities of macroscopic energies, since each of these energies is divided by the volume of the body $\Omega$. The minimum principle stated above extends the classical complementary energy principle to eigenstrained stress-gradient materials; its proof can be found in Appendix A.

**Remark 2.** *Eqs.* (27a) *and* (27b) *show why* $\boldsymbol{\phi}^*$ *is required to be trace-free. Indeed, only the trace-free part of the gradient of the stresses carries elastic energy (Forest and Sab, 2012; Tran et al., 2018), as expressed by Eq.* (15)*. On the other hand, if* $\boldsymbol{\phi}^*$ *was* not *trace-free, then the* whole *gradient of the stresses (rather than its trace-free part only) would contribute to* $V^{\mathrm{c}}$*, which would be inconsistent.*

**Remark 3.** *Note that the same variational result holds if the periodic boundary conditions* (25e) $\wedge$ (25f) $\wedge$ (25g) *are replaced with stress-boundary conditions* $\boldsymbol{\sigma}|_{\partial\Omega} = \overline{\boldsymbol{\sigma}}$*. It is again emphasized that for stress-gradient materials, the* full *stress tensor* can *be prescribed at the boundary.*

### 3.2. Clapeyron's theorem

To close this section, we state the extension to eigenstrained, stress-gradient materials of Clapeyron's theorem, which gives an expression of the minimum complementary energy (see derivation in Appendix B)

$$\min_{\overline{\boldsymbol{\sigma}}+\mathcal{S}_0(\Omega)} \Pi^{\mathrm{c}}(\bullet, \mathbf{e}^*, \boldsymbol{\phi}^*) = \tfrac{1}{2}\overline{\boldsymbol{\sigma}}:\langle \mathbf{e}\rangle + \tfrac{1}{2}\langle \boldsymbol{\sigma}:\mathbf{e}^*\rangle + \tfrac{1}{2}\langle (\boldsymbol{\sigma}\otimes\nabla) \therefore \boldsymbol{\phi}^*\rangle, \tag{28}$$

where $\mathbf{e} = \mathbf{S} : \boldsymbol{\sigma} + \mathbf{e}^*$ and

$$\boldsymbol{\sigma} = \operatorname*{arg\,min}_{\overline{\boldsymbol{\sigma}}+\mathcal{S}_0(\Omega)} \Pi^{\mathrm{c}}(\bullet, \mathbf{e}^*, \boldsymbol{\phi}^*). \tag{29}$$

Note that in the above equations and in the remainder of this paper, "$\bullet$" is a placeholder that stands for the optimization variable. In other words, $\min_{\overline{\boldsymbol{\sigma}}+\mathcal{S}_0(\Omega)} \Pi^{\mathrm{c}}(\bullet, \mathbf{e}^*, \boldsymbol{\phi}^*)$ should be understood as $\min\{\Pi^{\mathrm{c}}(\boldsymbol{\sigma}', \mathbf{e}^*, \boldsymbol{\phi}^*), \boldsymbol{\sigma}' \in \overline{\boldsymbol{\sigma}} + \mathcal{S}_0(\Omega)\}$.

In particular, for $\mathbf{e}^* = \mathbf{0}$ and $\boldsymbol{\phi}^* = \mathbf{0}$, $V^{\mathrm{c}}$ vanishes, and we find that

$$\min_{\overline{\boldsymbol{\sigma}}+\mathcal{S}_0(\Omega)} W^{\mathrm{c}} = \min_{\overline{\boldsymbol{\sigma}}+\mathcal{S}_0(\Omega)} \Pi^{\mathrm{c}} = \tfrac{1}{2}\overline{\boldsymbol{\sigma}} : \langle \mathbf{e}\rangle = \tfrac{1}{2}\overline{\boldsymbol{\sigma}} : \mathbf{S}^{\mathrm{eff}} : \overline{\boldsymbol{\sigma}}, \tag{30}$$

which provides a vartiational definition of the effective compliance and extends a classical result of homogenization theory.

## 4. Homogeneous, eigenstrained materials – The Green operator

We now consider a *homogeneous* stress-gradient material with compliances $\mathbf{S}_0$ and $\mathbf{M}_0$, occupying the domain $\Omega = (0, L_1)\times(0, L_2) \times (0, L_3)$, subjected to second- and third-order eigenstrains only. In other words, we specialize Problem (25) to homogeneous materials

$$\boldsymbol{\sigma} \cdot \nabla = \mathbf{0}, \tag{31a}$$

$$\mathbf{e} = \mathbf{S}_0 : \boldsymbol{\sigma} + \mathbf{e}^* \tag{31b}$$

$$\boldsymbol{\phi} = \mathbf{M}_0 \therefore (\boldsymbol{\sigma} \otimes \nabla) + \boldsymbol{\phi}^*, \tag{31c}$$

$$\mathbf{e} = \boldsymbol{\phi} \cdot \nabla + \mathbf{sym}(\mathbf{u} \otimes \nabla), \tag{31d}$$

$$\boldsymbol{\sigma} \text{ and } \mathbf{u} - \langle \mathbf{e}\rangle \cdot \mathbf{x} \text{ are } \Omega\text{-periodic}, \tag{31e}$$

$$\boldsymbol{\phi} \cdot \mathbf{n} \text{ is } \Omega\text{-skew-periodic}, \tag{31f}$$

$$\langle \boldsymbol{\sigma}\rangle = \overline{\boldsymbol{\sigma}}. \tag{31g}$$

The solution to the above problem is unique, and depends linearly on the loading parameters, namely: $\overline{\boldsymbol{\sigma}}$, $\mathbf{e}^*$ and $\boldsymbol{\phi}^*$. This linear relationship is most conveniently expressed in Fourier space. Owing to the periodic boundary conditions, all mechanical fields are expanded in Fourier series

$$\begin{Bmatrix} \mathbf{u}(\mathbf{x}) - \langle \mathbf{e}\rangle \cdot \mathbf{x} \\ \boldsymbol{\phi}(\mathbf{x}) \\ \boldsymbol{\sigma}(\mathbf{x}) \\ \mathbf{e}^*(\mathbf{x}) \\ \boldsymbol{\phi}^*(\mathbf{x}) \end{Bmatrix} = \sum_{n\in\mathbb{Z}^3} \begin{Bmatrix} \hat{\mathbf{u}}_n \\ \hat{\boldsymbol{\phi}}_n \\ \hat{\boldsymbol{\sigma}}_n \\ \hat{\mathbf{e}}^*_n \\ \hat{\boldsymbol{\phi}}^*_n \end{Bmatrix} \mathrm{e}^{\mathrm{i}\mathbf{k}_n\cdot\mathbf{x}}, \tag{32}$$

with

$$\begin{Bmatrix} \hat{\mathbf{u}}_n \\ \hat{\boldsymbol{\phi}}_n \\ \hat{\boldsymbol{\sigma}}_n \\ \hat{\mathbf{e}}^*_n \\ \hat{\boldsymbol{\phi}}^*_n \end{Bmatrix} = \frac{1}{|\Omega|}\int_\Omega \begin{Bmatrix} \mathbf{u}(\mathbf{x}) - \langle \mathbf{e}\rangle \cdot \mathbf{x} \\ \boldsymbol{\phi}(\mathbf{x}) \\ \boldsymbol{\sigma}(\mathbf{x}) \\ \mathbf{e}^*(\mathbf{x}) \\ \boldsymbol{\phi}^*(\mathbf{x}) \end{Bmatrix} \mathrm{e}^{-\mathrm{i}\mathbf{k}_n\cdot\mathbf{x}} \mathrm{d}V \tag{33}$$

and

$$\mathbf{k}_n = \frac{2\pi n_1}{L_1}\mathbf{e}_1 + \frac{2\pi n_2}{L_2}\mathbf{e}_2 + \frac{2\pi n_3}{L_3}\mathbf{e}_3, \tag{34}$$

which allow to write Problem (31) in Fourier space [note that Eqs. (31e) and (31f) are automatically satisfied by the Fourier expansions (32)]

$$\hat{\boldsymbol{\sigma}}_n \cdot \mathbf{k}_n = \mathbf{0}, \tag{35a}$$

$$\hat{\mathbf{e}}_n = \mathbf{S}_0 : \hat{\boldsymbol{\sigma}}_n + \hat{\mathbf{e}}^*_n, \tag{35b}$$

$$\hat{\boldsymbol{\phi}}_n = \mathrm{i}\mathbf{M}_0 \therefore (\hat{\boldsymbol{\sigma}}_n \otimes \mathbf{k}_n) + \hat{\boldsymbol{\phi}}^*_n, \tag{35c}$$

$$\hat{\mathbf{e}}_n = \mathrm{i}\hat{\boldsymbol{\phi}}_n \cdot \mathbf{k}_n + \mathrm{i}\,\mathbf{sym}(\hat{\mathbf{u}}_n \otimes \mathbf{k}_n). \tag{35d}$$

Introducing the fourth order, frequency dependent tensor $\hat{\mathbf{S}}^\ell_0(\mathbf{k})$, with components

$$\hat{S}^{\ell}_{0,ijpq}(\mathbf{k}) = S_{0,ijpq} + M_{0,ijmpqn}k_m k_n \tag{36}$$

and plugging Eq. (35c) into Eq. (35d), we find that

$$\hat{\mathbf{e}}_n = -[\hat{\mathbf{S}}^\ell_0(\mathbf{k}_n) - \mathbf{S}_0] : \hat{\boldsymbol{\sigma}}_n + \mathrm{i}\,\mathbf{sym}(\hat{\mathbf{u}}_n \otimes \mathbf{k}_n) + \mathrm{i}\hat{\boldsymbol{\phi}}^*_n \cdot \mathbf{k}_n. \tag{37}$$

Substituting Eq. (36) in Eq. (35b), it is finally found that the Fourier coefficients $\hat{\boldsymbol{\sigma}}_n$ solve the following problem

$$\hat{\boldsymbol{\sigma}}_n \cdot \mathrm{i}\mathbf{k}_n = \mathbf{0}, \tag{38a}$$

$$\hat{\boldsymbol{\varepsilon}}_n = \hat{\mathbf{S}}^\ell_0 : \hat{\boldsymbol{\sigma}}_n + \hat{\mathbf{e}}^*_n - \mathrm{i}\hat{\boldsymbol{\phi}}^*_n \cdot \mathbf{k}_n, \tag{38b}$$

$$\hat{\boldsymbol{\varepsilon}}_n = \mathrm{i}\,\mathbf{sym}(\hat{\mathbf{u}}_n \otimes \mathbf{k}_n). \tag{38c}$$

It results from the above analysis that for fixed $n \in \mathbb{Z}^3$, the Fourier coefficient $\hat{\boldsymbol{\sigma}}_n$ depends linearly on the combination $\hat{\mathbf{e}}^*_n - \mathrm{i}\hat{\boldsymbol{\phi}}^*_n \cdot \mathbf{k}_n$ (same $n \in \mathbb{Z}^3$). We write formally

$$\hat{\boldsymbol{\sigma}}_n = -\hat{\boldsymbol{\Lambda}}_0(\mathbf{k}_n) : (\hat{\mathbf{e}}^*_n - \mathrm{i}\hat{\boldsymbol{\phi}}^*_n \cdot \mathbf{k}_n), \tag{39}$$

where, for any vector $\mathbf{k}$, $\hat{\boldsymbol{\Lambda}}_0(\mathbf{k})$ is a fourth order tensor with major and minor symmetries. It is fully derived in Appendix C.1. It should be noted that $\hat{\boldsymbol{\Lambda}}_0(\mathbf{0}) = \mathbf{0}$; from the condition (31g), we find that $\hat{\boldsymbol{\sigma}}_0 = \overline{\boldsymbol{\sigma}}$. Synthesis of the Fourier series expansion of $\boldsymbol{\sigma}$ finally leads to

$$\boldsymbol{\sigma}(\mathbf{x}) = \overline{\boldsymbol{\sigma}} - \sum_{n\in\mathbb{Z}^d} \hat{\boldsymbol{\Lambda}}_0(\mathbf{k}_n) : (\hat{\mathbf{e}}^*_n - \mathrm{i}\hat{\boldsymbol{\phi}}^*_n \cdot \mathbf{k}_n)\mathrm{e}^{\mathrm{i}\mathbf{k}_n\cdot\mathbf{x}}. \tag{40}$$

The above result suggests to introduce two operators, $\boldsymbol{\Delta}_0$ ant $\boldsymbol{\Lambda}_0$ that map second and third order tensors to second order tensors as follows

$$\boldsymbol{\Delta}_0(\mathbf{e}^*)(\mathbf{x}) = \sum_{n\in\mathbb{Z}^3} \hat{\boldsymbol{\Delta}}_0(\mathbf{k}_n) : \hat{\mathbf{e}}^*_n \tag{41a}$$

$$\boldsymbol{\Lambda}_0(\boldsymbol{\phi}^*)(\mathbf{x}) = \sum_{n\in\mathbb{Z}^3} -\mathrm{i}[\hat{\boldsymbol{\Delta}}_0(\mathbf{k}_n) \otimes \mathbf{k}_n] \therefore \hat{\boldsymbol{\phi}}^*_n. \tag{41b}$$

Note that these operators are *linear* with respect to the tensor fields $\mathbf{e}^*$ and $\boldsymbol{\phi}^*$, respectively; besides $\boldsymbol{\Delta}_0(\mathbf{e}^*)$ and $\boldsymbol{\Lambda}_0(\boldsymbol{\phi}^*)$ are both second-order tensor fields. Combining Eqs. (40) and (41), we express the solution to Problem (31) as follows

$$\boldsymbol{\sigma} = \overline{\boldsymbol{\sigma}} - \boldsymbol{\Delta}_0(\mathbf{e}^*) - \boldsymbol{\Lambda}_0(\boldsymbol{\phi}^*). \tag{42}$$

The above identity extends to stress-gradient materials the classical definition of the Delta operator (Korringa, 1973; Kröner, 1974; Zeller and Dederichs, 1973). It is recalled that the classical Delta operator is defined as the operator $\boldsymbol{\sigma} = -\boldsymbol{\Delta}^0_0(\mathbf{e}^*)$, where $\boldsymbol{\sigma}$ solves the following problem

$$\boldsymbol{\sigma} \cdot \nabla = \mathbf{0}, \tag{43a}$$
$$\boldsymbol{\varepsilon} = \mathbf{S}_0 : \boldsymbol{\sigma} + \mathbf{e}^*, \tag{43b}$$
$$\boldsymbol{\varepsilon} = \mathbf{sym}(\mathbf{u} \otimes \nabla), \tag{43c}$$
$$\mathbf{u} - \langle\mathbf{e}\rangle \cdot \mathbf{x} \text{ is } \Omega\text{-periodic}, \tag{43d}$$
$$\boldsymbol{\sigma} \cdot \mathbf{n} \text{ is } \Omega\text{-skew-periodic}, \tag{43e}$$
$$\langle\boldsymbol{\sigma}\rangle = \mathbf{0}. \tag{43f}$$

In particular, it is shown in Appendix C.3 that, for the simplified model of Tran et al. (2018) introduced in Sec. 2.2

$$\hat{\boldsymbol{\Lambda}}_0(\mathbf{k}) = (1 + k^2\ell_0^2)^{-1}\hat{\boldsymbol{\Lambda}}^0_0(\mathbf{k}), \tag{44}$$

where $\ell_0$ denotes the sole internal material length of the reference material. Note that this remarkable connection between classical and generalized Delta operators does not hold for the Gamma operator (that maps eigenstresses onto total strains), which largely explains why we adopted a stress-based approach in this work.

**Remark 4.** *In principle, Eq. (42) could also be written:* $\boldsymbol{\sigma} = \overline{\boldsymbol{\sigma}} - \boldsymbol{\Delta}_0(\mathbf{e}^* - \boldsymbol{\phi}^* \cdot \nabla)$*, since the expression* $\hat{\boldsymbol{\phi}}^*_n \cdot \mathrm{i}\mathbf{k}_n$ *that appears in Eq. (40) is the n-th Fourier coefficient of* $\boldsymbol{\phi}^* \cdot \nabla$*. However, we will refrain from using this compact expression, since* $\boldsymbol{\phi}^*$ *might not have sufficient regularity for* $\boldsymbol{\phi}^* \cdot \nabla$ *to be meaningful. Note that the* $k^2$ *in the denominator of Eq. (44) has a regularizing effect that ensures the convergence of the series in Eq. (40) even if* $\boldsymbol{\phi}^* \cdot \nabla$ *is not defined.*

The Delta operator enjoys the following elementary properties, the proof of which can be inferred from the work of Willis (2001) (for the classical Gamma operator)

1. As a result of the Hill–Mandel lemma, $\boldsymbol{\Delta}_0$ is self-adjoint: for all $\boldsymbol{\eta}_1, \boldsymbol{\eta}_2 \in \mathcal{T}_2(\Omega)$
$$\langle\boldsymbol{\eta}_1 : \boldsymbol{\Delta}_0(\boldsymbol{\eta}_2)\rangle = \langle\boldsymbol{\eta}_2 : \boldsymbol{\Delta}_0(\boldsymbol{\eta}_1)\rangle. \tag{45}$$
2. For all $\boldsymbol{\eta} \in \mathcal{T}_2(\Omega)$, $\langle\boldsymbol{\Delta}_0(\boldsymbol{\eta})\rangle = \mathbf{0}$ (by construction).
3. "Square" of the Delta-operator: for all $\boldsymbol{\eta} \in \mathcal{T}_2(\Omega)$,
$$\boldsymbol{\Delta}_0[\mathbf{S}_0 : \boldsymbol{\Delta}_0(\boldsymbol{\eta})] = \boldsymbol{\Delta}_0(\boldsymbol{\eta}). \tag{46}$$
4. If $\boldsymbol{\eta}$ is constant, then $\boldsymbol{\Delta}_0(\boldsymbol{\eta}) = \mathbf{0}$.

To close this section, we introduce the total complementary energy $\Pi^{\mathrm{c}}_0(\boldsymbol{\sigma}, \mathbf{e}^*, \boldsymbol{\phi}^*)$ of the homogeneous material. For constant compliance and generalized compliance, Eq. (28) reads

$$\begin{aligned}\min_{\overline{\boldsymbol{\sigma}}+\mathcal{S}_0(\Omega)} \Pi^{\mathrm{c}}_0(\bullet, \mathbf{e}^*, \boldsymbol{\phi}^*) &= \tfrac{1}{2}\overline{\boldsymbol{\sigma}} : \langle\mathbf{S}_0 : \boldsymbol{\sigma} + \mathbf{e}^*\rangle + \tfrac{1}{2}\langle\boldsymbol{\sigma} : \mathbf{e}^*\rangle \\ &\quad + \tfrac{1}{2}\langle(\boldsymbol{\sigma} \otimes \nabla) \therefore \boldsymbol{\phi}^*\rangle \\ &= \tfrac{1}{2}\overline{\boldsymbol{\sigma}} : \mathbf{S}_0 : \overline{\boldsymbol{\sigma}} + \overline{\boldsymbol{\sigma}} : \langle\mathbf{e}^*\rangle \\ &\quad + \tfrac{1}{2}\langle(\boldsymbol{\sigma} - \overline{\boldsymbol{\sigma}}) : \mathbf{e}^*\rangle \\ &\quad + \tfrac{1}{2}\langle(\boldsymbol{\sigma} \otimes \nabla) \therefore \boldsymbol{\phi}^*\rangle,\end{aligned} \tag{47}$$

where the stress-strain relationship (31b) has been used. The last two volume averages are evaluated in Fourier space. From Parseval's identity and expression (39) of the Fourier coefficient of $\boldsymbol{\sigma}$

$$\begin{aligned}\langle(\boldsymbol{\sigma} - \overline{\boldsymbol{\sigma}}) : \mathbf{e}^*\rangle &= \sum_{\substack{n\in\mathbb{Z}^3 \\ n\neq(0,0,0)}} \mathrm{conj}(\hat{\mathbf{e}}^*_n) : \hat{\boldsymbol{\sigma}}_n \\ &= -\sum_{n\in\mathbb{Z}^3} \mathrm{conj}(\hat{\mathbf{e}}^*_n) : \hat{\boldsymbol{\Lambda}}_0(\mathbf{k}_n) : \hat{\boldsymbol{\eta}}_n,\end{aligned} \tag{48}$$

where conj denotes the complex conjugate and

$$\hat{\boldsymbol{\eta}}_n = \hat{\mathbf{e}}^*_n - \mathrm{i}\hat{\boldsymbol{\phi}}^*_n \cdot \mathbf{k}_n. \tag{49}$$

Similarly,

$$\begin{aligned}\langle(\boldsymbol{\sigma} \otimes \nabla) \therefore \boldsymbol{\phi}^*\rangle &= \sum_{n\in\mathbb{Z}^3} \mathrm{conj}(\hat{\boldsymbol{\phi}}^*_n) \therefore (\hat{\boldsymbol{\sigma}}_n \otimes \mathrm{i}\mathbf{k}_n) \\ &= \sum_{n\in\mathbb{Z}^3} \mathrm{conj}(-\mathrm{i}\hat{\boldsymbol{\phi}}^*_n \cdot \mathbf{k}_n) : \hat{\boldsymbol{\sigma}}_n \\ &= -\sum_{n\in\mathbb{Z}^3} \mathrm{conj}(-\mathrm{i}\hat{\boldsymbol{\phi}}^*_n \cdot \mathbf{k}_n) : \hat{\boldsymbol{\Lambda}}_0(\mathbf{k}_n) : \hat{\boldsymbol{\eta}}_n.\end{aligned} \tag{50}$$

Gathering the above results, we find

$$\begin{aligned}\min_{\overline{\boldsymbol{\sigma}}+\mathcal{S}_0(\Omega)} \Pi^{\mathrm{c}}_0(\bullet, \mathbf{e}^*, \boldsymbol{\phi}^*) &= \tfrac{1}{2}\overline{\boldsymbol{\sigma}} : \mathbf{S}_0 : \overline{\boldsymbol{\sigma}} + \overline{\boldsymbol{\sigma}} : \langle\mathbf{e}^*\rangle \\ &\quad - \tfrac{1}{2}\sum_{n\in\mathbb{Z}^3} \mathrm{conj}(\hat{\boldsymbol{\eta}}_n) : \hat{\boldsymbol{\Lambda}}_0(\mathbf{k}_n) : \hat{\boldsymbol{\eta}}_n.\end{aligned} \tag{51}$$

In the previous section, we have introduced the Delta operator $\boldsymbol{\Delta}_0$. We have shown that this sole operator suffices to construct the solution to problems with both second- and third-order eigenstrains and general periodic boundary conditions, since the Lambda operator that is also needed is related to the Delta operator through Eq. (41b). This result can be used to extend the Lippmann–Schwinger equation (Korringa, 1973; Kröner, 1974; Zeller and Dederichs, 1973) to stress-gradient materials, as discussed in Sec. 5 below.

## 5. The Lippmann–Schwinger equation

In the present section, we derive an integral equation that is equivalent to Problem (21) $\wedge$ (23). This integral equation can be seen as an extension to stress-gradient materials of the classical Lippmann–Schwinger equation for linear elasticity (Korringa, 1973; Kröner, 1974; Zeller and Dederichs, 1973). We first rewrite Problem (21) $\wedge$ (23) as follows

$$\boldsymbol{\sigma} \cdot \nabla = \mathbf{0}, \tag{52a}$$
$$\mathbf{e} = \mathbf{S}_0 : \boldsymbol{\sigma} + \mathbf{e}^*, \tag{52b}$$
$$\boldsymbol{\phi} = \mathbf{M}_0 \therefore (\boldsymbol{\sigma} \otimes \nabla) + \boldsymbol{\phi}^*, \tag{52c}$$
$$\mathbf{e} = \boldsymbol{\phi} \cdot \nabla + \mathbf{sym}(\mathbf{u} \otimes \nabla), \tag{52d}$$
$$\boldsymbol{\sigma} \text{ and } \mathbf{u} - \langle \mathbf{e} \rangle \cdot \mathbf{x} \text{ are } \Omega\text{-periodic}, \tag{52e}$$
$$\boldsymbol{\phi} \cdot \mathbf{n} \text{ is } \Omega\text{-skew-periodic}, \tag{52f}$$
$$\langle \boldsymbol{\sigma} \rangle = \overline{\boldsymbol{\sigma}}, \tag{52g}$$
$$\mathbf{e}^* = (\mathbf{S} - \mathbf{S}_0) : \boldsymbol{\sigma}, \tag{52h}$$
$$\boldsymbol{\phi}^* = (\mathbf{M} - \mathbf{M}_0) \therefore (\boldsymbol{\sigma} \otimes \nabla), \tag{52i}$$

where we have introduced two new unknowns ($\mathbf{e}^*$ and $\boldsymbol{\phi}^*$), as well as two supplementary equations, namely: Eqs. (52h) and (52i). As shown in Sec. 4, Eqs. (52a) to (52g) lead to Eq. (42). In other words, the stress field $\boldsymbol{\sigma}$ that solves Problem (21) $\wedge$ (23) is fully defined by

$$\boldsymbol{\sigma} = \overline{\boldsymbol{\sigma}} - \boldsymbol{\Delta}_0(\mathbf{e}^*) - \boldsymbol{\Lambda}_0(\boldsymbol{\phi}^*), \tag{53a}$$
$$\mathbf{e}^* = (\mathbf{S} - \mathbf{S}_0) : \boldsymbol{\sigma}, \tag{53b}$$
$$\boldsymbol{\phi}^* = (\mathbf{M} - \mathbf{M}_0) \therefore (\boldsymbol{\sigma} \otimes \nabla), \tag{53c}$$

and, eliminating $\mathbf{e}^*$ and $\boldsymbol{\phi}^*$, we find the integral equation

$$\boldsymbol{\sigma} + \boldsymbol{\Delta}_0[(\mathbf{S} - \mathbf{S}_0) : \boldsymbol{\sigma}] + \boldsymbol{\Lambda}_0[(\mathbf{M} - \mathbf{M}_0) \therefore (\boldsymbol{\sigma} \otimes \nabla)] = \overline{\boldsymbol{\sigma}}. \tag{54}$$

The classical Lippmann–Schwinger equation is retrieved when $\mathbf{M} = \mathbf{M}_0 = \mathbf{0}$.

**Remark 5.** *In order to apply Eq. (42), we must check that $\boldsymbol{\phi}^*$ defined by (52i) is indeed trace-free, or, equivalently, that $\mathbf{I}_6' \therefore \boldsymbol{\phi}^* = \boldsymbol{\phi}^*$. This is readily verified, since $\mathbf{I}_6' \therefore \mathbf{M} = \mathbf{M}$ and $\mathbf{I}_6' \therefore \mathbf{M}_0 = \mathbf{M}_0$.*

We are now ready to state the principle of Hashin and Shtrikman (1962a), extended to stress-gradient materials. The proof of this principle can be found in Appendix D; it follows closely that of Willis (1977, 1991).

## 6. The principle of Hashin and Shtrikman

We consider again the setting introduced in Sec. 2.3 for periodic homogenization. We further introduce a homogeneous, reference stress-gradient material with compliance $\mathbf{S}_0$ and generalized compliance $\mathbf{M}_0$ and eliminate the stresses $\boldsymbol{\sigma}$ in Problem (53)

$$(\mathbf{S} - \mathbf{S}_0)^{-1} : \mathbf{e}^* + \boldsymbol{\Delta}_0(\mathbf{e}^*) + \boldsymbol{\Lambda}_0(\boldsymbol{\phi}^*) = \overline{\boldsymbol{\sigma}}, \tag{55a}$$
$$(\mathbf{M} - \mathbf{M}_0)^{-1} \therefore \boldsymbol{\phi}^* + [\boldsymbol{\Delta}_0(\mathbf{e}^*) + \boldsymbol{\Lambda}_0(\boldsymbol{\phi}^*)] \otimes \nabla = \mathbf{0}. \tag{55b}$$

Then, multiplying with the test functions $\delta\mathbf{e}^*$ and $\delta\boldsymbol{\phi}^*$ and averaging over the unit-cell $\Omega$ delivers the following weak form of the Lippmann–Schwinger equation

$$\begin{aligned}\langle \overline{\boldsymbol{\sigma}} : \delta\mathbf{e}^* \rangle = {} & \langle \mathbf{e}^* : (\mathbf{S} - \mathbf{S}_0)^{-1} : \delta\mathbf{e}^* \rangle \\ & + \langle \boldsymbol{\phi}^* \therefore (\mathbf{M} - \mathbf{M}_0)^{-1} \therefore \delta\boldsymbol{\phi}^* \rangle \\ & + \langle [\boldsymbol{\Delta}_0(\mathbf{e}^*) + \boldsymbol{\Lambda}_0(\boldsymbol{\phi}^*)] : \delta\mathbf{e}^* \rangle \\ & + \langle \{[\boldsymbol{\Delta}_0(\mathbf{e}^*) + \boldsymbol{\Lambda}_0(\boldsymbol{\phi}^*)] \otimes \nabla\} \therefore \delta\boldsymbol{\phi}^* \rangle,\end{aligned} \tag{56}$$

for all $\delta\mathbf{e}^* \in \mathcal{T}_2(\Omega)$ and $\delta\boldsymbol{\phi}^* \in \mathcal{T}_3'(\Omega)$. Again, the last two terms are expressed in Fourier space by means of Parseval's identity (see Sec. 4)

$$\begin{aligned}\langle \overline{\boldsymbol{\sigma}} : \delta\mathbf{e}^* \rangle = {} & \langle \mathbf{e}^* : (\mathbf{S} - \mathbf{S}_0)^{-1} : \delta\mathbf{e}^* \rangle \\ & + \langle \boldsymbol{\phi}^* \therefore (\mathbf{M} - \mathbf{M}_0)^{-1} \therefore \delta\boldsymbol{\phi}^* \rangle \\ & + \sum_{n \in \mathbb{Z}^3} \mathrm{conj}(\hat{\boldsymbol{\eta}}_n) : \hat{\boldsymbol{\Delta}}_0(\mathbf{k}_n) : \delta\hat{\boldsymbol{\eta}}_n,\end{aligned} \tag{57}$$

for all $\delta\mathbf{e}^* \in \mathcal{T}_2(\Omega)$ and $\delta\boldsymbol{\phi}^* \in \mathcal{T}_3'(\Omega)$. In the above variational equation, $\hat{\boldsymbol{\eta}}_n$ is defined by Eq. (49) and

$$\delta\hat{\boldsymbol{\eta}}_n = \delta\hat{\mathbf{e}}_n^* - \mathrm{i}\delta\hat{\boldsymbol{\phi}}_n^* \cdot \mathbf{k}_n. \tag{58}$$

Eq. (57) suggests to introduce the functional of Hashin and Shtrikman, HS, defined for all so-called trial *strain-polarizations* $\mathbf{e}^* \in \mathcal{T}_2(\Omega)$ and $\boldsymbol{\phi}^* \in \mathcal{T}_3'(\Omega)$ as follows

$$\begin{aligned}\mathrm{HS}(\mathbf{e}^*, \boldsymbol{\phi}^*, \overline{\boldsymbol{\sigma}}) = {} & \tfrac{1}{2}\overline{\boldsymbol{\sigma}} : \mathbf{S}_0 : \overline{\boldsymbol{\sigma}} + \overline{\boldsymbol{\sigma}} : \langle \mathbf{e}^* \rangle \\ & - \tfrac{1}{2}\langle \mathbf{e}^* : (\mathbf{S} - \mathbf{S}_0)^{-1} : \mathbf{e}^* \rangle \\ & - \tfrac{1}{2}\langle \boldsymbol{\phi}^* \therefore (\mathbf{M} - \mathbf{M}_0)^{-1} \therefore \boldsymbol{\phi}^* \rangle \\ & - \tfrac{1}{2}\sum_{n \in \mathbb{Z}^3} \mathrm{conj}(\hat{\boldsymbol{\eta}}_n) : \hat{\boldsymbol{\Delta}}_0(\mathbf{k}_n) : \hat{\boldsymbol{\eta}}_n\end{aligned} \tag{59}$$

and it results from Eq. (57) that HS is stationary. This is the stationarity principle of Hashin and Shtrikman that will be stated below. We first note that Eq. (51) leads to the following alternative expression of HS

$$\begin{aligned}\mathrm{HS}(\mathbf{e}^*, \boldsymbol{\phi}^*, \overline{\boldsymbol{\sigma}}) = {} & \min_{\overline{\boldsymbol{\sigma}} + \mathcal{S}_0(\Omega)} \Pi_0^{\mathrm{c}}(\bullet, \mathbf{e}^*, \boldsymbol{\phi}^*) \\ & - \tfrac{1}{2}\langle \mathbf{e}^* : (\mathbf{S} - \mathbf{S}_0)^{-1} : \mathbf{e}^* \rangle \\ & - \tfrac{1}{2}\langle \boldsymbol{\phi}^* \therefore (\mathbf{M} - \mathbf{M}_0)^{-1} \therefore \boldsymbol{\phi}^* \rangle.\end{aligned} \tag{60}$$

*Critical point of the functional of Hashin and Shtrikman.* The functional of Hashin and Shtrikman has a unique critical point $\mathbf{e}^*_{\text{crit}}, \boldsymbol{\phi}^*_{\text{crit}}$ defined by

$$\mathbf{e}^*_{\text{crit}} = (\mathbf{S} - \mathbf{S}_0) : \boldsymbol{\sigma} \quad \text{and} \quad \boldsymbol{\phi}^*_{\text{crit}} = (\mathbf{M} - \mathbf{M}_0) : (\boldsymbol{\sigma} \otimes \nabla), \tag{61}$$

where $\boldsymbol{\sigma}$ is the solution to Problem (21). At this point, the value of the Hashin–Shtrikman functional is

$$\text{HS}(\mathbf{e}^*_{\text{crit}}, \boldsymbol{\phi}^*_{\text{crit}}, \overline{\boldsymbol{\sigma}}) = \tfrac{1}{2}\overline{\boldsymbol{\sigma}} : \mathbf{S}^{\text{eff}} : \overline{\boldsymbol{\sigma}}, \tag{62}$$

see proof in Appendix D.1.

The above *stationarity* principle can be complemented with an *extremum* principle, provided that the reference material is less compliant or more compliant than all constituants of the composite. This is discussed below.

*Maximum of the functional of Hashin and Shtrikman.* If $\mathbf{S} \geq \mathbf{S}_0$ and $\mathbf{M} \geq \mathbf{M}_0$ in the sense of quadratic forms[1], then the critical point of the functional of Hashin and Shtrikman is a *maximum*: for all $\mathbf{e}^* \in \mathcal{T}_2(\Omega)$ and $\boldsymbol{\phi}^* \in \mathcal{T}'_3(\Omega)$

$$\tfrac{1}{2}\overline{\boldsymbol{\sigma}} : \mathbf{S}^{\text{eff}} : \overline{\boldsymbol{\sigma}} \geq \text{HS}(\mathbf{e}^*, \boldsymbol{\phi}^*, \overline{\boldsymbol{\sigma}}). \tag{63}$$

(The proof of this result is given in Appendix D.2).

*Minimum of the functional of Hashin and Shtrikman.* Conversely, if $\mathbf{S} \leq \mathbf{S}_0$ and $\mathbf{M} \leq \mathbf{M}_0$ in the sense of quadratic forms, then the critical point of the functional of Hashin and Shtrikman is a *minimum*: for all $\mathbf{e}^* \in \mathcal{T}_2(\Omega)$ and $\boldsymbol{\phi}^* \in \mathcal{T}'_3(\Omega)$

$$\tfrac{1}{2}\overline{\boldsymbol{\sigma}} : \mathbf{S}^{\text{eff}} : \overline{\boldsymbol{\sigma}} \leq \text{HS}(\mathbf{e}^*, \boldsymbol{\phi}^*, \overline{\boldsymbol{\sigma}}). \tag{64}$$

(The proof of this result is given in Appendix D.3).

The variational principle stated in the previous section allows the derivation of rigorous bounds on the effective compliance within the framework of *periodic* homogenization. In the remainder of this paper, we extend this result to *random* homogenization. To do so, we take implicitly advantage of the formal analogy between periodic and statistically homogeneous, ergodic, media that was first put forward by Sab (1994).

## 7. Apparent and effective compliances of random composites

In the present section we show how the effective compliance of a random heterogeneous, stress-gradient material can be derived. Most symbols defined previously keep the same meaning, except that now, the microstructure is no longer *periodic*, but *random*: the heterogeneous properties of the composite $\mathbf{S}(\mathbf{x}, \omega)$ and $\mathbf{M}(\mathbf{x}, \omega)$ are random variables, indexed by the realization $\omega$ (which fills the whole space $\mathbb{R}^3$). We emphasize that Eq. (20) no longer holds. Separation of scales in the sense of Sec. 2.3 does hold: the sides $L_i$ of the unit-cell $\boldsymbol{\Omega}$ should be replaced with the typical size $L$ of the structure.

Determination of the effective properties of a random heterogeneous material in theory requires the solution to a corrector problem defined over the whole space $\mathbb{R}^3$, which is highly unpractical. It is however known in classical (cauchy) elasticity that solving the corrector problem with *periodic boundary conditions* on a large (but finite) microstructure to obtain a satisfactory estimate of the effective properties. This is also true for stress-gradient elasticity (Tran et al., 2018).

More precisely, let us define the *apparent* compliance. To do so, we consider a fixed, cubic, unit-cell $\Omega = (0, L)^3 \subset \mathbb{R}^3$. The restriction to $\Omega$ of any realization of the random heterogeneous material under consideration will be called a statistical volume element (SVE) (Ostoja-Starzewski, 2006). For each of these SVEs, we can solve Problem (21) $\wedge$ (23) (same corrector problem as before). The solution is now indexed by $\omega$ (the realization) and depends on $L$ (the size of the SVE). Owing to the linearity of this problem, the strain field $\mathbf{e}$ and its volume average $\langle \mathbf{e} \rangle$ depend linearly on the loading parameter $\overline{\boldsymbol{\sigma}}$. The apparent compliance $\mathbf{S}^{\text{app}}(L, \omega)$ of the SVE $\Omega$ is defined as the linear operator that maps the prescribed macroscopic stress $\overline{\boldsymbol{\sigma}}$ onto the macroscopic strain $\langle \mathbf{e} \rangle$

$$\langle \mathbf{e} \rangle = \mathbf{S}^{\text{app}}(L, \omega) : \overline{\boldsymbol{\sigma}} = \mathbf{S}^{\text{app}}(L, \omega) : \langle \boldsymbol{\sigma} \rangle, \tag{65}$$

(note the similarity with Eq. (24) that defines the *effective* compliance of a periodic microstructure). It is emphasized that $\mathbf{S}^{\text{app}}$ is a random variable that depends on the realization (the SVE). Under the assumption of statistical homogeneity and ergodicity of the microstructure, the apparent compliance converges to the effective compliance as the size of the SVE $\Omega$ tends to infinity: $\mathbf{S}^{\text{eff}} = \lim_{L \to +\infty} \mathbf{S}^{\text{app}}(L, \omega)$.

Although not necessary (owing to ergodicity), it is often convenient to take in the previous limit the ensemble average $\mathbb{E}[\bullet]$ over all realizations, prior to letting the domain grow to infinity: $\mathbf{S}^{\text{eff}} = \lim_{L \to +\infty} \mathbb{E}_\omega[\mathbf{S}^{\text{app}}(L, \omega)]$.

## 8. The principle of Hashin and Shtrikman for random homogenization

We are now in a position to extend the variational principle of Hashin and Shtrikman presented in Sec. 6 to random homogenization. We can first write this principle realization-by-realization, for a fixed-size SVE:

$$\tfrac{1}{2}\overline{\boldsymbol{\sigma}} : \mathbf{S}^{\text{app}}(L, \omega) : \overline{\boldsymbol{\sigma}} \overset{\geq}{\leq} \text{HS}(\mathbf{e}^*, \boldsymbol{\phi}^*, \overline{\boldsymbol{\sigma}}, L, \omega), \tag{66}$$

subjected to

$$\mathbf{S} \overset{\geq}{\leq} \mathbf{S}_0 \quad \text{and} \quad \mathbf{M} \overset{\geq}{\leq} \mathbf{M}_0. \tag{67}$$

In the above equation, $\text{HS}(\bullet, \bullet, \overline{\boldsymbol{\sigma}}, L, \omega)$ denotes the value of the functional of Hashin and Shtrikman [see Eq. (59)], evaluated for the realization $\omega$, on a unit-cell of size $L$. It is observed that the *critical* strain polarizations $\mathbf{e}^*_{\text{crit}}$ and $\boldsymbol{\phi}^*_{\text{crit}}$ are now

[1] $\boldsymbol{\sigma} : (\mathbf{S} - \mathbf{S}_0) : \boldsymbol{\sigma} \geq 0$ and $\mathbf{R} \therefore (\mathbf{M} - \mathbf{M}_0) : \mathbf{R} \geq \mathbf{0}$ for all second-order, symmetric tensor $\boldsymbol{\sigma} \in \mathcal{T}_2$ and third-order, trace-free tensor $\mathbf{R} \in \mathcal{T}'_3$.

also size-dependent, random fields. We will therefore use random fields as *trial* strain-polarizations. More precisely, we consider $\mathbf{e}^*(\mathbf{x},\omega)$ and $\boldsymbol{\phi}^*(\mathbf{x},\omega)$ two random fields, defined over the whole space $\mathbb{R}^3$ (of course, only their restriction to the unit-cell $\Omega$ will be used to compute the functional of Hashin and Shtrikman). We assume that both fields are statistically homogeneous (their ensemble averages and cross-correlations are translation invariant) and ergodic. We introduce for further use the cross-correlations

$$\mathbf{R}_{ee}(\mathbf{r}) = \mathbb{E}[\mathbf{e}^*(\mathbf{x})\otimes\mathbf{e}^*(\mathbf{x}+\mathbf{r})] - \mathbb{E}[\mathbf{e}^*]\otimes\mathbb{E}[\mathbf{e}^*], \tag{68a}$$

$$\mathbf{R}_{\phi\phi}(\mathbf{r}) = \mathbb{E}[\boldsymbol{\phi}^*(\mathbf{x})\otimes\boldsymbol{\phi}^*(\mathbf{x}+\mathbf{r})] - \mathbb{E}[\boldsymbol{\phi}^*]\otimes\mathbb{E}[\boldsymbol{\phi}^*], \tag{68b}$$

$$\mathbf{R}_{e\phi}(\mathbf{r}) = \mathbb{E}[\mathbf{e}^*(\mathbf{x})\otimes\boldsymbol{\phi}^*(\mathbf{x}+\mathbf{r})] - \mathbb{E}[\mathbf{e}^*]\otimes\mathbb{E}[\boldsymbol{\phi}^*], \tag{68c}$$

which not depend on the observation point $\mathbf{x}\in\Omega$ owing to statistical homogeneity.

Then, the right-hand side of Eq. (66) owes its randomness to the randomness of the microstructure *and* the trial strain-polarizations. We can take in this inequality the ensemble average over all SVEs, which delivers the following bound

$$\tfrac{1}{2}\overline{\boldsymbol{\sigma}} : \mathbb{E}[\mathbf{S}^{\text{app}}(L)] : \overline{\boldsymbol{\sigma}} \overset{\geq}{\leq} \mathbb{E}_\omega[\text{HS}(\mathbf{e}^*,\boldsymbol{\phi}^*,\overline{\boldsymbol{\sigma}},L,\omega)], \tag{69}$$

the size $L$ of the SVE being fixed. Finally, taking the limit when $L\to+\infty$ delivers a bound on the effective compliance

$$\tfrac{1}{2}\overline{\boldsymbol{\sigma}} : \mathbf{S}^{\text{eff}} : \overline{\boldsymbol{\sigma}} \overset{\geq}{\leq} \text{HS}^\infty(\mathbf{e}^*,\boldsymbol{\phi}^*,\overline{\boldsymbol{\sigma}}), \tag{70}$$

where we have introduced the following functional

$$\text{HS}^\infty(\mathbf{e}^*,\boldsymbol{\phi}^*,\overline{\boldsymbol{\sigma}}) = \lim_{L\to+\infty} \mathbb{E}_\omega[\text{HS}(\mathbf{e}^*,\boldsymbol{\phi}^*,\overline{\boldsymbol{\sigma}},L,\omega)], \tag{71}$$

which is evaluated in Appendix E using a technique similar to the work of Sab and Nedjar (2005). In this appendix, it is shown that

$$\begin{aligned}
\text{HS}^\infty(\mathbf{e}^*,\boldsymbol{\phi}^*,\overline{\boldsymbol{\sigma}}) = {} & \tfrac{1}{2}\overline{\boldsymbol{\sigma}} : \mathbf{S}_0 : \overline{\boldsymbol{\sigma}} + \overline{\boldsymbol{\sigma}} : \mathbb{E}[\mathbf{e}^*] \\
& - \tfrac{1}{2}\,\mathbb{E}[\mathbf{e}^* : (\mathbf{S}-\mathbf{S}_0)^{-1} : \mathbf{e}^*] \\
& - \tfrac{1}{2}\,\mathbb{E}[\boldsymbol{\phi}^* \therefore (\mathbf{M}-\mathbf{M}_0)^{-1} \therefore \boldsymbol{\phi}^*] \\
& - \tfrac{1}{2}(2\pi)^{-3}\int_{\mathbf{k}\in\mathbb{R}^3} \hat{\boldsymbol{\Delta}}_0(\mathbf{k}) \odot \hat{\mathbf{R}}_{ee}(\mathbf{k})\,\mathrm{d}^3\mathbf{k} \\
& - \tfrac{1}{2}(2\pi)^{-3}\int_{\mathbf{k}\in\mathbb{R}^3} \hat{\boldsymbol{\Delta}}''_0(\mathbf{k}) \odot \hat{\mathbf{R}}_{\phi\phi}(\mathbf{k})\,\mathrm{d}^3\mathbf{k} \\
& - (2\pi)^{-3}\int_{\mathbf{k}\in\mathbb{R}^3} [\hat{\boldsymbol{\Delta}}_0(\mathbf{k})\otimes\mathbf{k}] \odot \Im[\hat{\mathbf{R}}_{e\phi}(\mathbf{k})]\mathrm{d}^3\mathbf{k},
\end{aligned} \tag{72}$$

where "$\odot$" denotes the total contraction, $\hat{\mathbf{R}}_{ee}$, $\hat{\mathbf{R}}_{\phi\phi}$ and $\hat{\mathbf{R}}_{e\phi}$ are the (continuous) Fourier transforms of the cross-correlations

$$\begin{Bmatrix} \hat{\mathbf{R}}_{ee}(\mathbf{k}) \\ \hat{\mathbf{R}}_{\phi\phi}(\mathbf{k}) \\ \hat{\mathbf{R}}_{e\phi}(\mathbf{k}) \end{Bmatrix} = \int_{\mathbf{r}\in\mathbb{R}^3} \begin{Bmatrix} \mathbf{R}_{ee}(\mathbf{r}) \\ \mathbf{R}_{\phi\phi}(\mathbf{r}) \\ \mathbf{R}_{e\phi}(\mathbf{r}) \end{Bmatrix} \mathrm{e}^{-\mathrm{i}\mathbf{k}\cdot\mathbf{r}}\mathrm{d}^3\mathbf{r}, \tag{73}$$

and the components of $\hat{\boldsymbol{\Delta}}''_0$ are defined as follows

$$\hat{\Delta}''_{0,ijpmnq}(\mathbf{k}) = \hat{\Delta}_{0,ijmn}(\mathbf{k})k_p k_q. \tag{74}$$

In the previous section, we have shown that bounds on the effective compliance of random, heterogeneous, stress-gradient materials can be produced by means of statistically homogeneous and ergodic trial-strain fields $\mathbf{e}^*$ and $\boldsymbol{\phi}^*$. The bounds are given by Eqs. (70) and (72). In the next section, we show that, under very mild assumptions, these bounds can be significantly simplified.

## 9. Simplifications of the bounds

We assume in this section that $\mathbf{R}_{e\phi}(-\mathbf{r}) = \mathbf{R}_{e\phi}(\mathbf{r})$. At this point, this assumption should be seen as purely mathematical; it will be shown in Sec. 10 that, for $N$-phase, isotropic materials and strain polarizations that are constant in each phase, this assumption holds. Under this assumption, $\hat{\mathbf{R}}_{e\phi}$ is *real* and the last term in Eq. (72) vanishes

$$\begin{aligned}
\text{HS}^\infty(\mathbf{e}^*,\boldsymbol{\phi}^*,\overline{\boldsymbol{\sigma}}) = {} & \tfrac{1}{2}\overline{\boldsymbol{\sigma}} : \mathbf{S}_0 : \overline{\boldsymbol{\sigma}} + \overline{\boldsymbol{\sigma}} : \mathbb{E}[\mathbf{e}^*] \\
& - \tfrac{1}{2}\,\mathbb{E}[\mathbf{e}^* : (\mathbf{S}-\mathbf{S}_0)^{-1} : \mathbf{e}^*] \\
& - \tfrac{1}{2}\,\mathbb{E}[\boldsymbol{\phi}^* \therefore (\mathbf{M}-\mathbf{M}_0)^{-1} \therefore \boldsymbol{\phi}^*] \\
& - \tfrac{1}{2}(2\pi)^{-3}\int_{\mathbf{k}\in\mathbb{R}^3} \hat{\boldsymbol{\Delta}}_0(\mathbf{k}) \odot \hat{\mathbf{R}}_{ee}(\mathbf{k})\,\mathrm{d}^3\mathbf{k} \\
& - \tfrac{1}{2}(2\pi)^{-3}\int_{\mathbf{k}\in\mathbb{R}^3} \hat{\boldsymbol{\Delta}}''_0(\mathbf{k}) \odot \hat{\mathbf{R}}_{\phi\phi}(\mathbf{k})\,\mathrm{d}^3\mathbf{k} \\
= {} & \text{HS}^\infty(\mathbf{e}^*,\mathbf{0},\overline{\boldsymbol{\sigma}}) + \text{HS}^\infty(\mathbf{0},\boldsymbol{\phi}^*,\mathbf{0}).
\end{aligned} \tag{75}$$

The last identity shows that, under the assumption: $\mathbf{R}_{e\phi}(-\mathbf{r}) = \mathbf{R}_{e\phi}(\mathbf{r})$, there is no coupling between $\mathbf{e}^*$ and $\boldsymbol{\phi}^*$ in the bounds on the effective compliance. To further simplify the bounds on the effective compliance, we must discuss on the compliance and generalized compliance of the reference material.

If the reference material is such that $\mathbf{S}\geq\mathbf{S}_0$ and $\mathbf{M}\geq\mathbf{M}_0$ at any point, then (see Sec. 6) for fixed SVE size $L$ and for each realization $\omega$, the functional of Hashin and Shtrikman has a maximum. In other words, the quadratic part of HS is negative; therefore, the quadratic part of $\text{HS}^\infty$ is also negative. In particular, $\text{HS}^\infty(\mathbf{0},\boldsymbol{\phi}^*,\mathbf{0})\leq 0$. Therefore

$$\text{HS}^\infty(\mathbf{e}^*,\boldsymbol{\phi}^*,\overline{\boldsymbol{\sigma}}) \leq \text{HS}^\infty(\mathbf{e}^*,\mathbf{0},\overline{\boldsymbol{\sigma}}), \tag{76}$$

which shows that, to maximize $\text{HS}^\infty$, it is possible to assume *a priori* that $\boldsymbol{\phi}^*=\mathbf{0}$.

Conversely, if the reference material is such that $\mathbf{S}\geq\mathbf{S}_0$ and $\mathbf{M}\geq\mathbf{M}_0$ at any point, then (see Sec. 6), the functional of Hashin and Shtrikman has a minimum. In other words, the quadratic part of HS is positive; therefore, the quadratic part of $\text{HS}^\infty$ is also positive. In particular, $\text{HS}^\infty(\mathbf{0},\boldsymbol{\phi}^*,\mathbf{0})\geq 0$. Therefore

$$\text{HS}^\infty(\mathbf{e}^*,\boldsymbol{\phi}^*,\overline{\boldsymbol{\sigma}}) \geq \text{HS}^\infty(\mathbf{e}^*,\mathbf{0},\overline{\boldsymbol{\sigma}}), \tag{77}$$

which shows that, to minimize $\text{HS}^\infty$, it is possible to assume again *a priori* that $\boldsymbol{\phi}^*=\mathbf{0}$.

As a conclusion, under the assumption: $\mathbf{R}_{e\phi}(-\mathbf{r}) = \mathbf{R}_{e\phi}(\mathbf{r})$,

we have the following bound on the effective stiffness

$$\begin{aligned}\tfrac{1}{2}\overline{\boldsymbol{\sigma}} : \mathbf{S}^{\text{eff}} : \overline{\boldsymbol{\sigma}} \overset{\geq}{\leq} \tfrac{1}{2}\overline{\boldsymbol{\sigma}} : \mathbf{S}_0 : \overline{\boldsymbol{\sigma}} + \overline{\boldsymbol{\sigma}} : \mathbb{E}[\mathbf{e}^*] \\ - \tfrac{1}{2}\,\mathbb{E}[\mathbf{e}^* : (\mathbf{S} - \mathbf{S}_0)^{-1} : \mathbf{e}^*] \\ - \tfrac{1}{2}(2\pi)^{-3} \int_{\mathbf{k}\in\mathbb{R}^3} \hat{\boldsymbol{\Delta}}_0(\mathbf{k}) \odot \hat{\mathbf{R}}_{ee}(\mathbf{k})\, \mathrm{d}^3\mathbf{k}, \end{aligned} \tag{78}$$

where the simplification $\boldsymbol{\phi}^* = \mathbf{0}$ does not cause any degradation of the bound.

A final simplification results from the following assumptions: the reference material follows the simplified stress-gradient model of Tran et al. (2018) and the random field $\mathbf{e}^*$ is statistically isotropic (in the weak sense): $\mathbf{R}_{ee}$ depends on the norm $r = \|\mathbf{r}\|$ of the lag-vector $\mathbf{r}$ only: $\mathbf{R}_{ee}(\mathbf{r}) = \mathbf{R}_{ee}(r)$. Then its Fourier transform depends on the norm $k = \|\mathbf{k}\|$ of the wave-vector $\mathbf{k}$ only: $\hat{\mathbf{R}}_{ee}(\mathbf{k}) = \hat{\mathbf{R}}_{ee}(k)$ and

$$\int_{\mathbf{k}\in\mathbb{R}^3} \hat{\boldsymbol{\Delta}}_0(\mathbf{k}) \odot \hat{\mathbf{R}}_{ee}(\mathbf{k})\, \mathrm{d}^3\mathbf{k} = \int_0^{+\infty} 4\pi k^2 \hat{\boldsymbol{\Delta}}_0^{\text{iso}}(k) \odot \hat{\mathbf{R}}_{ee}(k)\, \mathrm{d}k, \tag{79}$$

where

$$\hat{\boldsymbol{\Delta}}_0^{\text{iso}}(k) = \frac{1}{4\pi} \int_{\|\mathbf{n}\|=1} \hat{\boldsymbol{\Delta}}_0(k\mathbf{n})\, \mathrm{d}^2\mathbf{n}. \tag{80}$$

We have shown in Appendix C.3 that

$$\hat{\boldsymbol{\Delta}}_0^{\text{iso}}(k) = (1 + k^2\ell_0^2)^{-1}\mathbf{Q}_0, \tag{81}$$

where $\ell_0$ denotes the material internal length of the reference material. The fourth-order tensor $\mathbf{Q}_0$ is defined as follows

$$\mathbf{Q}_0 = \frac{4\mu_0}{3}\frac{1+\nu_0}{1-\nu_0}\mathbf{J}_4 + \frac{2\mu_0}{15}\frac{7-5\nu_0}{1-\nu_0}\mathbf{K}_4, \tag{82}$$

and is related to the classical Hill tensor $\mathbf{P}_0$ of spherical inclusions embedded in the homogeneous material $\mathbf{C}_0$ (Eshelby, 1957)

$$\mathbf{Q}_0 = \mathbf{C}_0 - \mathbf{C}_0 : \mathbf{P}_0 : \mathbf{C}_0. \tag{83}$$

Gathering the above results, the bound given by Eq. (78) reduces to

$$\begin{aligned}\tfrac{1}{2}\overline{\boldsymbol{\sigma}} : \mathbf{S}^{\text{eff}} : \overline{\boldsymbol{\sigma}} \overset{\geq}{\leq} \tfrac{1}{2}\overline{\boldsymbol{\sigma}} : \mathbf{S}_0 : \overline{\boldsymbol{\sigma}} + \overline{\boldsymbol{\sigma}} : \mathbb{E}[\mathbf{e}^*] \\ - \tfrac{1}{2}\,\mathbb{E}[\mathbf{e}^* : (\mathbf{S} - \mathbf{S}_0)^{-1} : \mathbf{e}^*] \\ - \tfrac{1}{2}\int_0^{+\infty} \frac{1}{2\pi^2}\frac{k^2}{1+k^2\ell_0^2}\mathbf{Q}_0 \odot \hat{\mathbf{R}}_{ee}(\mathbf{k})\, \mathrm{d}k. \end{aligned} \tag{84}$$

In the next section, we show how the above general derivations can be specialized to $N$-phase materials. In the spirit of the classical bounds of Hashin and Shtrikman (1962b), we select phase-wise constant trial strain-polarizations.

## 10. Specialization to isotropic, $N$-phase materials

We assume that the composite is a $N$-phase material; $\chi_\alpha$ denotes the indicator function of phase $\alpha = 1, \ldots, N$: $\mathbf{x} \in \Omega$ belongs to phase $\alpha$ if, and only if, $\chi_\alpha(\mathbf{x}) = 1$ (note that $\chi_\alpha$ depends on the realization). The microstructure is statistically homogeneous, ergodic and isotropic; $f_\alpha = \mathbb{E}[\chi_\alpha]$ denotes the volume fraction of phase $\alpha$. Finally, $S_{\alpha\beta}$ denotes the cross-correlation

$$S_{\alpha\beta}(r) = \mathbb{E}[\chi_\alpha(\mathbf{x})\chi_\beta(\mathbf{x}+\mathbf{r})] - f_\alpha f_\beta, \tag{85}$$

which depends on the norm $r = \|\mathbf{r}\|$ of the lag-vector only. The compliance and generalized compliance of phase $\alpha$ are $\mathbf{S}_\alpha$ and $\mathbf{M}_\alpha$, respectively

$$\begin{Bmatrix}\mathbf{S}(\mathbf{x}) \\ \mathbf{M}(\mathbf{x})\end{Bmatrix} = \sum_\alpha \chi_\alpha(\mathbf{x}) \begin{Bmatrix}\mathbf{S}_\alpha \\ \mathbf{M}_\alpha\end{Bmatrix} \quad (\mathbf{x} \in \Omega), \tag{86}$$

where the sum runs over all phase indices $\alpha = 1, \ldots, N$. Following Hashin and Shtrikman (1962b); Willis (1977), we use phase-wise constant trial strain-polarizations to derive bounds on the effective properties. More precisely, we consider the following trial strain-polarization

$$\begin{Bmatrix}\mathbf{e}^*(\mathbf{x}) \\ \boldsymbol{\phi}^*(\mathbf{x})\end{Bmatrix} = \sum_\alpha \chi_\alpha(\mathbf{x}) \begin{Bmatrix}\mathbf{e}_\alpha^* \\ \boldsymbol{\phi}_\alpha^*\end{Bmatrix} \quad (\mathbf{x} \in \Omega), \tag{87}$$

where $\mathbf{e}_\alpha^* \in \mathcal{T}_2$ and $\boldsymbol{\phi}_\alpha^* \in \mathcal{T}_3'(\alpha = 1, \ldots, N)$ are *constant*, *deterministic* tensors, which are yet unknown. It is emphasized that the only source of randomness in the trial strain-polarizations thus constucted comes from the $\chi_\alpha$ factors. For such trial strain-polarizations, we have

$$\mathbf{R}_{ee}(\mathbf{r}) = \sum_{\alpha,\beta} S_{\alpha\beta}(r)\, \mathbf{e}_\alpha^* \otimes \mathbf{e}_\beta^*, \tag{88a}$$

$$\mathbf{R}_{e\phi}(\mathbf{r}) = \sum_{\alpha,\beta} S_{\alpha\beta}(r)\, \mathbf{e}_\alpha^* \otimes \boldsymbol{\phi}_\beta^*, \tag{88b}$$

which shows that $\mathbf{R}_{e\phi}(-\mathbf{r}) = \mathbf{R}_{e\phi}(\mathbf{r})$, while $\mathbf{R}_{ee}$ is a function of the norm of the lag-vector only. If we select a reference material that follows the simplified model of Tran et al. (2018), then the simplifications of the previous sections apply, and the trial field $\boldsymbol{\phi}^*$ becomes superfluous. Using the following identities

$$\mathbb{E}[\mathbf{e}^*] = \sum_\alpha f_\alpha \mathbf{e}_\alpha^*, \tag{89a}$$

$$\mathbb{E}[\mathbf{e}^* : (\mathbf{S} - \mathbf{S}_0)^{-1} : \mathbf{e}^*] = \sum_\alpha f_\alpha \mathbf{e}_\alpha^* : (\mathbf{S}_\alpha - \mathbf{S}_0)^{-1} : \mathbf{e}_\alpha^*, \tag{89b}$$

we find for the bound given by Eq. (84)

$$\begin{aligned}\tfrac{1}{2}\overline{\boldsymbol{\sigma}} : \mathbf{S}^{\text{eff}} : \overline{\boldsymbol{\sigma}} \overset{\geq}{\leq} \tfrac{1}{2}\overline{\boldsymbol{\sigma}} : \mathbf{S}_0 : \overline{\boldsymbol{\sigma}} + \overline{\boldsymbol{\sigma}} : \sum_\alpha f_\alpha \mathbf{e}_\alpha^* \\ - \tfrac{1}{2}\sum_\alpha f_\alpha \mathbf{e}_\alpha^* : (\mathbf{S}_\alpha - \mathbf{S}_0)^{-1} : \mathbf{e}_\alpha^* \\ - \tfrac{1}{2}\sum_{\alpha,\beta} F_{\alpha\beta}\mathbf{e}_\alpha^* : \mathbf{Q}_0 : \mathbf{e}_\beta^*, \end{aligned} \tag{90}$$

with

$$F_{\alpha\beta} = \frac{1}{2\pi^2} \int_0^{+\infty} \frac{k^2}{1 + k^2 \ell_0} \hat{S}_{\alpha\beta}(k) \, \mathrm{d}k. \tag{91}$$

This bound is then optimized with respect to the $\mathbf{e}^*_\alpha$. The stationarity conditions read

$$f_\alpha (\mathbf{S}_\alpha - \mathbf{S}_0)^{-1} : \mathbf{e}^*_\alpha + \mathbf{Q}_0 : \sum_\beta F_{\alpha\beta} \mathbf{e}^*_\beta = f_\alpha \, \overline{\boldsymbol{\sigma}}, \tag{92}$$

and we find, for this choice of the $\mathbf{e}^*_\alpha$

$$\tfrac{1}{2} \overline{\boldsymbol{\sigma}} : \mathbf{S}^{\mathrm{eff}} : \overline{\boldsymbol{\sigma}} \overset{\geq}{\leq} \tfrac{1}{2} \overline{\boldsymbol{\sigma}} : \mathbf{S}_0 : \overline{\boldsymbol{\sigma}} + \tfrac{1}{2} \, \overline{\boldsymbol{\sigma}} : \sum_\alpha f_\alpha \mathbf{e}^*_\alpha. \tag{93}$$

Eqs. (92) and (93) extend to stress-gradient materials the classical bounds of Hashin and Shtrikman (1962a,b). Unlike the classical case, they cannot be expressed in closed-form in general, and the linear system (92) must in general be solved numerically. Two particular cases are examined below.

*The classical bounds.* When $\ell_0 = 0$ (classical reference material), we find from Eq. (91) that

$$\begin{aligned} F_{\alpha\beta} &= \frac{1}{2\pi^2} \int_0^{+\infty} k^2 \hat{S}_{\alpha\beta}(k) \, \mathrm{d}k \\ &= \frac{1}{8\pi^3} \int_{\|\mathbf{n}\|=1} \int_{k \geq 0} \hat{S}_{\alpha\beta}(k) \, k^2 \, \mathrm{d}k \, \mathrm{d}^2\mathbf{n} \\ &= (2\pi)^{-3} \int_{\mathbf{k} \in \mathbb{R}^3} \hat{S}_{\alpha\beta}(\|\mathbf{k}\|) \, \mathrm{d}^3\mathbf{k} \end{aligned} \tag{94}$$

and we recognize the inverse Fourier transform of $\hat{S}_{\alpha\beta}$, evaluated at $\mathbf{r} = \mathbf{0}$. In other words, $F_{\alpha\beta} = S_{\alpha\beta}(0) = f_\alpha(\delta_{\alpha\beta} - f_\beta)$ and Eq. (92) reads

$$[(\mathbf{S}_\alpha - \mathbf{S}_0)^{-1} + \mathbf{Q}_0] : \mathbf{e}^*_\alpha - \mathbf{Q}_0 : \sum_\beta f_\beta \mathbf{e}^*_\beta = \overline{\boldsymbol{\sigma}}, \tag{95}$$

and the classical Hashin–Shtrikman bounds are retrieved [see for example Eq. (3.12) in Willis (1977)].

*Two-phase materials.* For two-phase materials ($N = 2$) and $\ell_0 \neq 0$, we have $S_{11}(r) = S_{22}(r) = -S_{12}(r)$. Therefore $F_{11} = F_{22} = -F_{12}$, and we introduce $\Xi$ such that

$$F_{11} = F_{22} = -F_{12} = \Xi f_1 f_2. \tag{96}$$

The stationarity conditions (92) then read

$$[(\mathbf{S}_\alpha - \mathbf{S}_0)^{-1} + \Xi \, \mathbf{Q}_0] : \mathbf{e}^*_\alpha = \overline{\boldsymbol{\sigma}} + \Xi \, \mathbf{Q}_0 : (f_1 \mathbf{e}^*_1 + f_2 \mathbf{e}^*_2), \tag{97}$$

and the Hashin–Shtrikman bounds for stress-gradient materials can be deduced from the bounds for classical materials by the substitution: $\mathbf{Q}_0 \to \Xi \, \mathbf{Q}_0$. Using for example Eq. (3.16) in Willis (1977), we get

$$\mathbf{S}^{\mathrm{eff}} \overset{\geq}{\leq} \Big( \sum_\alpha f_\alpha \mathbf{S}_\alpha : \mathbf{B}^\infty_\alpha \Big) : \Big( \sum_\alpha f_\alpha \mathbf{B}^\infty_\alpha \Big)^{-1}, \tag{98}$$

where

$$\mathbf{B}^\infty_\alpha = [\mathbf{I}_4 + \Xi \, \mathbf{Q}_0 : (\mathbf{S}_\alpha - \mathbf{S}_0)]^{-1}. \tag{99}$$

It is remarkable that the generalized bounds of Hashin–Shtrikman-type obtained in the previous section depend explicitly on the cross-correlations $S_{\alpha\beta}$ of the microstructure. This result was expected, since stress-gradient materials introduce at least one material internal length which must be compared to a typical length-scale (e.g. the correlation length) of the microstructure. Note that, for the same reason, such size-effects are also observed with strain-gradient materials (Smyshlyaev and Fleck, 1994).

This size-effect is at odds with the classical bounds, for which it is well-known that the $S_{\alpha\beta}$ disappear, provided that the microstructure is isotropic (Willis, 1977). In that regard, the generalized bounds are "less universal" than their classical counterpart; they are arguably more sensitive to the fine details of the microstructure. This is illustrated quantitatively in the next section, where we consider a specific two-phase random material.

## 11. Applications

We consider in this section two applications of the above results. Both microstructures are distributions of monodisperse, spherical inclusions. The domain covered by the spheres will be referred to as "the inclusions" (index "i") while the complementary space will be referred to as "the matrix" (index "m"). The total volume fraction of inclusions is $f$; the radius of the spheres is $a$ and their volume is $v = \frac{4}{3}\pi a^3$.

In order to ease comparisons, we use the same numerical values as in the previous study by Tran et al. (2018)

$$\mu_\mathrm{i} = 10 \mu_\mathrm{m}, \tag{100a}$$

$$\nu_\mathrm{i} = \nu_\mathrm{m} = 0.25, \tag{100b}$$

$$\ell_\mathrm{i} = \ell_\mathrm{m} \in \{0.1a, 0.5a, a\}. \tag{100c}$$

Note that, in view of our assumption that scales are separated (see Sec. 2.3), we must ensure that $\|\mathbf{M}\|/\|\mathbf{S}\| \ll L^2$ or $\|\mathbf{M}\|/\|\mathbf{S}\| \sim L^2$, where $L$ is the size of the unit-cell (periodic microstructures) or the correlation length. Typically, $L$ is of the order of $a$, while in the simplified model of Tran et al. (2018), $\|\mathbf{M}\|/\|\mathbf{S}\|$ is of the order of $\ell^2$. Therefore, we must ensure that $\ell_\mathrm{i}, \ell_\mathrm{m} \ll a$ or $\ell_\mathrm{i}, \ell_\mathrm{m} \sim a$, which is consistent with the above values.

We first consider in Sec. 11.1 a *random* microstructure resulting from the random distribution of monodisperse overlapping spheres [the so-called *boolean model*, see Jeulin (2000)], as depicted in Fig. 1. This first model exhibits short-range correlations (spatial correlations vanish for distances greater than $2a$).

We then consider in Sec. 11.2 a *periodic* (cubic) array of spherical inclusions (see Fig. 1, bottom-right). Owing to periodicity, the correlation range is effectively infinite.

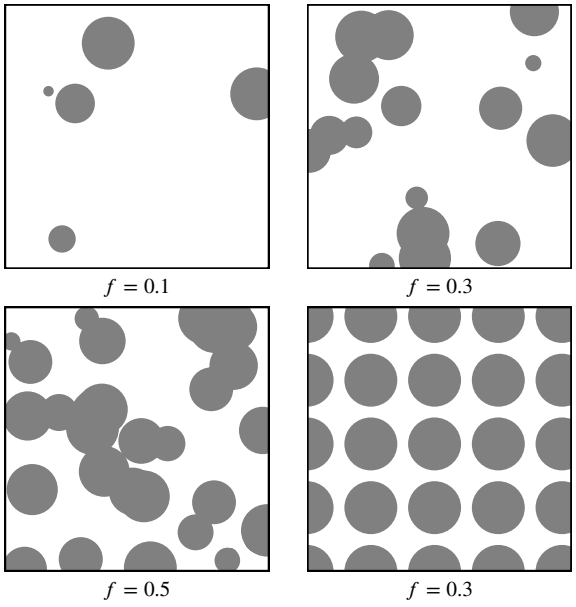


Figure 1: The microstructures considered in Sec. 11. *Top-left, top-right and bottom-left:* random distributions of monodisperse overlapping spheres for various volume fractions. Note that although all spheres share the same radius $a$, the radii of their intersections with a fixed plane are distributed in the range $(0, a)$. *Bottom-right:* periodic (cubic) distribution of spheres. Note that the periodic microstructure seems more densely packed because the section is taken through a plane that contains the centers of all the represented inclusions.

Comparing the bounds obtained for these two extreme cases will allow to quantify the role played by the microstructural cross-correlations. Note however that in the first application, the effective compliance has isotropic symmetry, while in the second application, the effective compliance has only cubic symmetry. Comparing the resulting bounds in both cases might therefore seem questionable. This is the reason why the comparison will be restricted to the effective bulk modulus $\kappa^{\text{eff}}$, defined as $\kappa^{\text{eff}} = \frac{1}{9}\mathbf{I}_2 : \mathbf{C}^{\text{eff}} : \mathbf{I}_2$ (regardless of the symmetries of $\mathbf{C}^{\text{eff}}$). Note that, for classical elasticity, the bounds of Hashin and Shtrikman (1962b) on the effective bulk modulus coincide for periodic and random microstructures (this will again be verified below).

### *11.1. A random microstructure*

For the random microstructure considered here, the results of Sec. 10 (in particular, the last part on two-phase materials) apply. Introducing the intensity $\rho$ of the Poisson process (number of inclusions per unit volume), we have the classical identities (Jeulin, 2000)

$$f = 1 - \exp(-\rho v) \quad S_{\text{ii}}(r) = S_{\text{mm}}(r) = f(1-f)\gamma(r) \tag{101}$$

with

$$\gamma(2ax) = \frac{\exp[\rho v \overline{w}(x)] - 1}{\exp(\rho v) - 1}, \tag{102}$$

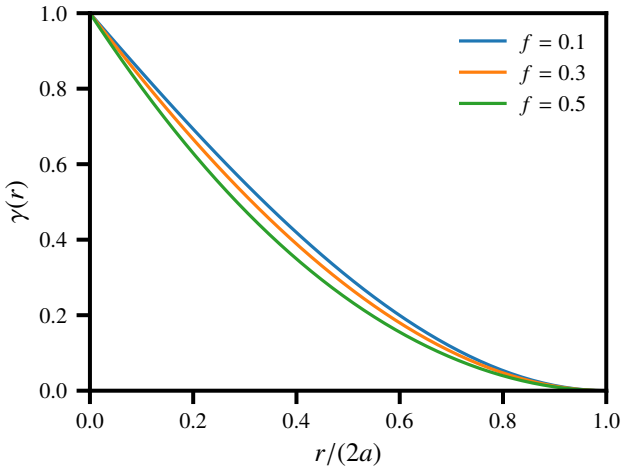


Figure 2: Covariance function $\gamma$ of the boolean model for various values of the volume fraction $f$ of inclusions.

where $\overline{w}(x)$ is the normalized volume of the intersection of two spheres of unit diameter ($x$: center-to-center distance)

$$\overline{w}(x) = \begin{cases} \frac{1}{2}x^3 - \frac{3}{2}x + 1 & \text{if } x \leq 1, \\ 0 & \text{otherwise.} \end{cases} \tag{103}$$

Fig. 2 shows the covariance function $\gamma$ for various values of the volume fraction $f$. The coefficient $\Xi$ is then given by the following integral [see Eq. (91)]

$$\Xi = \frac{1}{2\pi^2} \int_0^{+\infty} \frac{k^2}{1 + k^2 \ell_0} \hat{\gamma}(k)\, \mathrm{d}k, \tag{104}$$

where $\hat{\gamma}$ is the rotation-invariant 3D Fourier transform of $\gamma(\mathbf{r}) = \gamma(r)$

$$\begin{aligned} \hat{\gamma}(\mathbf{k}) &= \int_{\mathbf{r}\in\mathbb{R}^3} \gamma(\|\mathbf{r}\|) \exp(-\mathrm{i}\mathbf{k}\cdot\mathbf{r})\, \mathrm{d}^3\mathbf{r} \\ &= \int_{\|\mathbf{n}\|=1} \int_{r\geq 0} r^2 \gamma(r) \exp(-\mathrm{i}r\mathbf{k}\cdot\mathbf{n})\, \mathrm{d}r\, \mathrm{d}^2\mathbf{n} \\ &= \int_0^{2a} 4\pi r^2 \gamma(r) \frac{\sin kr}{kr}\, \mathrm{d}r, \end{aligned} \tag{105}$$

where the upper-bound in the last integral accounts for the fact that $\gamma(r) = 0$ for $r \geq 2a$. Numerical integration is used to compute the Fourier transform $\hat{\gamma}$ as well as the microstructural parameter $\Xi$. The procedure is detailed in Appendix F.

Fig. 3 shows for various values of the volume fraction $f$ the variations of $\Xi$ with respect to the internal length $\ell_0$ of the reference material. Clearly, $\Xi$ is not very sensitive to the volume fraction. It is however rather sensitive to the $\ell_0/2a$ ratio, that is to the internal length to correlation length ratio.

Only the numerical values relating to the effective bulk modulus $\kappa^{\text{eff}}$ are presentend in Figs. 4, 5 and 6; similar trends are observed with the effective shear modulus. To obtain this bounds, we selected first $\mathbf{S}_0 = \mathbf{S}_{\text{i}}$ and $\mathbf{M}_0 = \mathbf{M}_{\text{i}}$ (upper bound), then $\mathbf{S}_0 = \mathbf{S}_{\text{m}}$ and $\mathbf{M}_0 = \mathbf{M}_{\text{m}}$ (lower bound). It is observed that the Mori–Tanaka estimate of Tran et al. (2018) is close, but not equal to the lower bound. This is at odds with classical elasticity, but is

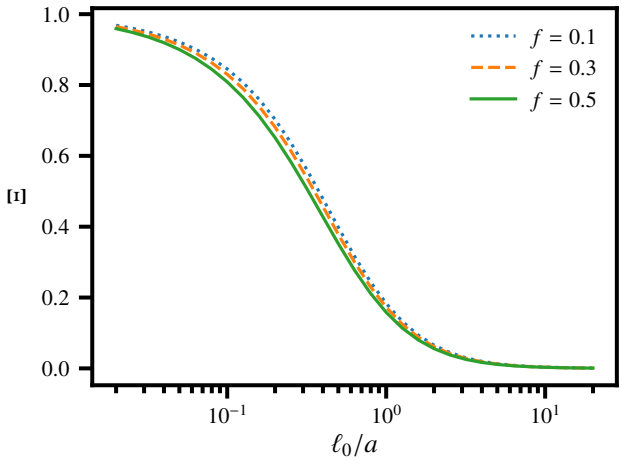


Figure 3: The value of $\Xi$ for various values of the volume fraction $f$ and the internal length $\ell_0$ of the reference material.

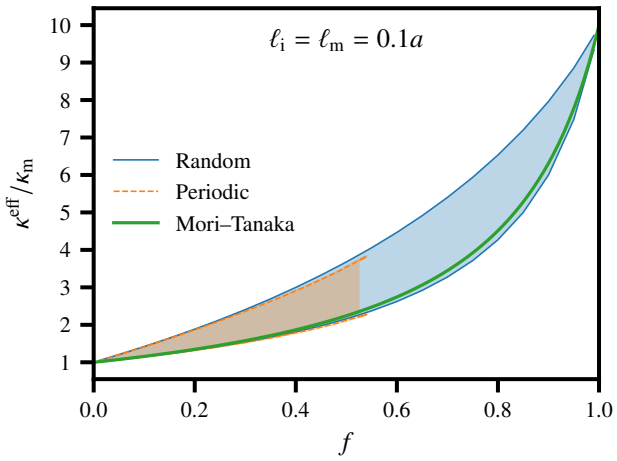


Figure 4: Upper and lower bounds on the effective bulk modulus $\kappa^\mathrm{eff}$, for $\ell_\mathrm{i} = \ell_\mathrm{m} = 0.1a$ and various values of the volume fraction. Both random (see Sec. 11.1) and periodic (see Sec. 11.2) microstructures are plotted on the same graph. For comparison, the thick line represents the Mori–Tanaka estimate derived by Tran et al. (2018).

readily explained by the fact that, for stress-gradient materials, the solution to Eshelby's inhomogeneity problem does not coincide with the solution to Eshelby's inclusion problem (Tran et al., 2018).

### *11.2. A periodic microstructure*

For the periodic microstructure considered here, it is convenient to consider that the unit-cell and the inclusion are centered at the origin: $\Omega = (-L/2, L/2)^3$ and

$$\chi(\mathbf{x}) = \begin{cases} 1 & \text{if } \|\mathbf{x}\| \leq a, \\ 0 & \text{otherwise,} \end{cases} \tag{106}$$

where $\chi$ denotes the indicator function of the inclusion. We will again consider phase-wise constant trial strain-polarizations:

$$\mathbf{e}^*(\mathbf{x}) = \chi(\mathbf{x})\mathbf{e}^*_\mathrm{i} + [1 - \chi(x)]\mathbf{e}^*_\mathrm{m}, \tag{107a}$$
$$\boldsymbol{\phi}^*(\mathbf{x}) = \chi(\mathbf{x})\boldsymbol{\phi}^*_\mathrm{i} + [1 - \chi(x)]\boldsymbol{\phi}^*_\mathrm{m}, \tag{107b}$$

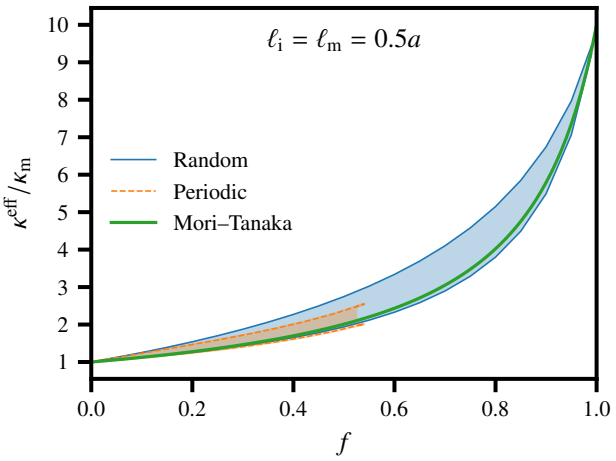


Figure 5: Upper and lower bounds on the effective bulk modulus $\kappa^\mathrm{eff}$, for $\ell_\mathrm{i} = \ell_\mathrm{m} = 0.5a$ and various values of the volume fraction. Both random (see Sec. 11.1) and periodic (see Sec. 11.2) microstructures are plotted on the same graph. For comparison, the thick line represents the Mori–Tanaka estimate derived by Tran et al. (2018).

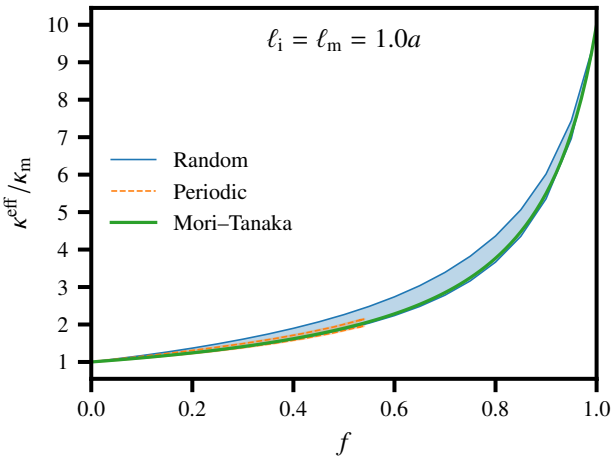


Figure 6: Upper and lower bounds on the effective bulk modulus $\kappa^\mathrm{eff}$, for $\ell_\mathrm{i} = \ell_\mathrm{m} = 0.5a$ and various values of the volume fraction. Both random (see Sec. 11.1) and periodic (see Sec. 11.2) microstructures are plotted on the same graph. For comparison, the thick line represents the Mori–Tanaka estimate derived by Tran et al. (2018).

where $\mathbf{e}^*_\mathrm{i}$, $\mathbf{e}^*_\mathrm{m}$, $\boldsymbol{\phi}^*_\mathrm{i}$ and $\boldsymbol{\phi}^*_\mathrm{m}$ are constant tensors. In the periodic setting considered here, we need to optimize the functional of Hashin and Shtrikman defined by Eq. (59).

We first prove that (as in the random case), the optimal third-order eigenstrain is null. Indeed, the Fourier coefficients of the trial strain-polarization $\mathbf{e}^*$ are

$$\hat{\mathbf{e}}^*_n = \begin{cases} \hat{\chi}_n(\mathbf{e}^*_\mathrm{i} - \mathbf{e}^*_\mathrm{m}) & \text{for } n \neq (0,0,0), \\ \langle \mathbf{e}^* \rangle = f\mathbf{e}^*_\mathrm{i} + (1-f)\mathbf{e}^*_\mathrm{m} & \text{for } n = (0,0,0), \end{cases} \tag{108}$$

with

$$\hat{\chi}_n = fF(k_n a) \quad \text{with} \quad F(\xi) = 3\frac{\sin\xi - \xi\cos\xi}{\xi^3}. \tag{109}$$

Similar expressions hold for $\hat{\boldsymbol{\phi}}^*_n$ and we find that $\hat{\mathbf{e}}^*_n$ and $\hat{\boldsymbol{\phi}}^*_n$ are *real*. Therefore, $\hat{\boldsymbol{\Delta}}_0(\mathbf{k}_n)$ being symmetric

$$\begin{aligned} &\mathrm{conj}(\hat{\boldsymbol{\eta}}_n) : \hat{\boldsymbol{\Delta}}_0(\mathbf{k}_n) : \hat{\boldsymbol{\eta}}_n \\ &\quad = (\hat{\mathbf{e}}^*_n + \mathrm{i}\hat{\boldsymbol{\phi}}^*_n \cdot \mathbf{k}_n) : \hat{\boldsymbol{\Delta}}_0(\mathbf{k}_n) : (\hat{\mathbf{e}}^*_n - \mathrm{i}\hat{\boldsymbol{\phi}}^*_n \cdot \mathbf{k}_n) \\ &\quad = \hat{\mathbf{e}}^*_n : \hat{\boldsymbol{\Delta}}_0(\mathbf{k}_n) : \hat{\mathbf{e}}^*_n + \hat{\boldsymbol{\phi}}^*_n \therefore [\mathbf{k}_n \otimes \hat{\boldsymbol{\Delta}}_0(\mathbf{k}_n) \otimes \mathbf{k}_n] \therefore \hat{\boldsymbol{\phi}}^*_n \end{aligned} \tag{110}$$

and [see Eq. (59)]

$$\mathrm{HS}(\mathbf{e}^*, \boldsymbol{\phi}^*, \overline{\boldsymbol{\sigma}}) = \mathrm{HS}(\mathbf{e}^*, \mathbf{0}, \overline{\boldsymbol{\sigma}}) + \mathrm{HS}(\mathbf{0}, \boldsymbol{\phi}^*, \mathbf{0}). \tag{111}$$

Stationarity with respect to $\boldsymbol{\phi}^*_\mathrm{i}$ and $\boldsymbol{\phi}^*_\mathrm{m}$ leads to $\boldsymbol{\phi}^*_\mathrm{i} = \boldsymbol{\phi}^*_\mathrm{m} = \mathbf{0}$ as announced. Then, recalling that $\hat{\boldsymbol{\Delta}}_0(\mathbf{k}_n) = \mathbf{0}$ for $n = (0,0,0)$ and using Eq. (108), we find that

$$\sum_{n\in\mathbb{Z}^3} \mathrm{conj}(\hat{\boldsymbol{\eta}}_n) : \hat{\boldsymbol{\Delta}}_0(\mathbf{k}_n) : \hat{\boldsymbol{\eta}}_n = f(1-f)(\mathbf{e}^*_\mathrm{i} - \mathbf{e}^*_\mathrm{m}) : \mathbf{Q} : (\mathbf{e}^*_\mathrm{i} - \mathbf{e}^*_\mathrm{m}), \tag{112}$$

with

$$f(1-f)\mathbf{Q} = \sum_{n\in\mathbb{Z}^3} |\hat{\chi}_n|^2 \hat{\boldsymbol{\Delta}}_0(\mathbf{k}_n), \tag{113}$$

where the $f(1-f)$ normalization will be justified below. We are therefore left with the optimization of

$$\begin{aligned} \mathrm{HS}(\mathbf{e}^*, \mathbf{0}, \overline{\boldsymbol{\sigma}}) = {} & \tfrac{1}{2}\overline{\boldsymbol{\sigma}} : \mathbf{S}_0 : \overline{\boldsymbol{\sigma}} + f\overline{\boldsymbol{\sigma}} : \mathbf{e}^*_\mathrm{i} + (1-f)\overline{\boldsymbol{\sigma}} : \mathbf{e}^*_\mathrm{m} \\ & - \tfrac{1}{2} f\mathbf{e}^*_\mathrm{i} : (\mathbf{S}_\mathrm{i} - \mathbf{S}_0)^{-1} : \mathbf{e}^*_\mathrm{i} \\ & - \tfrac{1}{2}(1-f)\mathbf{e}^*_\mathrm{m} : (\mathbf{S}_\mathrm{m} - \mathbf{S}_0)^{-1} : \mathbf{e}^*_\mathrm{m} \\ & - \tfrac{1}{2} f(1-f)(\mathbf{e}^*_\mathrm{i} - \mathbf{e}^*_\mathrm{m}) : \mathbf{Q} : (\mathbf{e}^*_\mathrm{i} - \mathbf{e}^*_\mathrm{m}), \end{aligned} \tag{114}$$

with respect to $\mathbf{e}^*_\mathrm{i}$ and $\mathbf{e}^*_\mathrm{m}$. This leads to the following stationarity conditions

$$[(\mathbf{S}_\mathrm{i} - \mathbf{S}_0)^{-1} + \mathbf{Q}] : \mathbf{e}^*_\mathrm{i} = \overline{\boldsymbol{\sigma}} + \mathbf{Q} : \langle \mathbf{e}^* \rangle, \tag{115a}$$

$$[(\mathbf{S}_\mathrm{m} - \mathbf{S}_0)^{-1} + \mathbf{Q}] : \mathbf{e}^*_\mathrm{m} = \overline{\boldsymbol{\sigma}} + \mathbf{Q} : \langle \mathbf{e}^* \rangle, \tag{115b}$$

with $\langle \mathbf{e}^* \rangle = f\mathbf{e}^*_\mathrm{i} + (1-f)\mathbf{e}^*_\mathrm{m}$. Observe the similarity with Eqs. (97) corresponding to the random case: Eqs. (98) and (99) would therefore apply with the substitution $\Xi\,\mathbf{Q}_0 \to \mathbf{Q}$.

However, in the present application, we seek a bound on the effective bulk modulus only, for which a direct derivation will deliver more simple expressions. We select a spherical (hydrostatic) macroscopic stress $\overline{\boldsymbol{\sigma}}$. Since $\mathbf{Q}$ has cubic symmetry, it can be shown that the solution $(\mathbf{e}^*_\mathrm{i}, \mathbf{e}^*_\mathrm{m})$ to the system (115a) $\wedge$ (115b) must also be spherical

$$\mathbf{e}^*_\mathrm{i} = e^*_\mathrm{i}\mathbf{I}_2 \quad \text{and} \quad \mathbf{e}^*_\mathrm{m} = e^*_\mathrm{m}\mathbf{I}_2 \quad \text{when} \quad \overline{\boldsymbol{\sigma}} = \overline{\sigma}\mathbf{I}_2, \tag{116}$$

where $e^*_\mathrm{i}$, $e^*_\mathrm{m}$ and $\overline{\sigma}$ are scalars. Contraction of Eqs. (115a) and (115b) with the second-order identity tensor then delivers the two scalar equations

$$[3(\kappa_\mathrm{i}^{-1} - \kappa_0^{-1})^{-1} + q]e^*_\mathrm{i} = \overline{\sigma} + q\langle e^* \rangle \tag{117a}$$

$$[3(\kappa_\mathrm{m}^{-1} - \kappa_0^{-1})^{-1} + q]e^*_\mathrm{m} = \overline{\sigma} + q\langle e^* \rangle \tag{117b}$$

where we have introduced $q = \mathbf{J}_4 :: \mathbf{Q} = \frac{1}{3}\mathbf{I}_2 : \mathbf{Q} : \mathbf{I}_2$. We show in Appendix C.3 that, for the simplified model of Tran et al. (2018) and for $n \neq (0,0,0)$

$$\mathbf{J}_4 :: \hat{\boldsymbol{\Delta}}_0(\mathbf{k}_n) = (1 + k_n^2\ell_0^2)^{-1} q_0 \quad \text{with} \quad q_0 = \mathbf{J}_4 :: \mathbf{Q}_0, \tag{118}$$

while $\mathbf{J}_4 :: \hat{\boldsymbol{\Delta}}_0(\mathbf{k}_n) = 0$ for $n = (0,0,0)$. Combining with Eq. (113), we find

$$f(1-f)\frac{q}{q_0} = \sum_{n\neq(0,0,0)} \frac{|\hat{\chi}_n|^2}{1 + k_n^2\ell_0^2} = \sum_{n\in\mathbb{Z}^3} \frac{|\hat{\chi}_n|^2}{1 + k_n^2\ell_0^2} - f^2, \tag{119}$$

since $\hat{\chi}(0) = \langle \chi \rangle = f$. Note that when $\ell_0 = 0$ (classical elasticity), we find from Parseval's identity that the sum in the right-hand side coincides with $f$. In other words, $q = q_0$ for $\ell_0 = 0$, which explains the $f(1-f)$ scaling in the definition (113) of $\mathbf{Q}$ and leads us to define $\Xi^\mathrm{per}$ as the ratio $\Xi^\mathrm{per} = q/q_0$. The resulting bound on the effective bulk modulus then becomes formally equivalent to expressions (98) and (99)

$$(\kappa^\mathrm{eff})^{-1} \overset{\geq}{\leq} \frac{f\kappa_\mathrm{i}^{-1} + (1-f)\kappa_\mathrm{m}^{-1}}{fb_\mathrm{i} + (1-f)b_\mathrm{m}}, \tag{120}$$

with

$$b_\alpha = [1 + \tfrac{1}{3}\Xi^\mathrm{per} q_0(\kappa_\alpha^{-1} - \kappa_0^{-1})]^{-1} \quad (\alpha = \mathrm{i}, \mathrm{m}). \tag{121}$$

Evaluation of the bounds on the effective bulk modulus therefore reduces to the evaluation of $\Xi^\mathrm{per}$ for various values of $f$ and $\ell_0$. Note that the microstructural parameter $\Xi^\mathrm{per}$ thus introduced is strictly equivalent to $\Xi$ introduced in the random case, albeit for spherical loadings only. Direct summation of the lattice sum (119) was performed; convergence was found to be fairly quick. Summing $121^3$ terms ($n \in \{-60, \ldots, 60\}^3$) resulted in about 1 % accuracy for $\Xi^\mathrm{per}$, which was deemed sufficient. Fig. 7 displays the values of $\Xi^\mathrm{per}$; comparison with Fig. 3 shows that this microstructural parameter is more sensitive to the value of the volume fraction than in the random case.

Bounds on $\kappa^\mathrm{eff}$ are again obtained by selecting first $\mathbf{S}_0 = \mathbf{S}_\mathrm{i}$ and $\mathbf{M}_0 = \mathbf{M}_\mathrm{i}$ (upper bound), then $\mathbf{S}_0 = \mathbf{S}_\mathrm{m}$ and $\mathbf{M}_0 = \mathbf{M}_\mathrm{m}$ (lower bound). These bounds are plotted on Figs. 4, 5 and 6 for three values of $\ell_0 = \ell_\mathrm{i} = \ell_\mathrm{m}$ and the whole range of volume fractions $0 \leq f \leq \pi/6$. For $\ell_0 \to 0$ (classical materials), we find that the bounds for both random and periodic microstructures coincide as announced, since both $\Xi \to 1$ and $\Xi^\mathrm{per} \to 1$ in that case. For finite values of $\ell_0$, the bounds differ as expected for both types of microstructures.

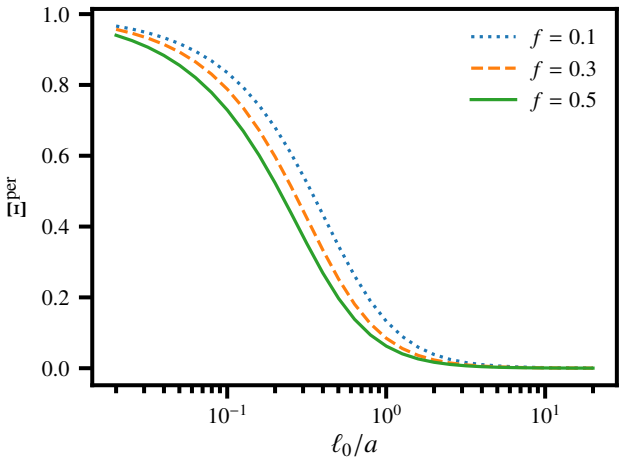


Figure 7: The value of $\Xi^{\mathrm{per}}$ for various values of the volume fraction $f$ and the internal length $\ell_0$ of the reference material.

## 12. Conclusions and perspectives

Adopting a stress-based approach, we have extended the classical variational principle of Hashin and Shtrikman (1962a) to stress-gradient materials, first for periodic homogenization, then for random homogenization. In both cases, we assumed that the material internal lengths were all of the order of the size of the heterogeneities or smaller, which led to homogenization as classical (rather than stress-gradient) materials.

The functional of Hashin and Shtrikman that we introduced involves two trial fields: a second-order eigenstrain, and a third-order eigenstrain. We have shown that in many cases of interest, the latter can be discarded for random homogenization, which significantly simplified the subsequent derivations. For isotropic microstructures and isotropic stress-gradient materials that follow the simplified model of Tran et al. (2018), we adopted an approach similar to the re-derivation by Willis (1977) of the classical bounds of Hashin and Shtrikman (1962b). Our bounds are similar to the classical ones, but for the fact that a microstructural parameter related to the covariance of the microstructure is involved. In that sense, the bounds that we obtained are "less universal" than the classical bounds of Hashin and Shtrikman (1962b).

We have identified two opportunities for improving the bounds proposed in the present work.

We first observe that the simplification that eventually leads to discarding the third-order eigenstrain is induced by the assumption that the cross-correlation of the second- and third- order eigenstrains is centro-symmetric. The price to pay for this simplification is the fact that the resulting bounds no longer depend on the the material internal lengths of the phases: they depend on the compliance of the phases, the compliance of the reference material and its material internal lengths. In those cases where the reference material coincides with one of the phases, the resulting bound may depend on the material internal lengths of this phase (but only this one).

Selecting trial fields such that their cross-corelations are not centro-symmetric may therefore deliver improved bounds on the effective compliance of heterogeneous, stress-gradient materials, since they would include more information on the microstructure (all material internal lengths would be accounted for simultaneously).

Second, Tran et al. (2018) have shown that boundary layers may arise at the interface between two phases of the composite. Clearly, adopting phase-wise constant trial fields as we did in this paper cannot capture, even approximately, such boundary layers. A natural extension to the present work would be to apply the *morphologically representative patterns* methodology introduced by Bornert et al. (1996). It was with this extension in mind that we derived in Sec. 8 quite general bounds with minimal assumptions on the random trial fields (the case of phase-wise constant trial fields being seen in Sec. 10 as a specialization of a much more general case).

These two perspectives will be explored in future work.

## Acknowledgments

This work has benefited from a French government grant managed by ANR within the frame of the national program Investments for the Future ANR-11-LABX-022-01.

## References

Altan, B.S., Aifantis, E.C., 1992. On the structure of the mode III crack-tip in gradient elasticity. Scripta Metallurgica et Materialia 26, 319–324. doi:10.1016/0956-716X(92)90194-J.

Altan, B.S., Aifantis, E.C., 1997. On Some Aspects in the Special Theory of Gradient Elasticity. Journal of the Mechanical Behavior of Materials 8, 231–282.

Askes, H., Aifantis, E.C., 2011. Gradient elasticity in statics and dynamics: An overview of formulations, length scale identification procedures, finite element implementations and new results. International Journal of Solids and Structures 48, 1962–1990. doi:10.1016/j.ijsolstr.2011.03.006.

Bornert, M., Stolz, C., Zaoui, A., 1996. Morphologically representative pattern-based bounding in elasticity. Journal of the Mechanics and Physics of Solids 44, 307–331. doi:10.1016/0022-5096(95)00083-6.

Eshelby, J.D., 1957. The Determination of the Elastic Field of an Ellipsoidal Inclusion, and Related Problems. Proceedings of the Royal Society of London. Series A, Mathematical and Physical Sciences 241, 376–396. doi:10.1098/rspa.1957.0133.

Forest, S., Sab, K., 2012. Stress gradient continuum theory. Mechanics Research Communications 40, 16–25. doi:10.1016/j.mechrescom.2011.12.002.

Forest, S., Sab, K., 2017. Finite-deformation second-order micromorphic theory and its relations to strain and stress gradient models. Mathematics and Mechanics of Solids , 1081286517720844doi:10.1177/1081286517720844.

Hashin, Z., Shtrikman, S., 1962a. On some variational principles in anisotropic and nonhomogeneous elasticity. Journal of the Mechanics and Physics of Solids 10, 335–342. doi:10.1016/0022-5096(62)90004-2.

Hashin, Z., Shtrikman, S., 1962b. A variational approach to the theory of the elastic behaviour of polycrystals. Journal of the Mechanics and Physics of Solids 10, 343–352. doi:10.1016/0022-5096(62)90005-4.

Hütter, G., Sab, K., Forest, S., 2020. Kinematics and constitutive relations in the stress-gradient theory: Interpretation by homogenization. International Journal of Solids and Structures 193-194, 90–97. doi:10.1016/j.ijsolstr.2020.02.014.

Jeulin, D., 2000. Random texture models for material structures. Statistics and Computing 10, 121–132. doi:10.1023/A:1008942325749.

Jikov, V.V., Kozlov, S.M., Oleinik, O.A., 1994. Homogenization of Differential Operators and Integral Functionals. Springer-Verlag, Berlin Heidelberg. doi:10.1007/978-3-642-84659-5.

Korringa, J., 1973. Theory of elastic constants of heterogeneous media. Journal of Mathematical Physics 14, 509–513. doi:doi:10.1063/1.1666346.
Kröner, E., 1974. On the Physics and Mathematics of Self-Stresses, in: Zeman, J.L., Ziegler, F. (Eds.), Topics in Applied Continuum Mechanics, Springer Verlag Wien, Vienna. pp. 22–38.
Mindlin, R.D., 1964. Micro-structure in linear elasticity. Archive for Rational Mechanics and Analysis 16, 51–78. doi:10.1007/BF00248490.
Moreau, J., 1979. Duality characterization of strain tensor distributions in an arbitrary open set. Journal of Mathematical Analysis and Applications 72, 760–770. doi:10.1016/0022-247X(79)90263-4.
Ostoja-Starzewski, M., 2006. Material spatial randomness: From statistical to representative volume element. Probabilistic Engineering Mechanics 21, 112–132. doi:10.1016/j.probengmech.2005.07.007.
Polizzotto, C., 2018. A micromorphic approach to stress gradient elasticity theory with an assessment of the boundary conditions and size effects. ZAMM - Journal of Applied Mathematics and Mechanics / Zeitschrift für Angewandte Mathematik und Mechanik 98, 1528–1553. doi:10.1002/zamm.201700364.
Sab, K., 1994. Homogenization of non-linear random media by a duality method. Application to plasticity. Asymptotic Analysis 9, 311–336. doi:10.3233/ASY-1994-9402.
Sab, K., Legoll, F., Forest, S., 2016. Stress Gradient Elasticity Theory: Existence and Uniqueness of Solution. Journal of Elasticity 123, 179–201. doi:10.1007/s10659-015-9554-1.
Sab, K., Nedjar, B., 2005. Periodization of random media and representative volume element size for linear composites. Comptes Rendus Mécanique 333, 187–195. doi:10.1016/j.crme.2004.10.003.
Smyshlyaev, V.P., Fleck, N.A., 1994. Bounds and estimates for linear composites with strain gradient effects. Journal of the Mechanics and Physics of Solids 42, 1851–1882. doi:10.1016/0022-5096(94)90016-7.
Suquet, P., 1990. A simplified method for the prediction of homogenized elastic properties of composites with a periodic structure. Comptes-rendus de l'Académie des sciences série II 311, 769–774.
Tran, V.P., 2016. Modeling of Random Heterogeneous Materials from Microscale to Macroscale. Ph.D. thesis. Université Paris Est, École des Ponts Paris Tech, 6-8 avenue Blaise Pascal, 77455 Marne La Vallée.
Tran, V.P., Brisard, S., Guilleminot, J., Sab, K., 2018. Mori–Tanaka estimates of the effective elastic properties of stress-gradient composites. International Journal of Solids and Structures 146, 55–68. doi:10.1016/j.ijsolstr.2018.03.020.
Walpole, L.J., 1984. Fourth-Rank Tensors of the Thirty-Two Crystal Classes: Multiplication Tables. Proceedings of the Royal Society of London. A. Mathematical and Physical Sciences 391, 149–179. doi:10.1098/rspa.1984.0008.
Willis, J., 1977. Bounds and self-consistent estimates for the overall properties of anisotropic composites. Journal of the Mechanics and Physics of Solids 25, 185–202. doi:10.1016/0022-5096(77)90022-9.
Willis, J., 1991. On methods for bounding the overall properties of nonlinear composites. Journal of the Mechanics and Physics of Solids 39, 73–86. doi:10.1016/0022-5096(91)90031-I.
Willis, J.R., 2001. Lectures on Mechanics of Random Media, in: Jeulin, D., Ostoja-Starzewski, M. (Eds.), Mechanics of Random and Multiscale Microstructures. Springer, Vienna. International Centre for Mechanical Sciences, pp. 221–267. doi:10.1007/978-3-7091-2780-3_5.
Zeller, R., Dederichs, P.H., 1973. Elastic Constants of Polycrystals. Physica Status Solidi (B) 55, 831–842. doi:10.1002/pssb.2220550241.

## Appendix A. Proof of the minimum complementary energy principle

In this section, we prove that $\boldsymbol{\sigma}$ is the unique solution to problem (25) if, and only if, $\boldsymbol{\sigma}$ is the unique minimizer of $\Pi^{\mathrm{c}}(\bullet, \mathbf{e}^*, \boldsymbol{\phi}^*)$. We consider two stress fields $\boldsymbol{\sigma} \in \overline{\boldsymbol{\sigma}} + \mathcal{S}_0(\Omega)$ and $\delta\boldsymbol{\sigma} \in \mathcal{S}_0(\Omega)$. Without further assumptions on these fields, we have

$$\begin{aligned}\Pi^{\mathrm{c}}(\boldsymbol{\sigma} + \delta\boldsymbol{\sigma}, \mathbf{e}^*, \boldsymbol{\phi}^*) = \Pi^{\mathrm{c}}(\boldsymbol{\sigma}, \mathbf{e}^*, \boldsymbol{\phi}^*) + W^{\mathrm{c}}(\delta\boldsymbol{\sigma}) \\ + \langle \mathbf{e} : \delta\boldsymbol{\sigma} \rangle + \langle \boldsymbol{\phi} \therefore (\delta\boldsymbol{\sigma} \otimes \nabla) \rangle,\end{aligned} \tag{A.1}$$

where we have introduced

$$\mathbf{e} = \mathbf{S} : \boldsymbol{\sigma} + \mathbf{e}^* \quad \text{and} \quad \boldsymbol{\phi} = \mathbf{M} \therefore (\boldsymbol{\sigma} \otimes \nabla) + \boldsymbol{\phi}^*. \tag{A.2}$$

Integrating by parts in the last volume integral in Eq. (A.1), we find

$$\langle \boldsymbol{\phi} \therefore (\delta\boldsymbol{\sigma} \otimes \nabla) \rangle = \frac{1}{|\Omega|} \int_{\partial\Omega} \delta\boldsymbol{\sigma} : \boldsymbol{\phi} \cdot \mathbf{n} \, \mathrm{d}S - \langle \delta\boldsymbol{\sigma} : (\boldsymbol{\phi} \cdot \nabla) \rangle, \tag{A.3}$$

where $\mathbf{n}$ denotes the outer unit normal to the boundary $\partial\Omega$ of the unit-cell $\Omega$. Gathering the above results, we get

$$\begin{aligned}\Pi^{\mathrm{c}}(\boldsymbol{\sigma} + \delta\boldsymbol{\sigma}, \mathbf{e}^*, \boldsymbol{\phi}^*) = \Pi^{\mathrm{c}}(\boldsymbol{\sigma}, \mathbf{e}^*, \boldsymbol{\phi}^*) + W^{\mathrm{c}}(\delta\boldsymbol{\sigma}) \\ + \langle (\mathbf{e} - \boldsymbol{\phi} \cdot \nabla) : \delta\boldsymbol{\sigma} \rangle \\ + \frac{1}{|\Omega|} \int_{\partial\Omega} \delta\boldsymbol{\sigma} : \boldsymbol{\phi} \cdot \mathbf{n} \, \mathrm{d}S.\end{aligned} \tag{A.4}$$

*Proof that any solution to problem (25) minimizes the complementary energy.* We first assume that $\boldsymbol{\sigma}$ is the solution to problem (25). Observing that $\boldsymbol{\phi} \cdot \mathbf{n}$ is $\Omega$-skew-periodic [see Eq. (25f)], it is found that the product $\delta\boldsymbol{\sigma} : \boldsymbol{\phi} \cdot \mathbf{n}$ is also $\Omega$-skew-periodic, since $\delta\boldsymbol{\sigma}$ is $\Omega$-periodic by construction. Therefore, the last term in Eq. (A.4) vanishes. Then, from Eq. (25d), $(\mathbf{e} - \boldsymbol{\phi} \cdot \nabla)$ is the symmetric part of the gradient of a vector field, $\mathbf{u}$, and

$$\begin{aligned}\langle (\mathbf{e} - \boldsymbol{\phi} \cdot \nabla) : \delta\boldsymbol{\sigma} \rangle &= \langle \mathbf{sym}(\mathbf{u} \otimes \nabla) : \delta\boldsymbol{\sigma} \rangle \\ &= \frac{1}{|\Omega|} \int_{\partial\Omega} \mathbf{u} \cdot \delta\boldsymbol{\sigma} \cdot \mathbf{n} \, \mathrm{d}S - \langle \mathbf{u} \cdot (\boldsymbol{\sigma} \cdot \nabla) \rangle,\end{aligned} \tag{A.5}$$

and the last term vanishes, since $\delta\boldsymbol{\sigma} \in \mathcal{S}_0(\Omega)$ is divergence-free in $\Omega$. Now, from Eq. (25e), $\mathbf{u} - \langle \mathbf{e} \rangle \cdot \mathbf{x}$ is $\Omega$-periodic. Since $\delta\boldsymbol{\sigma}$ is also $\Omega$-periodic, we have

$$\int_{\partial\Omega} \mathbf{u} \cdot \delta\boldsymbol{\sigma} \cdot \mathbf{n} \, \mathrm{d}S = \int_{\partial\Omega} (\langle \mathbf{e} \rangle \cdot \mathbf{x}) \cdot \delta\boldsymbol{\sigma} \cdot \mathbf{n} \, \mathrm{d}S. \tag{A.6}$$

Integrating again by parts, and using again the fact that, by construction, $\delta\boldsymbol{\sigma}$ is divergence-free with null average

$$\begin{aligned}\frac{1}{|\Omega|} \int_{\partial\Omega} (\langle \mathbf{e} \rangle \cdot \mathbf{x}) \cdot \delta\boldsymbol{\sigma} \cdot \mathbf{n} \, \mathrm{d}S &= \langle [(\langle \mathbf{e} \rangle \cdot \mathbf{x}) \otimes \nabla] : \delta\boldsymbol{\sigma} \rangle \\ &\quad + \langle (\langle \mathbf{e} \rangle \cdot \mathbf{x}) \cdot (\boldsymbol{\sigma} \cdot \nabla) \rangle \\ &= \langle \langle \mathbf{e} \rangle : \delta\boldsymbol{\sigma} \rangle \\ &= \langle \mathbf{e} \rangle : \langle \delta\boldsymbol{\sigma} \rangle = 0.\end{aligned} \tag{A.7}$$

Gathering the above results, we finally find that, for all $\delta\boldsymbol{\sigma} \in \mathcal{S}_0(\Omega)$

$$\begin{aligned}\Pi^{\mathrm{c}}(\boldsymbol{\sigma} + \delta\boldsymbol{\sigma}, \mathbf{e}^*, \boldsymbol{\phi}^*) = \Pi^{\mathrm{c}}(\boldsymbol{\sigma}, \mathbf{e}^*, \boldsymbol{\phi}^*) + W^{\mathrm{c}}(\delta\boldsymbol{\sigma}) \\ \geq \Pi^{\mathrm{c}}(\boldsymbol{\sigma}, \mathbf{e}^*, \boldsymbol{\phi}^*),\end{aligned} \tag{A.8}$$

since $W^{\mathrm{c}}$ is positive definite. Therefore, $\Pi^{\mathrm{c}}(\bullet, \mathbf{e}^*, \boldsymbol{\phi}^*)$ is minimum at the solution of problem (25).

*Proof that the minimizer of the complementary energy solves problem* (25). Conversely, we now assume that $\boldsymbol{\sigma}$ is a minimizer of $\Pi^{\mathrm{c}}(\bullet, \mathbf{e}^*, \boldsymbol{\phi}^*)$. Stationarity requires that the linear part of $\Pi^{\mathrm{c}}(\boldsymbol{\sigma} + \delta\boldsymbol{\sigma}, \mathbf{e}^*, \boldsymbol{\phi}^*) - \Pi^{\mathrm{c}}(\boldsymbol{\sigma}, \mathbf{e}^*, \boldsymbol{\phi}^*)$ in Eq. (A.4) must vanish for all $\delta\boldsymbol{\sigma} \in \mathcal{S}_0(\Omega)$

$$\int_\Omega (\mathbf{e} - \boldsymbol{\phi} \cdot \nabla) : \delta\boldsymbol{\sigma} \, \mathrm{d}V + \int_{\partial\Omega} \delta\boldsymbol{\sigma} : \boldsymbol{\phi} \cdot \mathbf{n} \, \mathrm{d}S = 0. \tag{A.9}$$

Considering first stress tensors $\delta\boldsymbol{\sigma}$ that vanish on $\partial\Omega$ and using a classical result by Moreau (1979), we find the existence of a vector field $\mathbf{u}$ such that

$$\mathbf{e} - \boldsymbol{\phi} \cdot \nabla = \mathbf{sym}(\mathbf{u} \otimes \nabla). \tag{A.10}$$

Plugging into Eq. (A.9), we then have for all $\delta\boldsymbol{\sigma} \in \mathcal{S}_0(\Omega)$

$$\int_{\partial\Omega} \delta\boldsymbol{\sigma} : \boldsymbol{\phi} \cdot \mathbf{n} \, \mathrm{d}S = 0, \tag{A.11}$$

which requires that $\boldsymbol{\phi} \cdot \mathbf{n}$ be $\Omega$-skew-periodic (since $\delta\boldsymbol{\sigma}$ is periodic). Substitution of Eqs. (A.10) and (A.11) in Eq. (A.9) shows that, for all $\delta\boldsymbol{\sigma} \in \mathcal{S}_0(\Omega)$

$$\int_\Omega \mathbf{sym}(\mathbf{u} \otimes \nabla) : \delta\boldsymbol{\sigma} \, \mathrm{d}V = 0, \tag{A.12}$$

and, from a classical orthogonality result (Jikov et al., 1994, §12.7), we find that $\mathbf{u} = \mathbf{F} \cdot \mathbf{x} + \mathbf{u}^{\mathrm{per}}$, where $\mathbf{F}$ is a constant tensor and $\mathbf{u}^{\mathrm{per}}$ is $\Omega$-periodic. Comparing with Eq. (A.10) and observing that $\langle \boldsymbol{\phi} \cdot \nabla \rangle = \mathbf{0}$ (since $\boldsymbol{\phi} \cdot \mathbf{n}$ is $\Omega$-skew-periodic)

$$\mathbf{F} = \langle \mathbf{e} \rangle - \langle \boldsymbol{\phi} \cdot \nabla \rangle = \langle \mathbf{e} \rangle, \tag{A.13}$$

which proves that $\mathbf{u} - \langle \mathbf{e} \rangle \cdot \mathbf{x}$ is $\Omega$-periodic. We have therefore proved that all equations of problem (25) are satisfied. In other words, the minimizer of the complementary energy $\Pi^{\mathrm{c}}$ solves problem (25). From uniqueness of this solution (Sab et al., 2016), it is further observed that this minimizer is unique, and the proof is complete.

## Appendix B. Critical value of the complementary energy – Clapeyron's theorem

In the present section, we derive a simplified expression of the minimum value of the complementary energy $\Pi^{\mathrm{c}}$. Let $\boldsymbol{\sigma} \in \overline{\boldsymbol{\sigma}} + \mathcal{S}_0(\Omega)$ denote the solution to Problem (25) [see Eq. (29)]. Then

$$\begin{aligned} \Pi^{\mathrm{c}}(\boldsymbol{\sigma}, \mathbf{e}^*, \boldsymbol{\phi}^*) &= \tfrac{1}{2} \langle \boldsymbol{\sigma} : \mathbf{S} : \boldsymbol{\sigma} + (\boldsymbol{\sigma} \otimes \nabla) \therefore \mathbf{M} \therefore (\boldsymbol{\sigma} \otimes \nabla) \rangle \\ &\quad + \langle \boldsymbol{\sigma} : \mathbf{e}^* \rangle + \langle (\boldsymbol{\sigma} \otimes \nabla) \therefore \boldsymbol{\phi}^* \rangle \\ &= \tfrac{1}{2} \langle \boldsymbol{\sigma} : (\mathbf{e} + \mathbf{e}^*) + (\boldsymbol{\sigma} \otimes \nabla) \therefore (\boldsymbol{\phi} + \boldsymbol{\phi}^*) \rangle, \end{aligned} \tag{B.1}$$

where we have introduced the constitutive relations (25b) and (25c). Then, integrating by parts the second term

$$\langle (\boldsymbol{\sigma} \otimes \nabla) \therefore \boldsymbol{\phi} \rangle = -\langle \boldsymbol{\sigma} : (\boldsymbol{\phi} \cdot \nabla) \rangle + \frac{1}{|\Omega|} \int_{\partial\Omega} \boldsymbol{\sigma} : \boldsymbol{\phi} \cdot \mathbf{n} \, \mathrm{d}S, \tag{B.2}$$

and the surface integral vanishes, since $\boldsymbol{\sigma}$ is $\Omega$-periodic, while $\boldsymbol{\phi} \cdot \mathbf{n}$ is $\Omega$-skew-periodic. Plugging into equation (B.1) and using the compatibility equation (25d)

$$2\Pi^{\mathrm{c}}(\boldsymbol{\sigma}, \mathbf{e}^*, \boldsymbol{\phi}^*) = \langle \boldsymbol{\sigma} : [\mathbf{sym}(\mathbf{u} \otimes \nabla) + \mathbf{e}^*] \rangle + \langle (\boldsymbol{\sigma} \otimes \nabla) \therefore \boldsymbol{\phi}^* \rangle. \tag{B.3}$$

Integrating again by parts and observing that $\boldsymbol{\sigma} \in \overline{\boldsymbol{\sigma}} + \mathcal{S}_0(\Omega)$ is divergence-free, we find

$$\begin{aligned} 2\Pi^{\mathrm{c}}(\boldsymbol{\sigma}, \mathbf{e}^*, \boldsymbol{\phi}^*) &= \frac{1}{|\Omega|} \int_{\partial\Omega} \mathbf{u} \cdot \boldsymbol{\sigma} \cdot \mathbf{n} \, \mathrm{d}S + \langle \boldsymbol{\sigma} : \boldsymbol{\eta} \rangle \\ &\quad + \langle (\boldsymbol{\sigma} \otimes \nabla) \therefore \boldsymbol{\phi}^* \rangle, \end{aligned} \tag{B.4}$$

and the surface integral is evaluated as follows

$$\begin{aligned} \int_{\partial\Omega} \mathbf{u} \cdot \boldsymbol{\sigma} \cdot \mathbf{n} \, \mathrm{d}S &= \int_{\partial\Omega} (\mathbf{u} - \langle \mathbf{e} \rangle \cdot \mathbf{x}) \cdot \boldsymbol{\sigma} \cdot \mathbf{n} \, \mathrm{d}S \\ &\quad + \int_{\partial\Omega} (\langle \mathbf{e} \rangle \cdot \mathbf{x}) \cdot \boldsymbol{\sigma} \cdot \mathbf{n} \, \mathrm{d}S. \end{aligned} \tag{B.5}$$

The first term vanishes since $(\mathbf{u} - \langle \mathbf{e} \rangle \cdot \mathbf{x})$ is $\Omega$-periodic; besides, the second term can again be integrated by parts

$$\begin{aligned} &\frac{1}{|\Omega|} \int_{\partial\Omega} (\langle \mathbf{e} \rangle \cdot \mathbf{x}) \cdot \boldsymbol{\sigma} \cdot \mathbf{n} \, \mathrm{d}S \\ &= \frac{1}{|\Omega|} \int_\Omega \boldsymbol{\sigma} : \langle \mathbf{e} \rangle \, \mathrm{d}V = \langle \boldsymbol{\sigma} \rangle : \langle \mathbf{e} \rangle = \overline{\boldsymbol{\sigma}} : \langle \mathbf{e} \rangle. \end{aligned} \tag{B.6}$$

Equation (28) is then readily retrieved.

## Appendix C. On the Delta operator

### *Appendix C.1. Expression in Fourier space of the Delta operator*

In the present section, we derive an expression of the Fourier components of the Delta operator. Our starting point is Problem (38), which is recalled below

$$\hat{\boldsymbol{\sigma}} \cdot \mathrm{i}\mathbf{k} = \mathbf{0}, \tag{C.1a}$$

$$\hat{\boldsymbol{\varepsilon}} = \hat{\mathbf{S}}_0^\ell : \hat{\boldsymbol{\sigma}} + \hat{\mathbf{e}}^* - \mathrm{i}\hat{\boldsymbol{\phi}}^* \cdot \mathbf{k}, \tag{C.1b}$$

$$\hat{\boldsymbol{\varepsilon}} = \mathrm{i}\,\mathbf{sym}(\hat{\mathbf{u}} \otimes \mathbf{k}), \tag{C.1c}$$

where we have dropped the lower indices for convenience. This problem is formally equivalent to the problem that defines the Delta operator for classical elasticity. The derivation of the generalized Delta operator is therefore identical to that of the classical Delta operator as outlined below [more details can be found in e.g. Suquet (1990)]. Problem (C.1) can be transformed

$$\hat{\boldsymbol{\sigma}} \cdot \mathrm{i}\mathbf{k} = \mathbf{0}, \tag{C.2a}$$

$$\hat{\boldsymbol{\sigma}} = \hat{\mathbf{C}}_0^\ell : \hat{\boldsymbol{\varepsilon}} + \hat{\boldsymbol{\tau}}, \tag{C.2b}$$

$$\hat{\boldsymbol{\varepsilon}} = \mathrm{i}\,\mathbf{sym}(\hat{\mathbf{u}} \otimes \mathbf{k}) = \mathrm{i}\mathbf{I}_4 : (\hat{\mathbf{u}} \otimes \mathbf{k}), \tag{C.2c}$$

where $\hat{\mathbf{C}}_0^\ell = (\hat{\mathbf{S}}_0^\ell)^{-1}$, $\hat{\boldsymbol{\tau}} = -\hat{\mathbf{C}}_0^\ell : \hat{\boldsymbol{\eta}}$ and $\hat{\boldsymbol{\eta}} = \hat{\mathbf{e}}^* - \mathrm{i}\hat{\boldsymbol{\phi}}^* \cdot \mathbf{k}$. Note that in Eq. (C.2c), we have used the fact that double contraction with

$\mathbf{I}_4$ is equivalent with symmetrization. Plugging Eq. (C.2c) into Eq. (C.2b), we find

$$\hat{\boldsymbol{\sigma}} = \mathrm{i}(\hat{\mathbf{C}}_0^\ell \cdot \mathbf{k}) \cdot \hat{\mathbf{u}} + \hat{\boldsymbol{\tau}}, \tag{C.3}$$

which, upon substitution in Eq. (C.2a) delivers the following linear relationship between $\hat{\mathbf{u}}$ and $\hat{\boldsymbol{\tau}}$

$$\hat{\mathbf{A}}_0^\ell \cdot \hat{\mathbf{u}} = \mathrm{i}\hat{\boldsymbol{\tau}} \cdot \mathbf{k}, \quad \text{with} \quad \hat{\mathbf{A}}_0^\ell(\mathbf{k}) = \mathbf{k} \cdot \hat{\mathbf{C}}_0^\ell(\mathbf{k}) \cdot \mathbf{k}. \tag{C.4}$$

Assuming that the "acoustic tensor" $\hat{\mathbf{A}}_0^\ell$ is non-singular (for $\mathbf{k} \neq \mathbf{0}$), we find from Eq. (C.4) (owing to the symmetry of $\hat{\boldsymbol{\tau}}$)

$$\hat{\mathbf{u}} = \mathrm{i}\hat{\mathbf{B}}_0^\ell \cdot (\hat{\boldsymbol{\tau}} \cdot \mathbf{k}) = \mathrm{i}(\hat{\mathbf{B}}_0^\ell \otimes \mathbf{k}) : \hat{\boldsymbol{\tau}} = \mathrm{i}[(\hat{\mathbf{B}}_0^\ell \otimes \mathbf{k}) : \mathbf{I}_4] : \hat{\boldsymbol{\tau}}, \tag{C.5}$$

where we have introduced the inverse $\hat{\mathbf{B}}_0^\ell$ of $\hat{\mathbf{A}}_0^\ell$. Then, using Eq. (C.2c)

$$\hat{\boldsymbol{\varepsilon}} = -\hat{\boldsymbol{\Gamma}}_0 : \hat{\boldsymbol{\tau}} \quad \text{with} \quad \hat{\boldsymbol{\Gamma}}_0 = \mathbf{I}_4 : [\mathbf{k} \otimes \hat{\mathbf{B}}_0^\ell \otimes \mathbf{k}] : \mathbf{I}_4. \tag{C.6}$$

The above expression is the extension to stress-gradient materials of the classical Gamma operator that relates the eigenstress $\boldsymbol{\tau}$ to the strain $\boldsymbol{\varepsilon}$ (Korringa, 1973; Kröner, 1974; Zeller and Dederichs, 1973). The stresses are finally deduced from Eq. (C.2b) and the definition of $\hat{\boldsymbol{\tau}}$

$$\begin{aligned}\hat{\boldsymbol{\sigma}} &= \hat{\mathbf{C}}_0^\ell : \hat{\boldsymbol{\varepsilon}} + \hat{\boldsymbol{\tau}} = -\hat{\mathbf{C}}_0^\ell : \hat{\boldsymbol{\Gamma}}_0 : \hat{\boldsymbol{\tau}} + \hat{\boldsymbol{\tau}} \\ &= \hat{\mathbf{C}}_0^\ell : \hat{\boldsymbol{\Gamma}}_0 : \hat{\mathbf{C}}_0^\ell : \hat{\boldsymbol{\eta}} - \hat{\mathbf{C}}_0^\ell : \hat{\boldsymbol{\eta}},\end{aligned} \tag{C.7}$$

and finally

$$\hat{\boldsymbol{\Delta}}_0(\mathbf{k}) = \hat{\mathbf{C}}_0^\ell(\mathbf{k}) - \hat{\mathbf{C}}_0^\ell(\mathbf{k}) : \hat{\boldsymbol{\Gamma}}_0(\mathbf{k}) : \hat{\mathbf{C}}_0^\ell(\mathbf{k}). \tag{C.8}$$

**Remark 6.** *The above derivation does not apply to the case* $\mathbf{k} = \mathbf{0}$*, since the acoustic tensor* $\hat{\mathbf{A}}_0^\ell$ *is singular. Since the average stress is required to vanish in the solution to Problem* (31) *when* $\overline{\boldsymbol{\sigma}} = \mathbf{0}$*, we must prescribe* $\hat{\boldsymbol{\Delta}}_0(\mathbf{k}) = \mathbf{0}$*.*

**Remark 7.** *Expressions* (C.6) *and* (C.8) *of the Gamma and Delta operators are unchanged for boundary conditions at infinity. In this case, the Fourier coefficients* $\hat{\mathbf{u}}_n$*,* $\hat{\boldsymbol{\phi}}_n$ *and* $\hat{\boldsymbol{\sigma}}_n$ *are to be replaced with the Fourier transforms* $\hat{\mathbf{u}}$*,* $\hat{\boldsymbol{\phi}}$ *and* $\hat{\boldsymbol{\sigma}}$ *and the synthesis formula* (40) *reads*

$$\boldsymbol{\sigma}(\mathbf{x}) = -(2\pi)^{-3} \int_{\mathbb{R}^3} \hat{\boldsymbol{\Delta}}_0(\mathbf{k}) : \hat{\boldsymbol{\eta}}(\mathbf{k}) \mathrm{e}^{\mathrm{i}\mathbf{k}\cdot\mathbf{x}} \, \mathrm{d}V_{\mathbf{k}}. \tag{C.9}$$

*Appendix C.2. The case of isotropic materials*

In this section, we derive the expression of the Delta operator for isotropic stress-gradient materials. The tensors $\mathbf{S}_0$ and $\mathbf{M}_0$ being in this case isotropic, the fourth-rank tensor $\hat{\mathbf{S}}_0^\ell(\mathbf{k})$ defined by Eq. (36) is transverse isotropic and is expanded in Walpole's basis (Walpole, 1984), which is recalled in Appendix G. We will find, formally

$$\hat{\mathbf{S}}_0^\ell = a\mathbf{E}^{\mathrm{I}} + b\mathbf{E}^{\mathrm{II}} + c(\mathbf{E}^{\mathrm{III}} + \mathbf{E}^{\mathrm{IV}}) + f\mathbf{F} + g\mathbf{G} = \{\left[\begin{smallmatrix} a & c \\ c & b \end{smallmatrix}\right], f, g\}, \tag{C.10}$$

where we used the compact notation introduced in Appendix G. In the above expansion, it is observed that the coefficients of $\mathbf{E}^{\mathrm{III}}$ and $\mathbf{E}^{\mathrm{IV}}$ are identical owing to major symmetry. Inversion delivers the non-local stiffness

$$\hat{\mathbf{C}}_0^\ell = \{d^{-1}\left[\begin{smallmatrix} b & -c \\ -c & a \end{smallmatrix}\right], 1/f, 1/g\} \quad \text{with} \quad d = ab - c^2. \tag{C.11}$$

Then, the acoustic tensor $\hat{\mathbf{A}}_0^\ell$ defined by Eq. (C.4) is obtained from Eq. (G.6)

$$\hat{\mathbf{A}}_0^\ell(\mathbf{k}) = k^2 \mathbf{n} \cdot \hat{\mathbf{C}}_0^\ell(\mathbf{k}) \cdot \mathbf{n} = k^2\Big(\frac{b}{d}\mathbf{p} + \frac{1}{2g}\mathbf{q}\Big). \tag{C.12}$$

For the inversion of the acoustic tensor, it is recalled that $\mathbf{p}$ and $\mathbf{q}$ are two mutually orthogonal projectors, which results in

$$\hat{\mathbf{B}}_0^\ell(\mathbf{k}) = \frac{1}{k^2}\Big(\frac{d}{b}\mathbf{p} + 2g\mathbf{q}\Big) \tag{C.13}$$

and

$$\mathbf{n} \otimes \hat{\mathbf{B}}_0^\ell(\mathbf{k}) \otimes \mathbf{n} = \frac{d}{b}\mathbf{n} \otimes \mathbf{p} \otimes \mathbf{n} + 2g\mathbf{n} \otimes \mathbf{q} \otimes \mathbf{n}. \tag{C.14}$$

Finally, using Eq. (G.2)

$$\hat{\boldsymbol{\Gamma}}_0 = \mathbf{I}_4 : [\mathbf{n} \otimes \hat{\mathbf{B}}_0^\ell(\mathbf{k}) \otimes \mathbf{n}] : \mathbf{I}_4 = \frac{d}{b}\mathbf{E}^{\mathrm{I}} + g\mathbf{G} = \{\left[\begin{smallmatrix} d/b & 0 \\ 0 & 0 \end{smallmatrix}\right], 0, g\}, \tag{C.15}$$

from which it results, using Eq. (C.8)

$$\begin{aligned}\hat{\boldsymbol{\Delta}}_0 &= \{d^{-1}\left[\begin{smallmatrix} b & -c \\ -c & a \end{smallmatrix}\right], 1/f, 1/g\} - \{d^{-1}\left[\begin{smallmatrix} b & -c \\ -c & c^2/b \end{smallmatrix}\right], 0, 1/g\} \\ &= \{\left[\begin{smallmatrix} 0 & 0 \\ 0 & 1/b \end{smallmatrix}\right], 1/f\} = \frac{\mathbf{E}^{\mathrm{II}}}{b} + \frac{\mathbf{F}}{f}.\end{aligned} \tag{C.16}$$

In other words, to compute the Delta operator of isotropic materials, it is sufficient to evaluate the $\mathbf{E}^{\mathrm{I}}$ and $\mathbf{F}$ coefficients of the expansion in Walpole's basis of the non-local compliance defined by Eq. (36).

*Appendix C.3. The simplified model of Tran et al. (2018)*

In the present section, we compute the coefficients $b$ and $f$ introduced above for the simplified model of Tran et al. (2018) defined by Eq. (18). It results from Eq. (36) that, for all $\mathbf{x}, \mathbf{y} \in \mathcal{T}_2$

$$\mathbf{x} : \hat{\mathbf{S}}_0^\ell(\mathbf{k}) : \mathbf{y} = \mathbf{x} : \mathbf{S}_0 : \mathbf{y} + k^2(\mathbf{x} \otimes \mathbf{n}) \therefore \mathbf{M}_0 \therefore (\mathbf{y} \otimes \mathbf{n}), \tag{C.17}$$

with $k = \|\mathbf{k}\|$ and $\mathbf{n} = \mathbf{k}/k$. Since the generalized compliance $\mathbf{M}_0$ is a linear combination of $\mathbf{I}_6'$ and $\mathbf{J}_6'$ [see Eq. (18)], evaluation of $\hat{\mathbf{S}}_0^\ell$ requires the evaluation of $(\mathbf{x} \otimes \mathbf{n}) \therefore \mathbf{I}_6' \therefore (\mathbf{y} \otimes \mathbf{n})$ and $(\mathbf{x} \otimes \mathbf{n}) \therefore \mathbf{J}_6' \therefore (\mathbf{y} \otimes \mathbf{n})$. From Eq. (7), we have

$$\mathbf{I}_6' \therefore (\mathbf{y} \otimes \mathbf{n}) = \mathbf{y} \otimes \mathbf{n} - \tfrac{1}{2}\mathbf{I}_4 \cdot (\mathbf{y} \otimes \mathbf{n}) : \mathbf{I}_2 = \mathbf{y} \otimes \mathbf{n} - \tfrac{1}{2}\mathbf{I}_4 \cdot \mathbf{y} \cdot \mathbf{n}, \tag{C.18}$$

and

$$\begin{aligned}(\mathbf{x} \otimes \mathbf{n}) \therefore \mathbf{I}_6' \therefore (\mathbf{y} \otimes \mathbf{n}) &= (\mathbf{x} \otimes \mathbf{n}) \therefore (\mathbf{y} \otimes \mathbf{n} - \tfrac{1}{2}\mathbf{I}_4 \cdot \mathbf{y} \cdot \mathbf{n}) \\ &= \mathbf{x} : \mathbf{y} - \tfrac{1}{2}(\mathbf{x} \otimes \mathbf{n}) \therefore \mathbf{I}_4 \cdot \mathbf{y} \cdot \mathbf{n} \\ &= \mathbf{x} : \mathbf{y} - \tfrac{1}{2}\mathbf{x} : \mathbf{I}_4 : [\mathbf{n} \otimes (\mathbf{y} \cdot \mathbf{n})] \\ &= \mathbf{x} : \mathbf{y} - \tfrac{1}{2}(\mathbf{x} \cdot \mathbf{n}) \cdot (\mathbf{y} \cdot \mathbf{n}) \\ &= \mathbf{x} : (\mathbf{I}_4 - \tfrac{1}{2}\mathbf{n} \otimes \mathbf{I}_2 \otimes \mathbf{n}) : \mathbf{y}.\end{aligned}$$

(C.19)

Since $\mathbf{x}$ and $\mathbf{y}$ are symmetric, we can perform the substitutions $\mathbf{x} \to \mathbf{I}_4 : \mathbf{x}$ and $\mathbf{y} \to \mathbf{I}_4 : \mathbf{y}$

$$\mathbf{x} : (\mathbf{I}_4 - \mathbf{n}\otimes\mathbf{I}_2\otimes\mathbf{n}) : \mathbf{y} = \mathbf{x} : [\mathbf{I}_4 - \tfrac{1}{2}\mathbf{I}_4 : (\mathbf{n}\otimes\mathbf{I}_2\otimes\mathbf{n}) : \mathbf{I}_4] : \mathbf{y} \quad \text{(C.20)}$$

and finally, using Eqs. (G.2) and (G.3)

$$(\mathbf{x}\otimes\mathbf{n}) \therefore \mathbf{I}'_6 \therefore (\mathbf{y}\otimes\mathbf{n}) = \mathbf{x} : (\tfrac{1}{2}\mathbf{E}^{\mathrm{I}} + \mathbf{E}^{\mathrm{II}} + \mathbf{F} + \tfrac{3}{4}\mathbf{G}) : \mathbf{y}. \quad \text{(C.21)}$$

We now turn to the $(\mathbf{x}\otimes\mathbf{n}) \therefore \mathbf{J}'_6 \therefore (\mathbf{y}\otimes\mathbf{n})$ term. From Eq. (7), we have

$$\begin{aligned}\mathbf{I}'_6 \therefore (\mathbf{I}_2\otimes\mathbf{e}_k) &= \mathbf{I}_2\otimes\mathbf{e}_k - \tfrac{1}{2}\mathbf{I}_4\cdot(\mathbf{I}_2\otimes\mathbf{e}_k) : \mathbf{I}_2 \\ &= \mathbf{I}_2\otimes\mathbf{e}_k - \tfrac{1}{2}\mathbf{I}_4\cdot\mathbf{e}_k \end{aligned} \quad \text{(C.22)}$$

and Eq. (8) shows that

$$\mathbf{J}_6 = \tfrac{2}{5}\delta_{ij}(\mathbf{I}_2\otimes\mathbf{e}_i - \tfrac{1}{2}\mathbf{I}_4\cdot\mathbf{e}_i)\otimes(\mathbf{I}_2\otimes\mathbf{e}_j - \tfrac{1}{2}\mathbf{I}_4\cdot\mathbf{e}_j). \quad \text{(C.23)}$$

Then

$$(\mathbf{I}_2\otimes\mathbf{e}_j - \tfrac{1}{2}\mathbf{I}_4\cdot\mathbf{e}_j) \therefore (\mathbf{y}\otimes\mathbf{n}) = n_j\mathbf{I}_2 : \mathbf{y} - \tfrac{1}{2}\mathbf{y} : (\mathbf{e}_j\otimes\mathbf{n}) \quad \text{(C.24)}$$

and

$$\begin{aligned}&\tfrac{5}{2}(\mathbf{x}\otimes\mathbf{n}) \therefore \mathbf{J}_6 \therefore (\mathbf{y}\otimes\mathbf{n}) \\ &\quad= \delta_{ij}[n_i\mathbf{I}_2 : \mathbf{x} - \tfrac{1}{2}\mathbf{x} : (\mathbf{n}\otimes\mathbf{e}_i)][n_j\mathbf{I}_2 : \mathbf{y} - \tfrac{1}{2}\mathbf{y} : (\mathbf{e}_j\otimes\mathbf{n})] \\ &\quad= \mathbf{x} : (\mathbf{I}_2\otimes\mathbf{I}_2 - \tfrac{1}{2}\mathbf{I}_2\otimes\mathbf{n}\otimes\mathbf{n} - \tfrac{1}{2}\mathbf{n}\otimes\mathbf{n}\otimes\mathbf{I}_2 + \tfrac{1}{4}\mathbf{n}\otimes\mathbf{I}_2\otimes\mathbf{n}) : \mathbf{y} \\ &\quad= \mathbf{x} : (\mathbf{I}_2\otimes\mathbf{I}_2 - \tfrac{1}{2}\mathbf{I}_2\otimes\mathbf{p} - \tfrac{1}{2}\mathbf{p}\otimes\mathbf{I}_2 + \tfrac{1}{4}\mathbf{n}\otimes\mathbf{I}_2\otimes\mathbf{n}) : \mathbf{y}.\end{aligned} \quad \text{(C.25)}$$

Replacing $\mathbf{I}_2$ with $\mathbf{p}+\mathbf{q}$, observing again that the symmetric tensors $\mathbf{x}$ and $\mathbf{y}$ can be replaced with $\mathbf{I}_4 : \mathbf{x}$ and $\mathbf{I}_4 : \mathbf{y}$, respectively, and using Eq. (G.3), we find that

$$\begin{aligned}&(\mathbf{x}\otimes\mathbf{n}) \therefore \mathbf{J}_6 \therefore (\mathbf{y}\otimes\mathbf{n}) \\ &\quad= \tfrac{2}{5}\mathbf{x} : (\mathbf{q}\otimes\mathbf{q} + \tfrac{1}{2}\mathbf{p}\otimes\mathbf{q} + \tfrac{1}{2}\mathbf{q}\otimes\mathbf{p} + \tfrac{1}{4}\mathbf{n}\otimes\mathbf{I}_2\otimes\mathbf{n}) : \mathbf{y} \\ &\quad= \tfrac{2}{5}\mathbf{x} : [2\mathbf{E}^{\mathrm{II}} + \tfrac{1}{2}\sqrt{2}(\mathbf{E}^{\mathrm{III}} + \mathbf{E}^{\mathrm{IV}}) + \tfrac{1}{4}\mathbf{n}\otimes\mathbf{I}_2\otimes\mathbf{n}] : \mathbf{y} \\ &\quad= \tfrac{2}{5}\mathbf{x} : [2\mathbf{E}^{\mathrm{II}} + \tfrac{1}{2}\sqrt{2}(\mathbf{E}^{\mathrm{III}} + \mathbf{E}^{\mathrm{IV}}) + \mathbf{I}_4 : (\mathbf{n}\otimes\mathbf{I}_2\otimes\mathbf{n}) : \mathbf{I}_4] : \mathbf{y} \\ &\quad= \mathbf{x} : [\tfrac{1}{10}\mathbf{E}^{\mathrm{I}} + \tfrac{4}{5}\mathbf{E}^{\mathrm{II}} + \tfrac{1}{5}\sqrt{2}(\mathbf{E}^{\mathrm{III}} + \mathbf{E}^{\mathrm{IV}}) + \tfrac{1}{20}\mathbf{G}] : \mathbf{y}.\end{aligned} \quad \text{(C.26)}$$

Gathering the above results, we get

$$\begin{aligned}&[16\mu_0(1+\nu_0)](\mathbf{x}\otimes\mathbf{n}) \therefore \mathbf{M}_0 \therefore (\mathbf{y}\otimes\mathbf{n}) \\ &\quad= \ell_0^2\mathbf{x} : [2(2+\nu_0)\mathbf{E}^{\mathrm{I}} + 8(1-\nu_0)\mathbf{E}^{\mathrm{II}} - 4\nu_0\sqrt{2}(\mathbf{E}^{\mathrm{III}} + \mathbf{E}^{\mathrm{IV}}) \\ &\qquad + 8(1+\nu_0)\mathbf{F} + (6+5\nu_0)\mathbf{G}] : \mathbf{y}\end{aligned} \quad \text{(C.27)}$$

and the non-local elasticity operator $\hat{\mathbf{S}}_0^{\ell}(\mathbf{k})$ reads

$$\begin{aligned}\hat{\mathbf{S}}_0^{\ell}(\mathbf{k}) = &\frac{4 + k^2\ell_0^2(2+\nu_0)}{8\mu_0(1+\nu_0)}\mathbf{E}^{\mathrm{I}} + \frac{(1+k^2\ell_0^2)(1-\nu_0)}{2\mu_0(1+\nu_0)}\mathbf{E}^{\mathrm{II}} \\ &- \frac{\nu_0\sqrt{2}(2+k^2\ell_0^2)}{4\mu_0(1+\nu_0)}(\mathbf{E}^{\mathrm{III}} + \mathbf{E}^{\mathrm{IV}}) + \frac{1+k^2\ell_0^2}{2\mu_0}\mathbf{F} \\ &+ \frac{8(1+\nu_0) + k^2\ell_0^2(6+5\nu_0)}{16\mu_0(1+\nu_0)}\mathbf{G}\end{aligned} \quad \text{(C.28)}$$

and

$$b = \frac{(1+k^2\ell_0^2)(1-\nu_0)}{2\mu_0(1+\nu_0)} \quad \text{and} \quad f = \frac{1+k^2\ell_0^2}{2\mu_0}. \quad \text{(C.29)}$$

Finally, Eqs. (C.16) and (C.29) deliver the closed-form expression of the Delta operator

$$\hat{\boldsymbol{\Delta}}_0(\mathbf{k}) = \frac{2\mu_0}{1+k^2\ell_0^2}\Big(\frac{1-\nu_0}{1+\nu_0}\mathbf{E}^{\mathrm{II}} + \mathbf{F}\Big). \quad \text{(C.30)}$$

Quite remarkably, for the simplified model of Tran et al. (2018), the Fourier components of the generalized Delta operator are deduced from its classical counterpart by the substitution $\mu_0 \to \mu_0/(1+k^2\ell_0^2)$ [see Eq. (44)].

The total contractions of $\hat{\boldsymbol{\Delta}}_0$ with the tensors $\mathbf{J}_4$ and $\mathbf{K}_4$ will also be used

$$\mathbf{J}_4 :: \hat{\boldsymbol{\Delta}}_0(\mathbf{k}) = \frac{4\mu_0}{3(1+k^2\ell_0^2)}\frac{1+\nu_0}{1-\nu_0}, \quad \text{(C.31a)}$$

$$\mathbf{K}_4 :: \hat{\boldsymbol{\Delta}}_0(\mathbf{k}) = \frac{2\mu_0}{3(1+k^2\ell_0^2)}\frac{7-5\nu_0}{1-\nu_0}. \quad \text{(C.31b)}$$

It is recalled that the orthogonal (in the sense of the ":" scalar product) projection $\mathbf{iso}\,\mathbf{T}$ of a fourth-order tensor $\mathbf{T} \in \mathcal{T}_4$ onto the space of isotropic, fourth-order tensors reads

$$\mathbf{iso}\,\mathbf{T} = [(\mathbf{J}_4 :: \mathbf{T})\mathbf{J}_4 + \tfrac{1}{5}(\mathbf{K}_4 :: \mathbf{T})\mathbf{K}_4] \quad \text{(C.32)}$$

and it is found from Eq. (C.31) that

$$\mathbf{iso}\,\hat{\boldsymbol{\Delta}}_0(\mathbf{k}) = (1+k^2\ell_0^2)^{-1}\mathbf{Q}_0, \quad \text{(C.33)}$$

where $\mathbf{Q}_0$ is defined by Eq. (82). Similarly, it can readily be verified that the angular average of $\hat{\boldsymbol{\Delta}}_0$ coincides with its isotropic projection

$$\frac{1}{4\pi}\int_{\|\mathbf{n}\|=1}\hat{\boldsymbol{\Delta}}_0(k\mathbf{n})\,\mathrm{d}V_{\mathbf{n}} = (1+k^2\ell_0^2)^{-1}\mathbf{Q}_0, \quad \text{(C.34)}$$

which extends the well-known expression of the isotropic average of the classical Green operator (Willis, 1977).

## Appendix D. On the Hashin–Shtrikman principle

In the present section, we prove the results stated in Sec. 6. We first show that the critical value of the functional of Hashin and Shtrikman is given by Eq. (62). Then we address the *maximum* of the functional. Finally, we discuss its *minimum*.

### *Appendix D.1. Critical value of the functional of Hashin and Shtrikman*

In order to prove identity (62), we first plug Eq. (61) in Eq. (59)

$$\begin{aligned}\mathrm{HS}(\mathbf{e}^*_{\mathrm{crit}}, \boldsymbol{\phi}^*_{\mathrm{crit}}, \overline{\boldsymbol{\sigma}}) = &\tfrac{1}{2}\overline{\boldsymbol{\sigma}} : \mathbf{S}_0 : \overline{\boldsymbol{\sigma}} + \overline{\boldsymbol{\sigma}} : \langle\mathbf{e}^*_{\mathrm{crit}}\rangle - \tfrac{1}{2}\langle\boldsymbol{\sigma} : \mathbf{e}^*_{\mathrm{crit}}\rangle \\ &- \tfrac{1}{2}\langle(\boldsymbol{\sigma}\otimes\nabla) \therefore \boldsymbol{\phi}^*_{\mathrm{crit}}\rangle \\ &- \tfrac{1}{2}\sum_{n\in\mathbb{Z}^3}\mathrm{conj}(\hat{\boldsymbol{\eta}}_{\mathrm{crit},n}) : \hat{\boldsymbol{\Delta}}_0(\mathbf{k}_n) : \hat{\boldsymbol{\eta}}_{\mathrm{crit},n},\end{aligned} \quad \text{(D.1)}$$

with $\hat{\boldsymbol{\eta}}_{\mathrm{crit},n} = \hat{\mathbf{e}}^*_{\mathrm{crit},n} - \mathrm{i}\hat{\boldsymbol{\phi}}^*_{\mathrm{crit},n} \cdot \mathbf{k}_n$. We then observe that $\hat{\boldsymbol{\Delta}}_0(\mathbf{k}_n) : \hat{\boldsymbol{\eta}}_{\mathrm{crit},n}$ is the $n$-th Fourier coefficient of $-\boldsymbol{\sigma}$ for $n \neq (0,0,0)$ [see Eq. (40)] and that, for $n = (0,0,0)$, $\hat{\boldsymbol{\sigma}}_0 = \overline{\boldsymbol{\sigma}}$ and $\hat{\boldsymbol{\eta}}_{\mathrm{crit},0} = \hat{\mathbf{e}}^*_{\mathrm{crit},0} = \langle \mathbf{e}^*_{\mathrm{crit}} \rangle$ we rewrite the last sum in Eq. (59)

$$\begin{aligned}
&\sum_{n\in\mathbb{Z}^3} \mathrm{conj}(\hat{\boldsymbol{\eta}}_{\mathrm{crit},n}) : \hat{\boldsymbol{\Delta}}_0(\mathbf{k}_n) : \hat{\boldsymbol{\eta}}_{\mathrm{crit},n} \\
&= -\sum_{n\in\mathbb{Z}^3} \mathrm{conj}(\hat{\boldsymbol{\eta}}_{\mathrm{crit},n}) : \hat{\boldsymbol{\sigma}}_n + \hat{\boldsymbol{\eta}}_{\mathrm{crit},0} : \hat{\boldsymbol{\sigma}}_0 \\
&= -\sum_{n\in\mathbb{Z}^3} [\mathrm{conj}(\hat{\mathbf{e}}^*_{\mathrm{crit},n}) : \hat{\boldsymbol{\sigma}}_n + \mathrm{conj}(\hat{\boldsymbol{\phi}}^*_{\mathrm{crit},n}) \therefore (\hat{\boldsymbol{\sigma}}_n \otimes \mathrm{i}\mathbf{k}_n)] + \overline{\boldsymbol{\sigma}} : \langle \mathbf{e}^*_{\mathrm{crit}} \rangle \\
&= -\langle \boldsymbol{\sigma} : \mathbf{e}^*_{\mathrm{crit}} \rangle - \langle (\boldsymbol{\sigma} \otimes \nabla) \therefore \boldsymbol{\phi}^*_{\mathrm{crit}} \rangle + \overline{\boldsymbol{\sigma}} : \langle \mathbf{e}^*_{\mathrm{crit}} \rangle.
\end{aligned} \tag{D.2}$$

In the last line, we have again used Parseval's identity, together with the fact that $\hat{\boldsymbol{\sigma}}_n \otimes \mathrm{i}\mathbf{k}_n$ is the $n$-th Fourier coefficient of $\boldsymbol{\sigma} \otimes \nabla$. Gathering the above results, we find

$$\begin{aligned}
\mathrm{HS}(\mathbf{e}^*_{\mathrm{crit}}, \boldsymbol{\phi}^*_{\mathrm{crit}}, \overline{\boldsymbol{\sigma}}) &= \tfrac{1}{2}\overline{\boldsymbol{\sigma}} : \mathbf{S}_0 : \overline{\boldsymbol{\sigma}} + \tfrac{1}{2}\overline{\boldsymbol{\sigma}} : \langle \mathbf{e}^*_{\mathrm{crit}} \rangle \\
&= \tfrac{1}{2}\overline{\boldsymbol{\sigma}} : \langle \mathbf{S}_0 : \boldsymbol{\sigma} + \mathbf{e}^*_{\mathrm{crit}} \rangle = \tfrac{1}{2}\overline{\boldsymbol{\sigma}} : \langle \mathbf{e} \rangle,
\end{aligned} \tag{D.3}$$

which proves Eq. (62).

### *Appendix D.2. Maximum of the functional of Hashin and Shtrikman*

In the present section, we show that if $\mathbf{S} \geq \mathbf{S}_0$ and $\mathbf{M} \geq \mathbf{M}_0$ at any point of the SVE, then the Hashin–Shtrikman functional is maximum at the solution to problem (21), (23). The proof follows closely that of Willis (1991). The arbitrary tensors $\mathbf{e}^* \in \mathcal{T}_2$ and $\boldsymbol{\phi}^* \in \mathcal{T}'_3$ being fixed, let

$$\begin{aligned}
u(\mathbf{e}^*, \boldsymbol{\phi}^*) = \sup_{\boldsymbol{\sigma},\mathbf{R}} \{ &\boldsymbol{\sigma} : \boldsymbol{\eta}_2 + \mathbf{R} \therefore \boldsymbol{\eta}_3 - \tfrac{1}{2}\boldsymbol{\sigma} : (\mathbf{S} - \mathbf{S}_0) : \boldsymbol{\sigma} \\
&- \tfrac{1}{2}\mathbf{R} \therefore (\mathbf{M} - \mathbf{M}_0) \therefore \mathbf{R} \},
\end{aligned} \tag{D.4}$$

where $\boldsymbol{\sigma} \in \mathcal{T}_2$ and $\mathbf{R} \in \mathcal{T}'_3$ are fixed. Trivially,

$$u(\mathbf{e}^*, \boldsymbol{\phi}^*) = \tfrac{1}{2}\mathbf{e}^* : (\mathbf{S} - \mathbf{S}_0)^{-1} : \mathbf{e}^* + \tfrac{1}{2}\boldsymbol{\phi}^* \therefore (\mathbf{M} - \mathbf{M}_0)^{-1} \therefore \boldsymbol{\phi}^*, \tag{D.5}$$

and, for all $\boldsymbol{\sigma}, \mathbf{e}^* \in \mathcal{T}_2$ and $\mathbf{R}, \boldsymbol{\phi}^* \in \mathcal{T}'_3$

$$\begin{aligned}
\tfrac{1}{2}\boldsymbol{\sigma} : \mathbf{S} : \boldsymbol{\sigma} + \tfrac{1}{2}\mathbf{R} \therefore \mathbf{M} \therefore \mathbf{R} \geq \tfrac{1}{2}\boldsymbol{\sigma} : \mathbf{S}_0 : \boldsymbol{\sigma} \\
+ \tfrac{1}{2}\mathbf{R} \therefore \mathbf{M}_0 \therefore \mathbf{R} + \boldsymbol{\sigma} : \mathbf{e}^* + \mathbf{R} \therefore \boldsymbol{\phi}^* - u(\mathbf{e}^*, \boldsymbol{\phi}^*).
\end{aligned} \tag{D.6}$$

In the above inequality, all tensors but $\mathbf{S}_0$ and $\mathbf{M}_0$ can be seen as tensor *fields*. In particular, for $\boldsymbol{\sigma} \in \overline{\boldsymbol{\sigma}} + \mathcal{S}_0(\Omega)$ and $\mathbf{R} = \boldsymbol{\sigma} \otimes \nabla \in \mathcal{T}'_3(\Omega)$, integration over the whole domain $\Omega$ delivers

$$W^{\mathrm{c}}(\boldsymbol{\sigma}) \geq \Pi^{\mathrm{c}}_0(\boldsymbol{\sigma}, \mathbf{e}^*, \boldsymbol{\phi}^*) - \langle u(\mathbf{e}^*, \boldsymbol{\phi}^*) \rangle, \tag{D.7}$$

with

$$\begin{aligned}
\langle u(\mathbf{e}^*, \boldsymbol{\phi}^*) \rangle = \tfrac{1}{2}\langle \mathbf{e}^* : (\mathbf{S} - \mathbf{S}_0)^{-1} : \mathbf{e}^* \rangle \\
+ \tfrac{1}{2}\langle \boldsymbol{\phi}^* \therefore (\mathbf{M} - \mathbf{M}_0)^{-1} \therefore \boldsymbol{\phi}^* \rangle.
\end{aligned} \tag{D.8}$$

Then, taking the infimum with respect to $\boldsymbol{\sigma} \in \overline{\boldsymbol{\sigma}} + \mathcal{S}_0(\Omega)$

$$\tfrac{1}{2}\overline{\boldsymbol{\sigma}} : \mathbf{S}^{\mathrm{eff}} : \overline{\boldsymbol{\sigma}} \geq \min_{\overline{\boldsymbol{\sigma}} + \mathcal{S}_0(\Omega)} \Pi^{\mathrm{c}}_0(\bullet, \mathbf{e}^*, \boldsymbol{\phi}^*) - \langle u(\mathbf{e}^*, \boldsymbol{\phi}^*) \rangle, \tag{D.9}$$

and Eq. (63) is a direct consequence of Eq. (60).

### *Appendix D.3. Minimum of the functional of Hashin and Shtrikman*

In the present section, we show that if $\mathbf{S} \leq \mathbf{S}_0$ and $\mathbf{M} \leq \mathbf{M}_0$ at any point of the SVE, then the Hashin–Shtrikman functional is minimum at the solution to problem (21) $\wedge$ (23). We follow closely the proof presented by Willis in the Appendix of his paper (Willis, 1977). We first observe that

$$\mathbf{S}_0 : (\mathbf{S} - \mathbf{S}_0)^{-1} : \mathbf{S}_0 = (\mathbf{C}_0 - \mathbf{C})^{-1} - \mathbf{S}_0, \tag{D.10a}$$

$$\mathbf{M}_0 \therefore (\mathbf{M} - \mathbf{M}_0)^{-1} \therefore \mathbf{M}_0 = (\mathbf{L}_0 - \mathbf{L})^{-1} - \mathbf{M}_0, \tag{D.10b}$$

where inversion in Eq. (D.10b) is performed in the space $\mathcal{T}'_3$ of trace-free, third-order tensors. It results from Eqs. (D.10a) and (D.10b) that

$$\begin{aligned}
\langle \mathbf{e}^* : (\mathbf{S} - \mathbf{S}_0)^{-1} : \mathbf{e}^* \rangle = \langle \boldsymbol{\sigma}^* : (\mathbf{C}_0 - \mathbf{C})^{-1} : \boldsymbol{\sigma}^* \rangle \\
- \langle \mathbf{e}^* : \mathbf{C}_0 : \mathbf{e}^* \rangle
\end{aligned} \tag{D.11a}$$

$$\begin{aligned}
\langle \boldsymbol{\phi}^* \therefore (\mathbf{M} - \mathbf{M}_0)^{-1} \therefore \boldsymbol{\phi}^* \rangle = \langle \mathbf{R}^* \therefore (\mathbf{L}_0 - \mathbf{L})^{-1} \therefore \mathbf{R}^* \rangle \\
- \langle \boldsymbol{\phi}^* \therefore \mathbf{L}_0 \therefore \boldsymbol{\phi}^* \rangle,
\end{aligned} \tag{D.11b}$$

where $\boldsymbol{\sigma}^* = -\mathbf{C}_0 : \mathbf{e}^*$ and $\mathbf{R}^* = -\mathbf{L}_0 \therefore \boldsymbol{\phi}^*$. Combining Eqs. (47) and (60) with the above results, we find

$$\begin{aligned}
2\,\mathrm{HS}(\mathbf{e}^*, \boldsymbol{\phi}^*, \overline{\boldsymbol{\sigma}}) = \overline{\boldsymbol{\sigma}} : \mathbf{S}_0 : \overline{\boldsymbol{\sigma}} + \overline{\boldsymbol{\sigma}} : \langle \mathbf{e}^* \rangle \\
+ \langle \boldsymbol{\sigma} : \mathbf{e}^* \rangle + \langle \mathbf{e}^* : \mathbf{C}_0 : \mathbf{e}^* \rangle \\
+ \langle (\boldsymbol{\sigma} \otimes \nabla) \therefore \boldsymbol{\phi}^* \rangle + \langle \boldsymbol{\phi}^* \therefore \mathbf{L}_0 \therefore \boldsymbol{\phi}^* \rangle \\
- \langle \boldsymbol{\sigma}^* : (\mathbf{C}_0 - \mathbf{C})^{-1} : \boldsymbol{\sigma}^* \rangle \\
- \langle \mathbf{R}^* \therefore (\mathbf{L}_0 - \mathbf{L})^{-1} \therefore \mathbf{R}^* \rangle,
\end{aligned} \tag{D.12}$$

where $\boldsymbol{\sigma} = \overline{\boldsymbol{\sigma}} - \boldsymbol{\Delta}_0(\mathbf{e}^*) - \boldsymbol{\Lambda}_0(\boldsymbol{\phi}^*)$ is the solution to Problem (31). Introducing the associated strains $\mathbf{e} = \mathbf{S}_0 : \boldsymbol{\sigma} + \mathbf{e}^*$ and $\boldsymbol{\phi} = \mathbf{M}_0 \therefore (\boldsymbol{\sigma} \otimes \nabla) + \boldsymbol{\phi}^*$, we find that the second line of Eq. (D.12) above reduce to

$$\begin{aligned}
\langle \boldsymbol{\sigma} : \mathbf{e}^* \rangle + \langle \mathbf{e}^* : \mathbf{C}_0 : \mathbf{e}^* \rangle &= \langle (\mathbf{e} - \mathbf{e}^*) : \mathbf{C}_0 : \mathbf{e}^* \rangle + \langle \mathbf{e}^* : \mathbf{C}_0 : \mathbf{e}^* \rangle \\
&= \langle \mathbf{e} : \mathbf{C}_0 : \mathbf{e}^* \rangle \\
&= \langle \mathbf{e} : \mathbf{C}_0 : (\mathbf{e} - \mathbf{S}_0 : \boldsymbol{\sigma}) \rangle \\
&= \langle \mathbf{e} : \mathbf{C}_0 : \mathbf{e} \rangle - \langle \boldsymbol{\sigma} : \mathbf{e} \rangle,
\end{aligned} \tag{D.13}$$

likewise

$$\begin{aligned}
\langle (\boldsymbol{\sigma} \otimes \nabla) \therefore \boldsymbol{\phi}^* \rangle + \langle \boldsymbol{\phi}^* \therefore \mathbf{L}_0 \therefore \boldsymbol{\phi}^* \rangle = \langle \boldsymbol{\phi} \therefore \mathbf{L}_0 \therefore \boldsymbol{\phi} \rangle \\
- \langle (\boldsymbol{\sigma} \otimes \nabla) \therefore \boldsymbol{\phi} \rangle.
\end{aligned} \tag{D.14}$$

Then, from the Hill–Mandel lemma,

$$\langle \boldsymbol{\sigma} : \mathbf{e} \rangle + \langle (\boldsymbol{\sigma} \otimes \nabla) \therefore \boldsymbol{\phi} \rangle = \langle \boldsymbol{\sigma} \rangle : \langle \mathbf{e} \rangle = \overline{\boldsymbol{\sigma}} : \langle \mathbf{e} \rangle = \overline{\boldsymbol{\sigma}} : \mathbf{S}^{\mathrm{eff}} : \overline{\boldsymbol{\sigma}}. \tag{D.15}$$

Gathering the above results, we find the following expression of HS

$$\begin{aligned}
2\,\mathrm{HS}(\mathbf{e}^*, \boldsymbol{\phi}^*, \overline{\boldsymbol{\sigma}}) = \overline{\boldsymbol{\sigma}} : \mathbf{S}_0 : \overline{\boldsymbol{\sigma}} + \overline{\boldsymbol{\sigma}} : \langle \mathbf{e}^* \rangle + \overline{\boldsymbol{\sigma}} : \mathbf{S}^{\mathrm{eff}} : \overline{\boldsymbol{\sigma}} \\
+ \langle \mathbf{e} : \mathbf{C}_0 : \mathbf{e} \rangle + \langle \boldsymbol{\phi} \therefore \mathbf{L}_0 \therefore \boldsymbol{\phi} \rangle \\
- \langle \boldsymbol{\sigma}^* : (\mathbf{C}_0 - \mathbf{C})^{-1} : \boldsymbol{\sigma}^* \rangle \\
- \langle \mathbf{R}^* \therefore (\mathbf{L}_0 - \mathbf{L})^{-1} \therefore \mathbf{R}^* \rangle,
\end{aligned} \tag{D.16}$$

which shows that the quadratic part of HS (namely, the last three lines of the above expression) is positive: therefore, the critical point of HS is a minimum in this case.

## Appendix E. Ensemble average over SVEs of fixed size

In the present section, we derive Eq. (69). The size $L$ of the SVE is fixed; the trial strain-polarizations $\mathbf{e}^*$ and $\boldsymbol{\phi}^*$ are statistically homogeneous, ergodic random fields. We start from the definition of HS [see Eq. (59)]

$$\begin{aligned}\mathrm{HS}(\mathbf{e}^*,\boldsymbol{\phi}^*,\overline{\boldsymbol{\sigma}},L,\omega) = {}& \tfrac{1}{2}\overline{\boldsymbol{\sigma}}:\mathbf{S}_0:\overline{\boldsymbol{\sigma}}+\overline{\boldsymbol{\sigma}}:\langle\mathbf{e}^*\rangle\\ &-\tfrac{1}{2}\langle\mathbf{e}^*:(\mathbf{S}-\mathbf{S}_0)^{-1}:\mathbf{e}^*\rangle\\ &-\tfrac{1}{2}\langle\boldsymbol{\phi}^*\therefore(\mathbf{M}-\mathbf{M}_0)^{-1}\therefore\boldsymbol{\phi}^*\rangle\\ &-\tfrac{1}{2}\sum_{n\in\mathbb{Z}^3}\mathrm{conj}(\hat{\boldsymbol{\eta}}_n):\hat{\boldsymbol{\Delta}}_0(\mathbf{k}_n):\hat{\boldsymbol{\eta}}_n\end{aligned}\tag{E.1}$$

with $\hat{\boldsymbol{\eta}}_n = \hat{\mathbf{e}}^*_n - \mathrm{i}\hat{\boldsymbol{\phi}}^*_n\cdot\mathbf{k}_n$. Expanding with respect to $\hat{\mathbf{e}}^*_n$ and $\hat{\boldsymbol{\phi}}^*_n$ in the last sum, we find

$$\begin{aligned}\mathrm{HS}(\mathbf{e}^*,\boldsymbol{\phi}^*,\overline{\boldsymbol{\sigma}},L,\omega) = {}& \tfrac{1}{2}\overline{\boldsymbol{\sigma}}:\mathbf{S}_0:\overline{\boldsymbol{\sigma}}+\overline{\boldsymbol{\sigma}}:\langle\mathbf{e}^*\rangle\\ &-\tfrac{1}{2}\langle\mathbf{e}^*:(\mathbf{S}-\mathbf{S}_0)^{-1}:\mathbf{e}^*\rangle\\ &-\tfrac{1}{2}\langle\boldsymbol{\phi}^*\therefore(\mathbf{M}-\mathbf{M}_0)^{-1}\therefore\boldsymbol{\phi}^*\rangle\\ &-\tfrac{1}{2}\sum_{n\in\mathbb{Z}^3}\hat{\boldsymbol{\Delta}}_0(\mathbf{k}_n)\odot[\mathrm{conj}(\hat{\mathbf{e}}^*_n)\otimes\hat{\mathbf{e}}^*_n]\\ &-\tfrac{1}{2}\sum_{n\in\mathbb{Z}^3}\hat{\boldsymbol{\Delta}}''_0(\mathbf{k}_n)\odot[\mathrm{conj}(\hat{\boldsymbol{\phi}}^*_n)\otimes\hat{\boldsymbol{\phi}}^*_n]\\ &-\sum_{n\in\mathbb{Z}^3}[\hat{\boldsymbol{\Delta}}_0(\mathbf{k}_n)\otimes\mathbf{k}_n]\odot\Im[\mathrm{conj}(\hat{\mathbf{e}}^*_n)\otimes\hat{\boldsymbol{\phi}}^*_n],\end{aligned}\tag{E.2}$$

Taking the ensemble average, and observing that $\mathbf{e}^*$ and $\boldsymbol{\phi}^*$ are ergodic (which allows to replace volume averages $\langle\bullet\rangle$ with volume averages $\mathbb{E}[\bullet]$)

$$\begin{aligned}\mathbb{E}_\omega[\mathrm{HS}(\mathbf{e}^*,\boldsymbol{\phi}^*,\overline{\boldsymbol{\sigma}},L,\omega)] = {}& \tfrac{1}{2}\overline{\boldsymbol{\sigma}}:\mathbf{S}_0:\overline{\boldsymbol{\sigma}}+\overline{\boldsymbol{\sigma}}:\mathbb{E}[\mathbf{e}^*]\\ &-\tfrac{1}{2}\mathbb{E}[\mathbf{e}^*:(\mathbf{S}-\mathbf{S}_0)^{-1}:\mathbf{e}^*]\\ &-\tfrac{1}{2}\mathbb{E}[\boldsymbol{\phi}^*\therefore(\mathbf{M}-\mathbf{M}_0)^{-1}\therefore\boldsymbol{\phi}^*]\\ &-\tfrac{1}{2}\sum_{n\in\mathbb{Z}^3}\hat{\boldsymbol{\Delta}}_0(\mathbf{k}_n)\odot\mathbb{E}[\mathrm{conj}(\hat{\mathbf{e}}^*_n)\otimes\hat{\mathbf{e}}^*_n]\\ &-\tfrac{1}{2}\sum_{n\in\mathbb{Z}^3}\hat{\boldsymbol{\Delta}}''_0(\mathbf{k}_n)\odot\mathbb{E}[\mathrm{conj}(\hat{\boldsymbol{\phi}}^*_n)\otimes\hat{\boldsymbol{\phi}}^*_n]\\ &-\sum_{n\in\mathbb{Z}^3}[\hat{\boldsymbol{\Delta}}_0(\mathbf{k}_n)\otimes\mathbf{k}_n]\odot\Im\,\mathbb{E}[\mathrm{conj}(\hat{\mathbf{e}}^*_n)\otimes\hat{\boldsymbol{\phi}}^*_n].\end{aligned}\tag{E.3}$$

We now need to evaluate the limit of the above quantity as $L\to+\infty$. The first three terms are constant, while the three last sums are of the same nature; we will therefore concentrate on the first sum. At fixed $L$ and $\omega$, $\hat{\mathbf{e}}^*_n$ is the $n$-th Fourier coefficient of $\mathbf{e}^*$

$$\hat{\mathbf{e}}^*_n(L,\omega) = L^{-3}\int_{(0,L)^3}\mathbf{e}^*(\mathbf{x},\omega)\,\mathrm{e}^{-\mathrm{i}\mathbf{k}_n\cdot\mathbf{x}}\mathrm{d}^3\mathbf{x},\tag{E.4}$$

where it is recalled that

$$\mathbf{k}_n = \frac{2\pi}{L}(n_1\mathbf{e}_1+n_2\mathbf{e}_2+n_3\mathbf{e}_3).\tag{E.5}$$

Then

$$\begin{aligned}&\mathbb{E}[\mathrm{conj}(\hat{\mathbf{e}}^*_n)\otimes\hat{\mathbf{e}}^*_n]\\ &= L^{-6}\int_{\mathbf{x},\mathbf{y}\in(0,L)^3}\mathbb{E}[\mathbf{e}^*(\mathbf{x})\otimes\mathbf{e}^*(\mathbf{y})]\mathrm{e}^{\mathrm{i}\mathbf{k}_n\cdot(\mathbf{x}-\mathbf{y})}\mathrm{d}^3\mathbf{x}\,\mathrm{d}^3\mathbf{y}\\ &= L^{-6}\int_{\mathbf{x},\mathbf{y}\in(0,L)^3}\mathbf{R}_{ee}(\mathbf{y}-\mathbf{x})\mathrm{e}^{-\mathrm{i}\mathbf{k}_n\cdot(\mathbf{y}-\mathbf{x})}\mathrm{d}^3\mathbf{x}\,\mathrm{d}^3\mathbf{y}\\ &= L^{-6}\int_{\mathbf{x}\in(0,L)^3}\int_{\mathbf{x}+\mathbf{r}\in(0,L)^3}\mathbf{R}_{ee}(\mathbf{r})\mathrm{e}^{-\mathrm{i}\mathbf{k}_n\cdot\mathbf{r}}\mathrm{d}^3\mathbf{x}\,\mathrm{d}^3\mathbf{y}\\ &\sim L^{-3}\hat{\mathbf{R}}_{ee}(\mathbf{k}_n)\qquad(L\to+\infty),\end{aligned}\tag{E.6}$$

where $\hat{\mathbf{R}}_{ee}$ denotes the Fourier transform of the cross-correlation $\mathbf{R}_{ee}$ [see Eq. (68a)]. Then

$$\begin{aligned}&\sum_{n\in\mathbb{Z}^3}\hat{\boldsymbol{\Delta}}_0(\mathbf{k}_n)\odot\mathbb{E}[\mathrm{conj}(\hat{\mathbf{e}}^*_n)\otimes\hat{\mathbf{e}}^*_n]\\ &\quad\sim(2\pi)^{-3}\sum_{n\in\mathbb{Z}^3}\hat{\boldsymbol{\Delta}}_0(\mathbf{k}_n)\odot\hat{\mathbf{R}}_{ee}(\mathbf{k}_n)\Delta k^3\qquad(L\to+\infty),\end{aligned}\tag{E.7a}$$

where $\Delta k = 2\pi/L$ denotes the spacing between to neighbouring wave-vector $\mathbf{k}_n$ in Fourier space. We recognize a Riemann sum, and finally find

$$\begin{aligned}&\sum_{n\in\mathbb{Z}^3}\hat{\boldsymbol{\Delta}}_0(\mathbf{k}_n)\odot\mathbb{E}[\mathrm{conj}(\hat{\mathbf{e}}^*_n)\otimes\hat{\mathbf{e}}^*_n]\\ &\quad\to(2\pi)^{-3}\int_{\mathbb{R}^3}\hat{\boldsymbol{\Delta}}_0(\mathbf{k})\odot\hat{\mathbf{R}}_{ee}(\mathbf{k})\,\mathrm{d}^3\mathbf{r}\qquad(L\to+\infty),\end{aligned}\tag{E.7b}$$

and, similarly

$$\begin{aligned}&\sum_{n\in\mathbb{Z}^3}\hat{\boldsymbol{\Delta}}''_0(\mathbf{k}_n)\odot\mathbb{E}[\mathrm{conj}(\hat{\boldsymbol{\phi}}^*_n)\otimes\hat{\boldsymbol{\phi}}^*_n]\\ &\quad\to(2\pi)^{-3}\int_{\mathbb{R}^3}\hat{\boldsymbol{\Delta}}''_0(\mathbf{k})\odot\hat{\mathbf{R}}_{\phi\phi}(\mathbf{k})\,\mathrm{d}^3\mathbf{r}\qquad(L\to+\infty),\end{aligned}\tag{E.7c}$$

$$\begin{aligned}&\sum_{n\in\mathbb{Z}^3}[\hat{\boldsymbol{\Delta}}_0(\mathbf{k}_n)\otimes\mathbf{k}_n]\odot\Im\,\mathbb{E}[\mathrm{conj}(\hat{\mathbf{e}}^*_n)\otimes\hat{\mathbf{e}}^*_n]\\ &\quad\to(2\pi)^{-3}\int_{\mathbb{R}^3}[\hat{\boldsymbol{\Delta}}_0(\mathbf{k})\otimes\mathbf{k}]\odot\Im\hat{\mathbf{R}}_{e\phi}(\mathbf{k})\,\mathrm{d}^3\mathbf{r}\qquad(L\to+\infty),\end{aligned}\tag{E.7d}$$

and expression (72) of $\mathrm{HS}^\infty$ is retrieved.

## Appendix F. On the numerical evaluation of the Ξ microstructural parameter

In the present section, we provide some details on the numerical evaluation of the Fourier transform of the covariance function $\gamma$ and the microstructural parameter $\Xi$ introduced in Sec. 11.

The Fourier transform of the covariance function $\gamma$ is evaluated as follows. For $k\le k_\mathrm{c}$ (where the value of the cut-off wave-number $k_\mathrm{c}$ will be specified below), the integration interval $0\le r\le 2a$ is decomposed in sub-intervals where the integrand has a constant sign

$$k\hat{\gamma}(k) = 4\pi\sum_{i=0}^{m-1}\int_{r_i}^{r_{i+1}} r\gamma(r)\sin(kr)\,\mathrm{d}r,\tag{F.1}$$

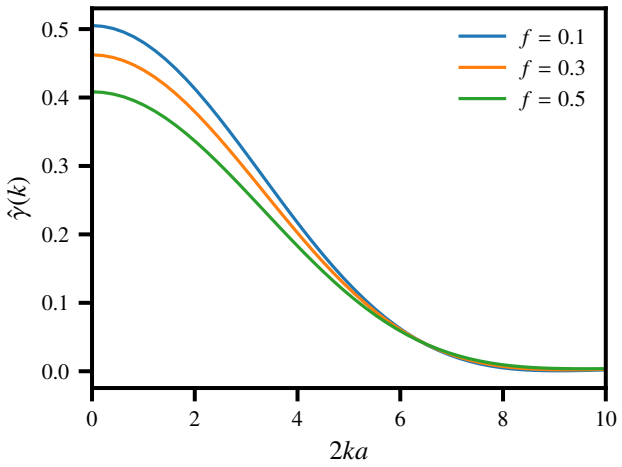


Figure F.8: Fourier transform $\hat{\gamma}$ of the covariance function of the boolean model, for various values of the volume fraction $f$ of inclusions.

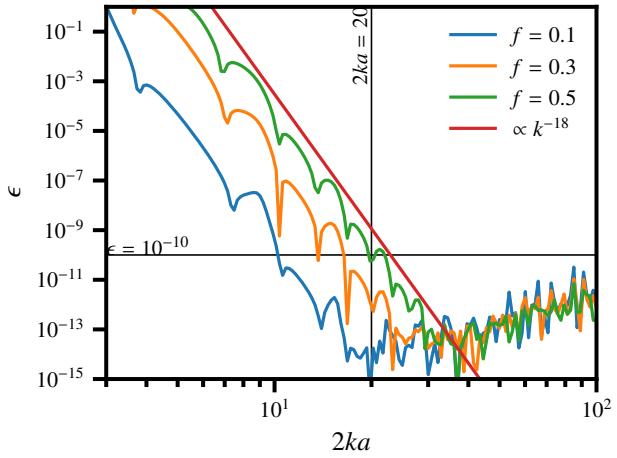


Figure F.9: The relative gap between the values of $\hat{\gamma}$ obtained through numerical integration and asymptotic expansion. For $2k_c a \sim 20$, an optimum is found between the truncation error of the asymptotic expansion and the round-off errors of numerical integration.

where $r_m = 2a$ and $r_i = i\pi/k$ $(i = 0, \ldots, m-1)$. On each subinterval, we use the standard function `scipy.integrate.quad`[2], which is a Python wrapper around the Fortran library QUADPACK. In order to minimize accumulation of rounding-off errors, positive and negative terms are then summed separately in increasing order of magnitude. Fig. F.8 shows $\hat{\gamma}$ for various values of the volume fraction of inclusions, $f$.

For $k \geq k_c$, the above method becomes impractical because of the large number of terms in Eq. (F.1). We resort to high-order asymptotic expansions

$$k\hat{\gamma}(k) = \sum_{p=3}^{n} \frac{a_p \cos 2ka + b_p \sin 2ka + c_p}{k^p} + O(k^{-n-1}), \qquad \text{(F.2)}$$

where the coefficients $a_p$, $b_p$ and $c_p$ are obtained by successive integrations by parts. The derivation is performed symbolically with the SymPy[3] computer algebra system. We find in particular the two-leading order terms of the expansion

$$a_4 = (1-f)c_4 \qquad b_4 = 0 \qquad c_4 = \frac{6\pi\rho v}{af}$$
$$a_5 = 0 \qquad b_5 = -\frac{12\pi\rho v}{a^2 f}(1-f) \qquad c_5 = 0.$$

The order of the expansion, and the cut-off value $k_c$ of $k$ beyond which the asymptotic expansion is used are selected in order to minimize the global relative error on $\hat{\gamma}$ as follows. Since $k\hat{\gamma}(k)$ behaves as $k^{-3}$ as $k \to +\infty$ we expect the relative error for this asymptotic expansion to behave as $k^{-n+2}$

$$\frac{\hat{\gamma}_{\mathrm{AE}}(k) - \hat{\gamma}(k)}{\hat{\gamma}(k)} = O(k^{-n+2}) \qquad (k \to +\infty), \qquad \text{(F.3)}$$

where $\hat{\gamma}_{\mathrm{AE}}$ denotes the asymptotic expansion (F.2). Since the exact value of $\hat{\gamma}$ is not known, we plot in Fig. F.9 the relative gap $\epsilon$ between $\hat{\gamma}_{\mathrm{AE}}$ and the approximation $\hat{\gamma}_{\mathrm{NI}}$ of $\hat{\gamma}$ obtained through numerical integration [Eq. (F.1)]

$$\epsilon = 2\frac{\hat{\gamma}_{\mathrm{AE}}(k) - \hat{\gamma}_{\mathrm{NI}}(k)}{\hat{\gamma}_{\mathrm{AE}}(k) + \hat{\gamma}_{\mathrm{NI}}(k)}. \qquad \text{(F.4)}$$

Fig. F.9 shows that the expected behavior $\epsilon = O(k^{-n+2})$ is indeed observed for "not-too-large" values of $k$. For large values of $k$, this behavior desappears and $\epsilon$ *increases*. This is due to numerical integration that becomes inaccurate, and $\epsilon$ is dominated in this range of $k$-values by the numerical integration error. We therefore set $k_c$ approximately at the location of the transition between the two regimes. Obviously, increasing the order $n$ of the asymptotic expansion increases its accuracy and therefore lowers the value of $k_c$, which is beneficial in terms of execution times. In all subsequent applications, we set $n = 20$. We then check that for $2k_c a \sim 20$, $\epsilon$ remains below $10^{-10}$, which is much lower than the prescribed relative tolerance for numerial integration (set here to $10^{-8}$).

In order to compute $\Xi$, its expression as an integral [see Eq. (104)] is split in two terms, $\Xi = \Xi_1 + \Xi_2$, with

$$\Xi_1 = \frac{1}{2\pi^2}\int_0^{k_c} \frac{k^2\hat{\gamma}(k)}{1+k^2\ell_0}\,\mathrm{d}k \simeq \frac{1}{2\pi^2}\int_0^{k_c} \frac{k^2\hat{\gamma}_{\mathrm{NI}}(k)}{1+k^2\ell_0}\,\mathrm{d}k \qquad \text{(F.5)}$$

and

$$\Xi_2 = \frac{1}{2\pi^2}\int_{k_c}^{+\infty} \frac{k^2\hat{\gamma}(k)}{1+k^2\ell_0}\,\mathrm{d}k \simeq \frac{1}{2\pi^2}\int_{k_c}^{+\infty} \frac{k^2\hat{\gamma}_{\mathrm{AE}}(k)}{1+k^2\ell_0}\,\mathrm{d}k. \qquad \text{(F.6)}$$

We again use numerical integration to evaluate $\Xi_1$. For $\Xi_2$, we need to evaluate integrals of the form

$$\begin{bmatrix}\mathcal{A}_p\\ \mathcal{B}_p\\ C_p\end{bmatrix} = \int_{k_c}^{+\infty} \frac{1}{k^{p-1}(1+k^2\ell_0^2)}\begin{bmatrix}\cos 2ka\\ \sin 2ka\\ 1\end{bmatrix}\mathrm{d}k, \qquad \text{(F.7)}$$

wich will be truncated to a yet unknown upper bound $K$

$$\begin{bmatrix}\mathcal{A}_p\\ \mathcal{B}_p\\ C_p\end{bmatrix} \simeq \int_{k_c}^{K} \frac{1}{k^{p-1}(1+k^2\ell_0^2)}\begin{bmatrix}\cos 2ka\\ \sin 2ka\\ 1\end{bmatrix}\mathrm{d}k, \qquad \text{(F.8)}$$

[2] https://www.scipy.org/, last retrieved June 6, 2020.
[3] https://www.sympy.org/, last retrieved June 6, 2020.

so that the residual is bounded in all three cases from above

$$\left|\int_K^{+\infty} \frac{1}{k^{p-1}(1+k^2\ell_0^2)} \begin{bmatrix}\cos 2ka\\ \sin 2ka\\ 1\end{bmatrix} \mathrm{d}k\right| \leq \int_K^{+\infty} \frac{\mathrm{d}k}{k^{p+1}\ell_0^2} = \frac{1}{p\ell_0^2 K^p}. \tag{F.9}$$

For the oscillatory integrals $\mathcal{A}_p$ and $\mathcal{B}_p$, we therefore proceed as follows. The integration range $(0, +\infty)$ is divided in subintervals where the integrand has a constant sign

$$\begin{bmatrix}\mathcal{A}_p\\ \mathcal{B}_p\end{bmatrix} = \sum_{i=0}^{+\infty} \int_{k_i}^{k_{i+1}} \frac{1}{k^{p-1}(1+k^2\ell_0^2)} \begin{bmatrix}\cos 2ka\\ \sin 2ka\end{bmatrix} \mathrm{d}k, \tag{F.10}$$

where $k_0 = k_c$ and $2a(k_{i+1} - k_i) = \pi$. The above sum is computed incrementally, one term at a time. Each time a new term is added to the sum, the residual is estimated through Eq. (F.9) and the iterations are stopped as soon as the residual is smaller than a prescribed fraction of the sum. For the non-oscillatory integrals $C_p$, we also proceed incrementally, using intervals of length $k_c\pi$ in that case.

## Appendix G. On the decomposition of fourth-order, transverse isotropic tensors

In the present section we gather the definition of the Walpole (1984) basis for fourth-order, transverse isotropic tensors. We also derive some expressions for the calculation of the acoustic tensor. The direction of anisotropy is denoted $\mathbf{n}$ (unit vector). We further introduce the two second-order projectors $\mathbf{p} = \mathbf{n}\otimes\mathbf{n}$ and $\mathbf{q} = \mathbf{I}_2 - \mathbf{p}$. Walpole (1984) proposed the $(\mathbf{E}^{\mathrm{I}}, \mathbf{E}^{\mathrm{II}}, \mathbf{E}^{\mathrm{III}}, \mathbf{E}^{\mathrm{IV}}, \mathbf{F}, \mathbf{G})$ basis for fourth-order, transverse isotropic tensors, with

$$\mathbf{E}^{\mathrm{I}} = \mathbf{p}\otimes\mathbf{p}, \qquad \sqrt{2}\mathbf{E}^{\mathrm{III}} = \mathbf{p}\otimes\mathbf{q}, \tag{G.1a}$$

$$\mathbf{E}^{\mathrm{II}} = \tfrac{1}{2}\mathbf{q}\otimes\mathbf{q}, \qquad \sqrt{2}\mathbf{E}^{\mathrm{IV}} = \mathbf{q}\otimes\mathbf{p} \tag{G.1b}$$

and

$$F_{ijkl} = \tfrac{1}{2}(q_{ik}q_{jl} + q_{jk}q_{il} - q_{ij}q_{kl}), \tag{G.1c}$$

$$G_{ijkl} = \tfrac{1}{2}(p_{ik}q_{jl} + p_{il}q_{jk} + p_{jk}q_{il} + p_{jl}q_{ik}), \tag{G.1d}$$

or, in component-free form

$$\mathbf{G} = 2\mathbf{I}_4 : (\mathbf{n}\otimes\mathbf{q}\otimes\mathbf{n}) : \mathbf{I}_4 \quad \text{and} \quad \mathbf{F} = \mathbf{I}_4 - \mathbf{E}^{\mathrm{I}} - \mathbf{E}^{\mathrm{II}} - \mathbf{G}. \tag{G.2}$$

It results from the above definitions that

$$\begin{aligned}\mathbf{I}_4 : (\mathbf{n}\otimes\mathbf{I}_2\otimes\mathbf{n}) : \mathbf{I}_4 &= \mathbf{I}_4 : [\mathbf{n}\otimes(\mathbf{p}+\mathbf{q})\otimes\mathbf{n}] : \mathbf{I}_4\\ &= \mathbf{I}_4 : (\mathbf{n}\otimes\mathbf{p}\otimes\mathbf{n} + \mathbf{n}\otimes\mathbf{q}\otimes\mathbf{n}) : \mathbf{I}_4\\ &= \mathbf{I}_4 : (\mathbf{p}\otimes\mathbf{p} + \mathbf{n}\otimes\mathbf{q}\otimes\mathbf{n}) : \mathbf{I}_4\\ &= \mathbf{E}^{\mathrm{I}} + \tfrac{1}{2}\mathbf{G}.\end{aligned} \tag{G.3}$$

The multiplication table for this table is best expressed through the following symbolic representation (Walpole, 1984)

$$\begin{aligned}\mathbf{T} &= a\mathbf{E}^{\mathrm{I}} + b\mathbf{E}^{\mathrm{II}} + c\mathbf{E}^{\mathrm{III}} + d\mathbf{E}^{\mathrm{IV}} + f\mathbf{F} + g\mathbf{G}\\ &= \{\left[\begin{smallmatrix}a & c\\ d & b\end{smallmatrix}\right], f, g\},\end{aligned} \tag{G.4a}$$

$$\begin{aligned}\mathbf{T}' &= a'\mathbf{E}^{\mathrm{I}} + b'\mathbf{E}^{\mathrm{II}} + c'\mathbf{E}^{\mathrm{III}} + d'\mathbf{E}^{\mathrm{IV}} + f'\mathbf{F} + g'\mathbf{G}\\ &= \{\left[\begin{smallmatrix}a' & c'\\ d' & b'\end{smallmatrix}\right], f', g'\},\end{aligned} \tag{G.4b}$$

which leads to the compact multiplication formula

$$\mathbf{T} : \mathbf{T}' = \{\left[\begin{smallmatrix}a & c\\ d & b\end{smallmatrix}\right] \cdot \left[\begin{smallmatrix}a' & c'\\ d' & b'\end{smallmatrix}\right], ff', gg'\}. \tag{G.5}$$

To close this section, we present some contractions of the Walpole tensors that will prove helpful for the derivation of the acoustic tensor

$$\begin{aligned}&\mathbf{n}\cdot\mathbf{E}^{\mathrm{I}}\cdot\mathbf{n} = \mathbf{p}, \quad \mathbf{n}\cdot\mathbf{E}^{\mathrm{III}}\cdot\mathbf{n} = \mathbf{0}, \quad \mathbf{n}\cdot\mathbf{F}\cdot\mathbf{n} = \mathbf{0},\\ &\mathbf{n}\cdot\mathbf{E}^{\mathrm{II}}\cdot\mathbf{n} = \mathbf{0}, \quad \mathbf{n}\cdot\mathbf{E}^{\mathrm{IV}}\cdot\mathbf{n} = \mathbf{0}, \quad \mathbf{n}\cdot\mathbf{G}\cdot\mathbf{n} = \tfrac{1}{2}\mathbf{q}.\end{aligned} \tag{G.6}$$